THESIS ON NATURAL AND EXACT SCIENCES B166

Estimation of the Complexity of the Electroencephalogram for Brain Monitoring in Intensive Care

ANDRES ANIER

TUT
PRESS

TALLINN UNIVERSITY OF TECHNOLOGY
Technomedicum
Department of Biomedical Engineering

Dissertation was accepted for the defense of the degree of Doctor of Philosophy (in Biomedical Technology) on December 20, 2013.

Supervisors: Professor **Tarmo Lipping**, PhD, Information Technology, Pori Department, Tampere University of Technology, Finland

Professor **Kalju Meigas**, PhD, Department of Biomedical Engineering, Technomedicum, Tallinn University of Technology, Estonia

Opponents: Chief Physicist **Antti Kulkas**, Dr.Tech., Department of Clinical Neurophysiology, Seinäjoki Central Hospital, Seinäjoki, Finland

Assistant Professor **Elzbieta Olejarczyk**, PhD, Nałęcz Institute of Biocybernetics and Biomedical Engineering, Polish Academy of Sciences, Warsaw, Poland

Defence of the thesis: February 7, 2014, Tallinn, Estonia

Declaration:

Hereby I declare that this doctoral thesis, my original investigation and achievement, submitted for the doctoral degree at Tallinn University of Technology has not been submitted for any academic degree.

/Andres Anier/

ISSN 1406-4723
ISBN 978-9949-23-581-0 (publication)
ISBN 978-9949-23-582-7 (PDF)

LOODUS- JA TÄPPISTEADUSED B166

Elektroentsefalogrammi kompleksuse hindamine aju monitooringul intensiivravis

ANDRES ANIER

TTÜ KIRJASTUS

CONTENTS

INTRODUCTION

Decades ago it was common to keep Intensive Care Unit (ICU) patients in deep anaesthesia. Fresh strategies consider patients' individual needs dynamic in nature as clinical circumstances and therpeutic targets change over time usually resulting in slightly sedated cooperative patient [109, 92].

Inaccurate pain assessment and the resulting inadequate treatment of pain in critically ill patients can have significant physiological and psychological consequences. For example, pain increases myocardial workload, which can lead to myocardial ischemia or to splinting, atelectasis and a cascade of events that in turn can lead to pneumonia [64]. There is also the risk of patient self injury resulting from removal of the endotracheal tube or vital catheters. Development of a post traumatic stress disorder can be caused by being awake and experiencing severe pain. There are risks related to oversedation as well, including venous thrombosis, reduced blood pressure and pneumonia [109]. As the common effect of most sedatives is respiratory depression, prolonged mechanical ventilation can be required resulting in the prolonged ICU and hospital stay which yields increased cost of care.

In order to achieve adequate anaesthesia it is important to understand the nature of anaesthesia. There are several components forming the state of the patient called as anaesthesia including amnesia, unconsciousness (hypnosis), antinociception, and neuromuscular blockade (paralysis). Amnesia is temporary loss of memory caused by sedative or hypnotic drugs. Unconciousness is the state of patient involving lack of responsivness to external stimuli. Antinociception is reduced sensitivity to painful stimuli. Neuromuscular blocade is inability to activate sceletal muscles as a result of a blockade at neuromuscular junction. General anaesthetic drugs induce all these components of anaesthesia depending on dosage. First to appear is unconciousness followed by antinociception and paralysis as dose increases. Each component of anaesthesia can be induced separately by a specific drug and must be assessed separately using adequate methods. Propofol, for example, is a pure hypnotic and the effect of propofol can be assessed using EEG analysis. For assessing the level of neuromuscular blocade the method called train-of-four test is used. The lack of responsiveness does not necessarily mean lack of awareness or lack of memory. Severe neuromuscular blocade accompanied with inadequate hypnosis and antinociception can result in memories of pain while the patient is not able to respond to the painful stimuli. Accurate measuring of pain, agitation, sedation and other related variables is essential to avoid excessive or prolonged sedation and ensure patient safety.

For communicative patients self-reporting is the best indicator of pain. Pain scales incorporating observed behavior and physiologic measures are used for non-communicative patients.

The main premises of the present thesis can be summarised as follows:

- in interference-free and artifact-free conditions the EEG signal becomes more regular (less complex) in deepening sedation of anaesthesia with most common sedative drugs. This change can be assessed and quantified by estimating the complexity of the signal
- wide variety of measures based on different mathematical frameworks have been used in commercial monitoring devices and proposed in scientific literature to assess this change
- in numerous studies EEG complexity based methods have been shown to give misleading results in situations like arousal, presence of muscle activity, epileptogenic patterns etc.

The main goal of the research presented in this thesis was to study the impact of the mathematical background of selected algorithms of signal complexity and entropy on the capability of these algorithms to follow the changes in the patient condition in the ICU. This goal is addressed by the following methodology:

- by changing the useful bandwidth of the EEG signal or calculation paradigm of the algorithms (signal windowing scheme or power spectrum calculation method, for example) the behaviour of the signal complexity measures with respect to clinical sedation scores is studied
- by fixing certain signal properties using surrogate analysis the capablility of the selected algorithms to follow the known change in either the patient condition or other properties of the signal is studied.

The results obtained will contribute to better understanding by clinicians and biomedical engineers of the tools used for brain monitoring in the ICU.

In the first part of the thesis the basic principles of assessing the level of sedation are discussed. The effect of common anaesthetic agents to human EEG are explained followed by an explanation of the methods applied in commercial anaesthesia monitors to detect these changes and estimate the level of sedation as a result.

In the second part of the thesis EEG signal complexity based methods are studied in-depth. Three studies are presented explaining the effect of the method used for power spectrum calculation on the spectral entropy measure, indicating the influence of the prefilter settings on the behavior of the entropy/complexity measures and showing the opposite behaviour of the spectral entropy and approximate entropy measures in the case of developing alpha rhythm.

In the third part entropy/complexity measures are studied further in their limits using surrogate analysis.

The present thesis is based on the following publications that are referred to in the text by their Roman numerals I-V:

I **Anier, A**., Lipping, T., Melto, S. and Hovilehto, S. Higuchi Fractal Dimension and Spectral Entropy as Measures of Depth of Sedation in Intensive Care Unit. *Engineering in Medicine and Biology Society, 2004. IEMBS'04. 26th Annual International Conference of the IEEE,* 1, pp. 526-529, 2004.

II Lipping, T., Ferenets, R., **Anier, A**., Melto, S. and Hovilehto, S. Power spectrum estimation in the calculation of spectral entropy to assess depth of sedation. *IFMBE Proc,* 11(1), 4p, 2005.

III Ferenets, R., Lipping, T., **Anier, A**., Jäntti, V., Melto, S. and Hovilehto, S. Comparison of Entropy and Complexity Measures for the Assessment of Depth of Sedation. *IEEE Transactions on Biomedical Engineering,* 53(6), pp. 1067-1077, 2006.

IV **Anier, A**., Lipping, T., Jäntti, V., Puumala, P. and Huotari, A-M. Entropy of the EEG in transition to burst suppression in deep anaesthesia: surrogate analysis. *Engineering in Medicine and Biology Society (EMBC), 2010 Annual International Conference of the IEEE,* pp. 2790-2793, 2010.

V **Anier, A**., Lipping, T., Ferenets, R., Puumala, P., Sonkajärvi, E., Rätsep, I. and Jäntti, V. Relationship between approximate entropy and visual inspection of irregularity in the EEG signal, a comparison with spectral entropy. *British journal of anaesthesia,* 109(6), pp. 928-934, 2012.

Approbation

26th Annual International Conference of the IEEE Engineering in Medicine and Biology Society San Francisco, California From 1-Sep-2004 to 4-Sep-2004

27th Annual International Conference of the IEEE Engineering in Medicine and Biology Society Shanghai, China From 1-Sep-2005 to 4-Sep-2005

5th International Workshop on Biosignal Interpretation September 6 - 8, 2005, Tokyo, Japan

29th Annual International Conference of the IEEE Engineering in Medicine and Biology Society Lyon, France From 23-Aug-2007 to 26-Aug-2007

11th Mediterranean Conference on Medical and Biological Engineering and Computing June 26 - 30, 2007, Ljubljana, Slovenia

30th Annual International Conference of the IEEE Engineering in Medicine and Biology Society Vancouver, Canada From 21-Aug-2008 to 24-Aug-2008

Author's own contribution

The author performed a substantial portion of analysing the experimental recordings, planning and performing of the EEG signal analysis, developed further custom signal analysis toolset [59] according to research needs and contributed to the writing of the papers.

Acknowledgements
My deepest appreciation belongs to my supervisor professor Tarmo Lipping for his continuous support, guidance and motivation spanning over more than decade, which made this work possible. I would like to express my sincere gratitude to everyone who contributed to the creation of this thesis, both directly and indirectly. Finally, I would like to express special thanks to my family for their support and understanding.

ABBREVIATIONS

ABS - Analgesia based sedation
BIS - Bispectral Index Score
BSR - Burst - Suppression Ratio
cEEG - continuous EEG monitoring
EEG - Electroencephalography
EMG - Electromyogram
HBS - Hypnotic based sedation
HDf - Higuchi Fractal Dimension
ICU - Intensive Care Unit
LZC - Lempel-Ziv complexity
OR - Operating Room
PrmEn - Permutation entropy
PSD - Power Density Distribution
RBR - Relative Beta Ratio
RE - Response Entropy
SAS - Riker Sedation-Agitation Scale
SE - State Entropy
SFS - SynchFastSlow
SmpEn - Sample entropy

1 PATIENT MANAGEMENT AND COMMON SEDATIVE DRUGS IN THE ICU

Historically patients were kept awake during mechanical ventilation [71, 75]. Since the introduction of infusion administered sedatives like diazepam, for example, in the late 1960s allowing titration to a desired level, sedation became a standard treatment in ICU patients undergoing mechanical ventilation as the first generation ventilators were not sensitive enough to avoid dyssynchrony between the patient and the ventilator [103].

Recently the focus of sedation management has shifted to the lenght of mechanical ventilation and duration of ICU and hospital stay [50, 12]. The simple intervention of stopping both sedation and analgesics until patients either become aroused or clearly uncomfortable, repeated on a daily basis, has become the best practice. Unfortunately such a practice is followed in less than half cases [52, 45, 22, 65, 107, 28].

Even fresher strategies suggest that successful management of ventilated patients is possible without sedation resulting significant reduction of stay in the ICU (reduction by 10 days on the average) and total hospital stay (reduction by 24 days on the average). Removing the reasons for patient discomfort like anger, depression, pain, inability to cooperate with the ventilator, hypoxia, and hypercapnia is suggested instead of using sedation. An unsedated comfortable patient allows to monitor central nervous system function, get feedback about organ perfusion and to detect the worsening of patient condition like the development of delirium, for example, earlier [103].

The management of critical care patient is complex and decision making in this setting is challenging involving about 50 variables related to assessment, physiology and treatment both pre- and post intervention. Sedation management is just one yet important integral component of care [4, 45] including itself several components like hypnosis and analgesia, for example.

The hypnotic based sedation (HBS) strategy involves maintaining certain level of sedation as the primary end-point using midazolam or propofol with analgesics added as needed. The analgesia based sedation (ABS) strategy optimises patient discomfort and pain by the titration of remifentanil while hypnotic agents are given as needed [70, 49]. This strategy results in signifcant reduction of duration of mechanical ventilation and ICU stay [83].

Analgestic therapy is usually delivered using opioids [98]. Opioids block neurons that transmit nociception but do not affect other modalities and motor functions. The depression of respiratory function is dose dependent and increases if used in combination with benzodiazepines. The most widely used opioids are morphine, fentanyl and its derviate remifentanil [30].

Fentanyl is highly lipid soluble synthetic narcotic analgesic able to cross blood-brain barrier quickly yielding in rapid onset of action. As also the duration of

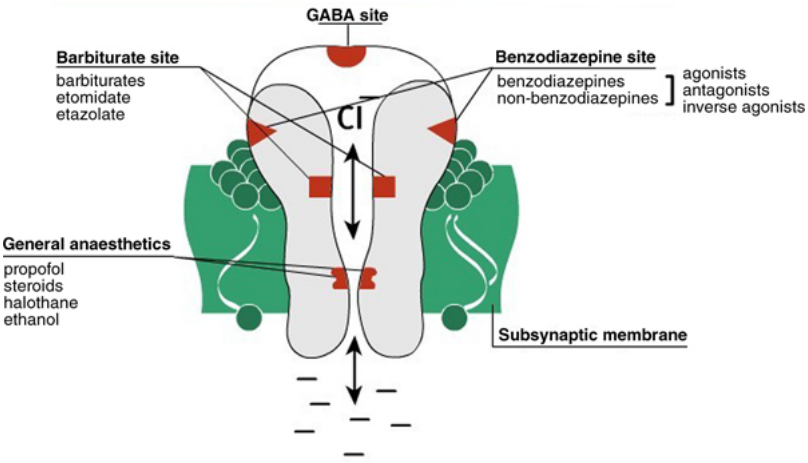

Figure 1.1: Functional binding sites on the GABA receptor. Adapted from [80].

action is short continuos infusion is required for sustained effect. Fentanyl has no histamine release or venodilating effects and no active metabolites [93].

While other opioids require hepatic transformation and renal excretion, remifentanil is metabolized by unspecific esterases that are widespread throughout the plasma, red blood cells, and interstitial tissues [8]. Remifentanil is the primary choice for ABS [11].

In **intravenous sedation** hypnotic drugs interact with the inhibitory γ-aminobutyric acid (GABA) system that counteracts excitatory neurotransmitters (see Figure 1.1).

Benzodiazepines limit the degree of modulation of GABA receptors, midazolam and lorazepam being the most common in ICU setting. Receptor occupancies around 20% are suggested to provide anxiolysis, 30-50% sedation, and more than 60% hypnosis [5]. They block the acquisition and encoding of new information (anterograde amnesia), but they do not induce retrograde amnesia. Benzodiazepines are the most widely used sedatives in medicine [122].

Propofol is a pure hypnotic with rapid onset and offset formulated in an oil-in-water emulsion. Propofol's rapid onset and offset actions are due to its lipophilic proprties allowing rapid crossing of the blood-brain barrier [30].
Propofol is preferred for the time period up to 72h and for longer terms midazolam is the preferred choice [63].

Dexmedetomidine is a relatively new centrally acting α2-agonist for ICU sedation having both sedative and analgesic properties [105, 62, 112]. The potential benefits of dexmedetomidine include modulation of the cardiovascular response to stressful procedures [111, 1], the absence of clinically significant respiratory depression [113], and the ability to sedate with only mild cognitive impairment [36].

The use of **volatile anaesthetics** as sedative agents in ICU have been restricted due to ambient air pollution risks. The introduction of new technologies like the AnaConDa® filter connected to normal ICU ventilators allows maintaining 90% of the volatile anaesthetic inside the patient and thus simplifying administration of volatile anaesthetics in this setting [9]. Volatile sedative agents are considered as the useful supplement to modern intravenous ABS techniques. The most frequently used volatile anaesthetics are isoflurane, desflurane and halothane [99, 100].

Isoflurane can be used for sedation in ICU patients undergoing mechanical ventilation providing adequate sedation with significally shorter awakening times compared with midazolam and without tolerance or withdrawal symptoms [51, 101, 66, 86]. Isoflurane is eliminated completely via exhalation if administration is discontinued making it one of the safest anaesthetic drugs [14].

There are several **subjective methods** for monitoring the depth of sedation in ICU including Ramsay Sedation Scale (RSS), Sedation Agitation Scale (SAS), Motor Activity Assessment Scale (MAAS), Richmond Agitation Sedation Scale (RASS) [89].

Although the Ramsay Sedation Scale was not intended for use as clinical monitoring tool, it appears to be one of the most commonly used sedation scales introduced nearly four decades ago [78]. It identifies six levels according to patient rousability (Table 1.1)

Table 1.1: Ramsay Sedation Scale

Score	Patient state
1	Patient awake, anxious and agitated or restless or both
2	Patient awake, co-operative, orientated, and tranquil
3	Patient awake, responds to commands only
4	Patient asleep, brisk response to a light glabellar tap or loud auditory stimulus
5	Patient asleep, sluggish response to a light glabellar tap or loud auditory stimulus
6	Patient asleep, no response to a light glabellar tap or loud auditory stimulus

The Riker Sedation-Agitation Scale (SAS) was developed and tested for ICU use identifying 7 levels, ranging from dangerous agitation to deep sedation (Table 1.2) [17, 81].

The Motor Activity Assessment Scale (MAAS) is similar to SAS (Table1.3) [24, 108].

The Richmond Agitation-Sedation Scale (RASS) is a 10-point scale (Table 1.4) developed at Virginia Commonwealth University in Richmond. It has has discrete criteria for levels of sedation and agitation and can be rated briefly using three

Table 1.2: Riker Sedation-Agitation Scale

Score	Diagnosis	Observation
7	Dangerously agitated	Pulls at endotracheal tube; tries to remove catheters; climbs over bed rail; strikes at staff; thrashes from side to side
6	Very agitated	Does not calm down despite frequent verbal reminding of limits; requires physical restraints; bites endotracheal tube
5	Agitated	Anxious or mildly agitated; attempts to sit up; calms down in response to verbal instructions
4	Calm and cooperative	Calm; awakens easily; follows commands
3	Sedated	Difficult to arouse; awakens to verbal stimuli or gentle shaking but drifts off again; follows simple commands
2	Very Sedated	Arouses to physical stimuli but does not communicate or follow commands; may move spontaneously
1	Unable to be aroused	Minimal or no response to noxious stimuli; does not communicate or follow commands

clearly defined steps. The duration of eye contact following verbal stimulation is used as the principal means of titrating sedation allowing assessment of thought content, the other component of conciousness beside arousal [91, 90, 74].

The known limitations of subjective sedation scales are inter-rater variablity, limited use in patients with cognitive dysfunction disorders, not useful in patients in neuromuscular blockers and incapability of discriminanting between deeper sedation levels [82]. The disturbance caused by patient stimulation for evaluation may arouse and agitate the patient and contribute to psychological sequelae [84].

Objective measures of depth of sedation include lower oesophageal sphincter contractility measurement, heart rate variability measurement, evoked potentials and electroencephalography (EEG) derived parameters such as Bispectral Index (BIS), Entropy, Patient State Index, Narcotrend etc. [124]. BIS offers a single value between 0 and 100 representing an integrated measure of cerebral activity [96, 104]. While the concept of a single number to guide how to titrate drug doses is certainly appealing the clear benefits of using sedation monitor are not clear [54]. The studies of correlation between BIS and subjective sedation have shown varying results [95, 26, 21]. There is significant overlap between BIS values and

Table 1.3: Motor Activity Assessment Scale

Score	Diagnosis	Observation
0	Unresponsive	Patient does not move with noxious stimulus
1	Responsive only to noxious stimuli	Patient opens eyes or raises eyebrows or turns head toward stimulus or moves limbs with noxious stimulus
2	Responsive to touch and name	Patient opens eyes or raises eyebrows or turns head toward stimulus or moves limbs when touched or name is loudly spoken
3	Calm and cooperative	Patient does not require external stimulus to elicit movement; adjusts sheets or clothes purposefully; follows commands
4	Restless but cooperative	Patient does not require external stimulus to elicit movement; picks at sheets or clothes or uncovers self; follows commands
5	Agitated	Patient does not require external stimulus to elicit movement; attempts to sit up or moves limbs out of bed; does not consistently follow commands
6	Dangerously agitated, uncooperative	Patient does not require external stimulus to elicit movement; pulls at tubes or catheters, thrashes from side to side, strikes at staff, or tries to climb out of bed; does not calm down when asked

clinical scores [85, 124]. BIS is unable to discriminate between different agitation levels and clinical scales are not able to discriminate between deeper levels of sedation in unresponsive patients.

The reduction of drug use with the help of BIS monitoring is questionable. The recent study by Olson et.al. shows higher doses of dexmedetomidine or benzodiazepines were given in BIS-augmented titration versus clinical assessment alone [68].

While clinical sedation scales are designed to address both agitation and sedation the EEG monitors were designed to measure depth of sedation to reduce risk of recall - amnesia [85], what may not be a valid endpoint for ICU sedation [47], especially in the era of ABS. Patients with factual memories are less likely to develop post traumatic stress disorder [103].

Table 1.4: Richmond Agitation Sedation Scale (RASS)

Score	Diagnosis	Observation
+4	Combative	Combative, violent, danger to staff
+3	Very agitated	Pulls or removes tubes or catheters, aggressive
+2	Agitated	Frequent nonpurposeful movement, fights ventilator
+1	Restless	Anxious, apprehensive, but not aggressive
0	Alert and calm	Alert and calm
-1	Drowsy	Not fully alert, but has sustained awakening, eye contact to voice > 10s
-2	Light sedation	Briefly awakens, eye contact to voice < 10s
-3	Moderate sedation	Movement or eye opening to voice, no eye contact
-4	Deep sedation	No response to voice, movement or eye opening to physical stimulation
-5	Unarousable	No response

2 EEG IN THE ICU

Continuous monitoring of the ICU patient EEG is becoming as common as monitoring of cardiac function. Although monitoring of celebral function is more difficult than monitoring of cardiac function, advancements in related technologies have made it more practical in recent years. The reasons not to use EEG monitoring are more logistical in nature like electrode maintenance, lack of effective computer algorithms to assist monitoring and lack of EEG experts. The advancements in computing power and algorithms development are essential to make continuous EEG monitoring (cEEG) more feasible as manual interpretation of EEG is impractical [42].

In this chapter the role of EEG monitoring in the ICU is discussed first and related commercial brain monitoring devices employing EEG signal analysis are described subsequently. These devices have been designed primarily for the assessment of the depth of general anaesthesia in the operating room, however, several of them have been approved also for brain monitoring in the ICU.

2.1 The advantages of EEG monitoring in the ICU

The goal of EEG monitoring in ICU is to detect the onset abnormalities at a reversible stage [10]. There has been a lot of discussion on the use of EEG monitoring in the ICU [27, 44, 48]. Recently Guerit et. al. published a review on the consensus of the use of neurophysiological tests, including EEG measurement, in the ICU [32]. It is commonly accepted that the detection of epileptic patterns is the most important aspect of EEG monitoring in neurological ICU [3]. However, numerous studies indicate that EEG, if interpreted by an experienced expert, contains a lot of useful information on, for example, the level of sedation, severity of brain damage or occurrence of hypoxic episodes. Also, EEG can have predictive value in patients suffering from severe brain damage or spontaneous haemorrhage [25, 118]. EEG can be used to detect delirium [73], a cognitive dysfunction causing inreased morbidity and prolonged ICU and hospital stay [119] with incidence rate ranging up to 50% [20].

It is strongly recommended to record audio and video together with all EEG studies in the ICU. It helps to identify clinical correlates of subtle seizures, and clinical events that mimic seizures. It is also very useful for artifact recognition as many artifacts like chewing/eating, patting/chest percussion, vibrating bed etc., mimic seizures and other important EEG patterns [43]. In addition to or in absence of video recordings notations by nurses and other staff regarding treatment, intentional stimulation are of great help in subsequent EEG interpretation.

2.2 Examples of Methods Applied in Commercial Anaesthesia Monitors

The key working principle of anaesthesia monitor is to follow and quantify the EEG changes that occur with the deepening of anaesthesia. In awake relaxed patients with the eyes closed α waves in frequency range 7.5 - 12.5 Hz dominate. With induction of light propofol or sevoflurane anaesthesia the power in the α range decreases and increases in the β frequency range 12.5 - 30Hz . The deepening of anaesthesia results in decrease of high frequency activity in α and β frequency band, slow waves begin to dominate in δ and θ ranges, 1.5 - 3.5 Hz and 3.5 - 7.5 Hz respectively [33]. Even deeper states of anaesthesia result in burst suppression EEG patterns where periodic epochs of electrical silence alternate with slow activity. Ultimately isolectrical silence appers with deep levels of anaesthesia.

The *Bispectral Index Score (BIS)* was developed by Aspect Medical Systems Inc. in the beginning of 90s and is validated for both Operating Room (OR) and ICU use. After applying artifact removal BIS combines the following parameters into single scalar between 0 and 100 using proprietary non-linear algorithm: Relative Beta Ratio (RBR), SynchFastSlow, Burst-Suppression Ratio [15]. Relative Beta Ratio is calculated in frequency domain

$$RBR = log(P_{30-47Hz}/P_{11-20Hz})$$

where $P_{f_1-f_2}$ denotes spectral power in EEG frequency band $f_1 - f_2$. Relative Beta Ratio follows power increase in β frequency range and is most influential parameter in light hypnotic states. SynchFastSlow (SFS) is bispectral domain parameter calculated as

$$SFS = log(B_{0.5-47Hz}/B_{40-47Hz})$$

where $B_{f_1-f_2}$ is the bispectral power in frequncy range $f_1 - f_2$. SynchFastSlow component of BIS predominates in surgical levels of anaesthesia.

Burst - Suppression Ratio (BSR) is calculated in the time domain and quantifies the extent of brain electrical inactivity during deep levels of the anaesthesia:

$$BSR = t_{suppression}/t_{epoch} * 100\%$$

While numerous studies [18, 29, 57, 60, 96, 124] confirm BIS correlates well with behavioral measures of sedation there are also several studies pointing at misbehaviours BIS. Discontiunuation of nitrous oxide N_2O was reported to cause declining BIS values as a result of an increase in δ and θ ranges showing deep anaesthesia - like patterns [77, 76, 37]. Ketamine administration causes different effects on EEG compared to general effects described above resulting in increase of BIS values [41, 38, 114]. A doubling or event tripling in isoflurane concentrations from 0.79% has reported to cause increase in BIS values result-

ing form increase in spectral power in α and β frequency bands similar to light anaesthesia [16, 23]. Onset of hypoglycemia produces EEG changes similar to general anaesthesia as described above and thus contribute to decrease in BIS values [110, 123, 117]. Electromyogram (EMG) frequency range overlaps with 30 - 47 Hz region of interest of RBR calculation and can therefore cause increased BIS values not reflecting the state of patient accurately [13, 6, 116, 97, 84]. This effect can be eliminated using bolus of neuromuscular blocking drug [19, 31].

M-Entropy module is a depth of anaesthesia monitoring module developed for the use in Datex-Ohmeda S/5 anaesthesia monitor. The method is based on the idea that the entropy of the EEG signal decreases with the deepening anaesthesia. Spectral entropy calculated over the frequency range of 0.8–32 Hz is called *State Entropy (SE)* and spectral entropy calculated over 0.8–47Hz is called *Response Entropy (RE).* Both parameters are normalised in a way that they become equal when the spectral power of EMG (32 - 47 Hz) is zero making RE - SE effectively a measure of EMG [115]. BIS being the *de facto* standard, Entropy Module has been compared with BIS and clinical measures in several studies [79, 106, 39, 61, 53, 94].

Despite several studies have also questioned the reliability of frontal EEG based depth of sedation monitors as BIS or Entropy Module [67, 120, 84, 85, 34, 35, 121] they cannot be replaced in patients receiving neuromuscular blocking drugs and/or at deeper, unresponsive levels of anaesthesia. In order to use such a devices in a proper manner one must have deeper understanding of underlying physiological processeses and signal processing aspects in order to be able to look behind numbers on the screen.

3 MEASURES OF EEG SIGNAL COMPLEXITY FOR ASSESSING DEPTH OF SEDATION

Besides the methods applied in the commercial brain monitoring devices, numerous other EEG signal measures have been proposed for brain monitoring in the operating room or ICU. Vast majority of these methods attempt to quantify the complexity or entropy of the EEG signal.

The algorithms can be divided into four categories according to their mathematical background:

- methods based on power spectrum analysis
  - Spectral Entropy
    quantifies the flatness of the power spectrum as a measure of regularity
- methods based on phase space analysis
  - Approximate Entropy
    measures dispersion of the trajectory in phase space when phase space dimension is increased by one
  - Sample Entropy
    is the enchanced version of the Approximate Entropy with, for example, self-matches excluded
  - Higuchi Fractal Dimension
    is the measure describing how signal is changed depending on the scale of measure
- methods quantifying pattern repetition in the signal
  - Lempel-Ziv complexity
    is a measure reflecting the rate of new pattern generation along given sequence of symbols
  - Permutation Entropy
    measures the randomness of the occurrence of symbols in a time series

In this chapter an overview on the entropy/complexity algorithms studied is given first and analysis of important aspects of their behaviour is presented subsequently. It appears that due to different mathematical background the different entropy/ complexity algorithms can behave in a quite different manner. This is particularly critical if the EEG signal contains artifacts or unexpected patterns. It is shown, for example, that the method used for the calculation of the power spectrum has significant impact on the value of *Spectral Entropy* (**Publication II**) and that the prefilter settings of the EEG measurement device have different effects on the performance of the signal complexity algorithms (**Publication I**). It is also shown

that *Approximate Entropy* and *Spectral Entropy* can change in opposite direction in certain conditions met in anaesthesia or sedation (**Publication V**).

3.1 Methods for the assessment of EEG signal entropy/complexity

In spite of the large variety of available methods for quantifying depth of hypnosis all of them seem to work in a satisfactory manner in most cases if surgical anaesthesia levels are considered. The situation is much more complicated in the Intensive Care Unit (ICU), however. In addition to the sedative drugs several other factors like various medication and the condition of the patient have influence on the EEG signal. Also, the environment in the ICU is hostile from the point of view of EEG measurement. Various kinds of equipment are used causing artifacts in the signal.

Due to these reasons the measures of the depth of anaesthesia used in the operating room often fail in the ICU and new parameters for quantifying depth of hypnosis are being proposed continuously. In the following, several algorithms quantifying the complexity of the EEG signal, proposed recently for the assessment of the level of hypnosis, are shortly reviewed.

Spectral Entropy (SpEn) is calculated

$$SpEn = \frac{-\sum_{i=f_{low}}^{f_{high}} P_i log P_i}{log N_f}, \tag{3.1}$$

where P is power density of signal, f_{low} and f_{high} define the frequency band of interest and N_f is the number of frequency components in the frequency band of interest. The calculated Spectral Entropy value is dependent on method used for estimating Power Density Distribution (PSD) of the signal (**Publication II**).

Approximate Entropy was introduced by Pincus [72] and quantifies the unpredictability of the signal. The approximate entropy of signal $s = \{x_1, ..., x_N\}$ for a chosen positive integer m (embedding dimension determining the dimension of the phase space) and a positive real number r (*a priori* fixed distance between the neighboring trajectory points) is calculated as follows. After forming $N - m + 1$ new vectors

$$v_m(i) = \{x_i, x_{i+1}, ..., x_{i+m-1}\}, \tag{3.2}$$

$C_i^m(r_f)$ is calculated for $1 \leq i \leq N - m + 1$

$$C_i^m(r) = \frac{number\,of\,such\,j\,that\,d[v_m(i), v_m(j)] \leq r}{N - m + 1}, \tag{3.3}$$

where d is the distance between vectors defined as

$$d[v_m(i), v_m(j)] = \max_{k=1,..,m} \left(\left| x_{i+k-1} - x_{j+k-1} \right| \right). \tag{3.4}$$

Approximate entropy is defined as

$$ApEn(m,r,N) = \Phi^m(r_f) - \Phi^{m+1}(r), \tag{3.5}$$

where

$$\Phi^m(r) = \frac{1}{N-m+1} \sum_{i=1}^{N-m+1} \log C_i^m(r). \tag{3.6}$$

Sample Entropy is calculated quite similar to Approximate Entropy (3.5) except in calculating the number of similar sequences (i.e., close data points in phase space) self-matches (i = j in equation 3.3) are excluded. Secondly equations 3.5 and 3.6 are replace with

$$C^m(r) = \frac{1}{N-m} \sum_{i=1}^{N-m} C_i^m(r), \tag{3.7}$$

and

$$SmpEn(m,r,N) = -\ln \frac{C^{m+1}(r)}{C^m(r)}. \tag{3.8}$$

The algorithm of the *Higuchi fractal dimension* (HDf)was proposed in [40] and is calculated as follows.

k new time series are constructed from a given time series $x\{1\},x\{2\},...,x\{N\}$ for $m = 1,...,k$

$$X_m^k = \left[x\{m\}, x\{m+k\}, ..., x\left\{ m + \left\lfloor \frac{N-m}{k} \right\rfloor k \right\} \right]. \tag{3.9}$$

The lenght of X_m^k is defined as:

$$L_m^k = \frac{1}{k} \left[\left(\sum_{i=1}^{\lfloor N-m/k \rfloor} |x\{m+ik\} - x\{m+(i-1)k\}| \right) \frac{N-1}{\lfloor N-m/k \rfloor} \right]. \tag{3.10}$$

Thus, L_m^k is proportional to the average difference of consecutive values of X_m^k . Averaging the lenghts L_m^k over m and calculating these averages for all k gives the sequence $L[k]$. If $L[k]$ is plotted against $1/k$, where $k = 1,...,k_{max}$, in double logarithmic scale the data points should fall into straight line with the slope S. The slope of the obtained line is calculated by applying linear fitting by means of least-squares to pairs $(log 1/k, logL(k)), k = 1,...,k_{max}$ giving the estimate of the fractal dimension HDf. Detailed description of the algorithm and its applicability to EEG signal analysis has been thoroughly studied in [2].

The *Lempel-Ziv normalised complexity (LZC)* is a measure reflecting the rate of new pattern generation along given sequence of symbols and was introduced in [56].

For the sequence of symbols $s = \left\{x_1^N\right\} = \{x_1, ..., x_N\}$ of length N the Lempel-Ziv Comlexity LZC calculated as follows. A block B of length l where $(1 \leq l \leq N)$ is a subsequence of l consecutive symbols from sequence s

$$B = \left\{x_i^{i+l-1}\right\} = \{x_i, ..., x_{i+l-1}\} \, (1 \leq i \leq N) \, . \tag{3.11}$$

The first block B_1 is equal to first symbol in the sequence s i.e. $B_1 = \{x_1\}$. The next block B_{k+1} defined to be the following consecutive block of minimal lenth such it does not occuew in sequence $\left\{x_1^{n_{k+1}-1}\right\}$

$$B_{k+1} = \left\{x_{n_k+1}^{n_{k+1}}\right\} (n_k + 1 \leq n_{k+1} \leq N. \tag{3.12}$$

By continuing this algorithm recursively until last symbol x_N is reached decomposition of sequence s into minimal number of blocks is obtained

$$s = B_1, ..., B_n. \tag{3.13}$$

The complexity C of X $C_\alpha(s)$ is defined as the number of blocks in the decomposition ($C = n$).

The normalised complexity of s is defined as

$$LZC = \frac{C_\alpha(x_1^N)}{N/log_\alpha N}, \tag{3.14}$$

where α denotes number of possible different symbols in s.

Permutation Entropy measures the randomness of the occurrence of symbols in a time series [7, 58]. The symbols are obtained by considering the rank order of signal samples in a fixed length sequence. Let the symbol length be 4. As an example, a sequence of signal values $x_4(t) = \{5, 9, 7, 3\}$ symbol $s =' 3021'$ as in this case $x(t+3) < x(t) < x(t+2) < x(t+1)$. All possible sequences of length 4 are considered and the probabilities p of occurrence of each of the 4! symbols are found. *Permutation Entropy* is calculated based on these probabilities according to the Shannon equation

$$PrmEn = -\sum_i p_i \log p_i. \tag{3.15}$$

3.2 The effect of the method used for power spectrum calculation on the spectral entropy measure

The problem discovered while comparing the entropy/complexity measures of the EEG signal – the dependence of *Spectral Entropy* on the length of the signal window – was investigated further in (**Publication II**). The aim was to test if this dependence was due to added information when incorporating more data or if it was due to the algorithm. The data set containing EEG recordings from 12 ICU

patients (age from 29 to 83 with the mean 63 years) with propofol as the sedative was used.

Four different schemes of the power spectrum estimation were compared in order to study the dependence of spectral entropy on data length:

Welch periodogram with averaging method A
The signal segment was divided into subsegments with 50% overlap. The subsegments were windowed using the Hamming window and the FFT was taken. The estimate of the power spectrum was obtained as the average of the FFTs of the subsegments. Four subsegment lengths: 1.25s, 2.5s, 5s and 10s. were used. The shorter the subsegment the more subsegments were incorporated into the average. The FFT size was increased together with the subsegment length. The results show that if the FFT size is varied, the obtained spectral entropy is highly dependent on the signal subsegment length over which the FFT is calculated.

Welch periodogram with averaging method B (the same as previous except that the FFT length was kept constant - 4096 samples) showed that power spectrum estimation dependence on data length is actually reversed.

In the third scheme of power spectrum estimation the *Autocorrelation* function was estimated first and power spectrum was obtained as the FFT of the Hamming-windowed middle part of the autocorrelation function. Four different window lengths were used for cutting the middle part of the autocorrelation function: 5s, 10s, 20s and 40s. The FFT size was equal to the window length. The dependence of the results on the window lenght was not eliminated as far as the FFT size changed together with the window length.

As the fourth method the power spectrum was estimated based on the coefficients of the *autoregressive* model. Model orders of 16, 32, 48 and 64 were used. The results show that if sufficiently high autoregressive model order is used, the obtained spectral entropy is fairly stable, not depending on the choice of the model order.

The results show that the entropy values obtained using autoregressive model coefficients are in the range of 0.75...0.87 while the other schemes give values in the range of approximately 0.5...0.7. Autoregressice model gives generally smoother power spectrum compared to the Welch periodogram averaging method. Thus the correlation between the smoothness of the power spectrum and the value of spectral entropy can be concluded. This behaviour can also be observed if constant FFT size is used in the case of Welch periodogram with averaging method B. The entropy value is higher for shorter subsegment lengths, corresponding to smoother power spectrum (shorter subsegments mean averaging over larger number of subsegment spectra).

As for all the calculation methods the amount of data available was equal we can conclude that the dependence of spectral entropy values on the length of the signal window is not caused by the variable amount of data available but rather the properties of the periodogram as the estimate of the power spectrum. Based on the results the autoregressive model based calculation scheme for spectral entropy

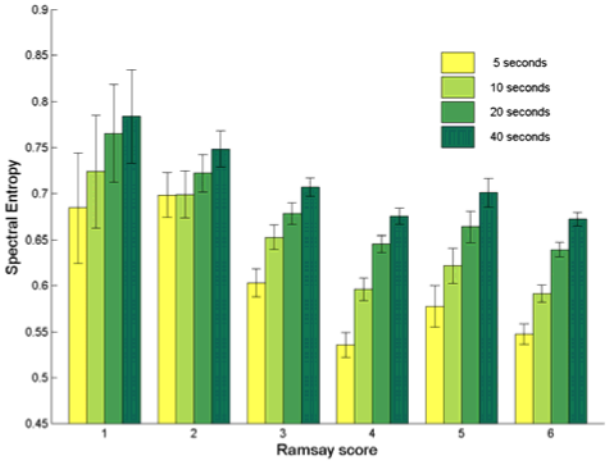

Figure 3.1: Spectral entropy (mean ± standard error) of 47 Hz low-pass filtered data for four window lengths (**Publication I**).

with models of order 32...48 can be suggested as the most stable with respect to data size.

It is important to note that the correlation of the entropy with depth of sedation was not affected by the choice of the method. This implies that as far as equal window lengths are used, the choice of the power spectrum estimation method is not critical.

3.3 The influence of the prefilter settings on the behavior of the entropy/complexity measures

In 2004 the feasibility of several entropy based algorithms were compared against clinically assessed levels of sedation. Some of the preliminary results were published in (**Publication I**). The results of more detailed study with introduction on surrogate analysis were published in (**Publication III**).

It is generally known that the EEG signal slows down becoming more regular and less complex as the subject becomes unconscious. For lighter leveles of sedation as in the ICU environment, changes in EEG can be quite different. As publisehd in (**Publication I**) and (**Publication III**) the study revealed that for light sedation leveles used in ICU entropy based algorithms struggle to match the depth of sedation assessed using clinical methods i.e. Ramsay scoring. The *Higuchi Fractal Dimension* algorithm gave the best discrimination between the light sedation leveles (Ramsay scores 2 – 4) while *relative β-ratio* was superior for deep sedation (Ramsay score 6). *Spectral Entropy* had reverse behavior for the sedation levels deeper than Ramsay score 4 (see Figure 3.1). The values of *Higuchi Fractal Dimension, Lempel-Ziv Complexity and Approximate Entropy* changed signifi-

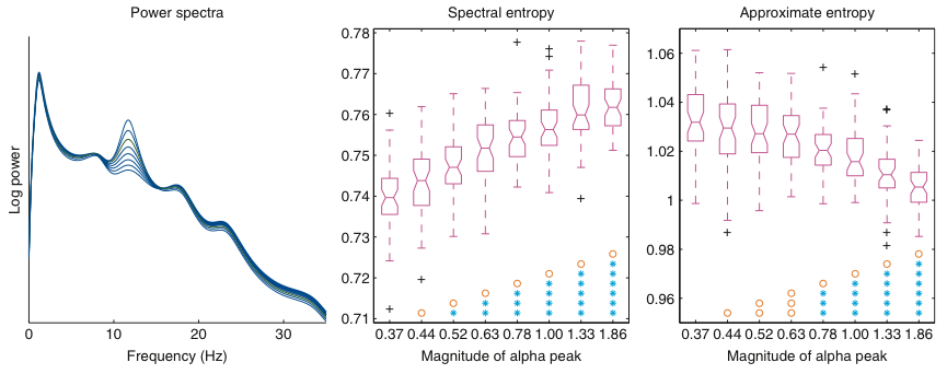

Figure 3.2: Sensitivity of spectral entropy and approximate entropy to rhythmic activity (**Publication V**).

cantly when higher frequencies were incorporated while *Spectral Entropy* was not very sensitive to the frequency content. On the other hand, the *Higuchi Fractal Dimension, Lempel-Ziv Complexity and Approximate Entropy* were insensitive to the window length while *Spectral Entropy* correlated highly with the length of the data.

All the methods seemed to have difficulty in discriminating Ramsay score 5. Our preliminary analysis using other data sets showed that this phenomenon is not related to the particular data set but is more general, indicating the need for further study. More comperhensive overview and analysis of results is presented in (**Publication III**).

3.4 Opposite behavior of the spectral entropy and approximate entropy measures in the case of developing alpha rhythm

To study the effect of increasingly rhythmic activity on *Spectral Entropy* and *Approximate Entropy* an EEG sample with spectral peak at about 11 Hz corresponding to the α-band was chosen. The signal was recorded from a patient in propofol anaesthesia. The amplitude of the rhythmic component was manipulated using the autoregressive moving average (ARMA) modelling technique to obtain test signals of similar spectral properties as the original EEG signal but of eight different proportions of the rhythmic activity.

The *Spectral Entropy* measure increased significantly with each increase in the peak level of the rhythmic activity (see Figure 3.2). The first three steps of increase in the α-band peak did not cause a significant change in the *Approximate Entropy*. However, the entropy decrease became significant with higher proportions of the rhythmic activity. The results show that *Spectral Entropy* increases significantly indicating the power spectrum becoming more flat and the signal more irregular when very low-frequency components (< 1.5 Hz) are present in the EEG signal. At

the same time *Approximate Entropy* decreases significantly (indicating the signal becoming more regular) when the EEG becomes more rhythmic.

4 SURROGATES IN EEG SIGNAL ANALYSIS

A surrogate can be defined as a substitute for something or a deputy. In signal analysis surrogates are mainly used to study certain properties of signals (or their underlying processes) or to test the sensitivity of certain methods to these properties. Here surrogate is a signal having similar properties to the original time series (i.e., the one whose surrogate is in question) except for a certain property to be tested. Probably the most common usage of surrogates is testing for nonlinearity by phase randomization. Linear processes are fully described by their second order statistics. As power spectrum is by definition the Fourier' transform of the autocorrelation function, it fully describes linear processes. Power spectrum, however, does not contain any phase information. Phase randomized surrogates are generated by taking the Fourier' transform of the original signal, randomizing the phase spectrum and taking the inverse Fourier' transform. If a signal measure cannot differentiate between the original signal and its phase randomized surrogates, the phase of the original signal does not carry any important information regarding this particular measure and can be considered as a realisation of a random phase.

There has been a lot of discussion on the linearity of the EEG signal [102, 46]. It has been found, for example, that in the case of epileptic patterns the EEG signal is highly non-linear while in other situations linear models might describe the signal quite well [55]. Quite obviously, the phase relations between the various rhythms present in the EEG signal are not random but reflect the complex synchronization patterns in neuronal networks. However, the phase relations might be too complex for our nonlinearity tests to sense.

4.1 Phase randomisation surrogates of the EEG signal in studying transition to burst suppression

The broad set of measures usually referred to as "entropy" and/or "complexity" actually reveal different properties of signals. While "classical" Shannon entropy is sensitive only to the amplitude distribution, *Spectral Entropy* depends purely on signal spectrum and the methods based on phase space and recurrence analysis are sensitive to both mentioned properties. To get even deeper insight into behaviour of different measures called entropy a case study was implemented. In the study described above we used EEG samples with known clinically assessed sedation level. Although Ramsay scoring is known to be inter-rater reliable [92] it still leaves room for human error.

In the present case study single EEG signal was used to compare behaviour of different entropy measures with known transition from continuous EEG to burst suppression in deep anaesthesia obtained from a 40 years old male patient undergoing a routine surgery. Propofol was used as the anaesthetic agent. The signal

was obtained from channel Cz-M2. The signal was prefiltered using a bandpass FIR filter with lower and upper cutoff frequencies of 0.5 and 35 Hz, respectively. The original sampling frequency was 20 kHz. Before applying the entropy algorithms the signal was downsampled to 100 Hz using appropriate anti-aliasing filtering.

To study the sensitivity of the measures to phase information in the signal, phase randomization as well as amplitude adjusted surrogates are also analyzed. *Spectral Entropy* was chosen as representative of entropy measures based purely on power spectrum of the signal. *Higuchi Fractal Dimension* (HDf)*, Approximate entropy* (ApEn) and *Sample entropy* (SmpEn), were chosen as entropy measured based on the phase space representation of the time series and *Permutation entropy* (PrmEn) was chosen over Lempel-Ziv Complexity as a measure based on occurrences of patterns in the time series.

In *surrogate analysis* some signal properties are fixed while others are varied to obtain a set of surrogate signals. If the response of an algorithm to the surrogates is similar to the response to the original signal it can be concluded that the algorithm is not sensitive to the properties of the signal varied in the surrogate generation process.

Surrogate data can be achieved using following algorithm:

1. Compute the Fourier transform (FT) of the original data;

2. Randomize the phases but keep the original absolute values of the Fourier coefficients (i.e., the spectrum);

3. Perform the inverse FT into the time domain.

Resulting surrogate data would have exactly the same spectrum as original data [69]. Phase randomization modifies the amplitude distribution of the time series towards Gaussian distribution with the consequence that the surrogate can be fully described by first and second order statistics. More realistic surrogates can be obtained by iteratively modifying the properties of a surrogate so that both the power spectrum as well as the amplitude distribution resemble that of the original signal as well as possible [87, 88] . In the study *IAAFT algorithm for surrogate generation* was used (**Publication IV**).

For each entropy measure the entropy of the original signal (blue curves), the average entropy of 10 phase-randomized surrogates (green curves), and the average entropy of 10 amplitude adjusted surrogates (red curves) were calculated. See Figure 4.1.

It was concluded that *Permutation Entropy* is highly sensitive while *Higuchi Fractal Dimension* is almost insensitive to phase information and nonlinearities in the signal. As power spectrum does not contain phase information, the three curves of *Spectral Entropy* are almost identical. For segments when the results for surrogates differ from those for the original signal, the IAAFT-surrogates give

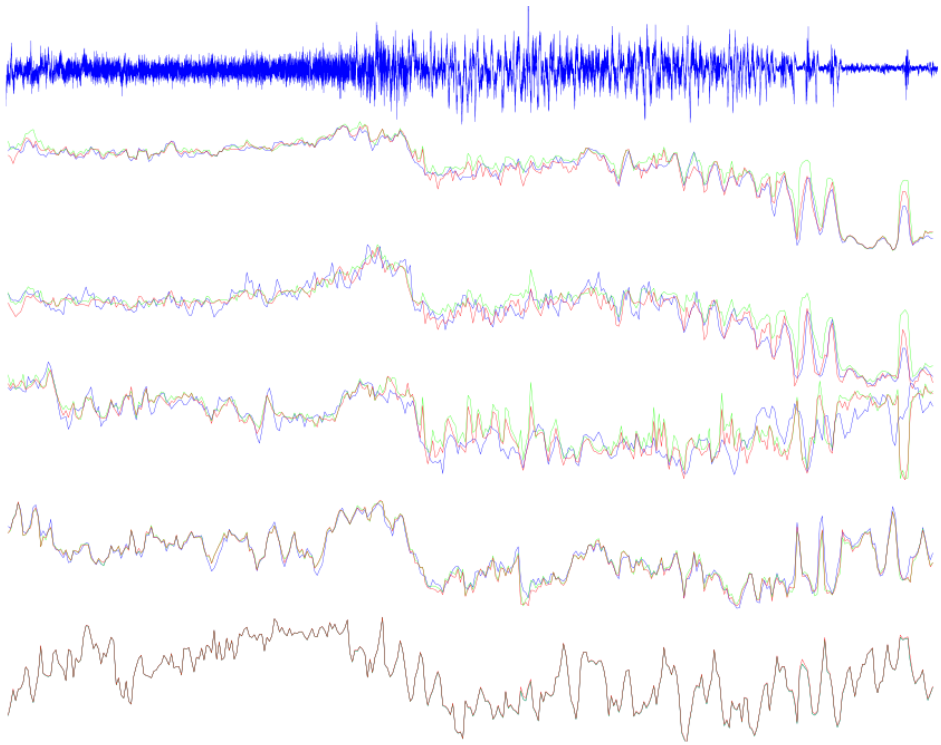

Figure 4.1: The original signal and the entropy measures (from top to bottom): *Approximate Entropy*, *Sample Entropy*, *Permutation Entropy*, *Higuchi Fractal Dimension*, and *Spectral Entropy* (**Publication IV**).

values between those for the the original signal and those for the phase randomisation surrogates (red curve lies between blue and green curves). The three curves disagree to greater extent during the period of high delta waves indicating higher degree of nonlinearities.

4.2 Spectral entropy surrogates in studying the propeties of entropy measures

The usefulness of the entropy measures in the assessment depth of sedation is commonly justified by the claims that the EEG becomes more regular with deepening anaesthesia and that these measures correctly quantify this increase in regularity. From all the entropy measures, only *Spectral Entropy* has been applied in commercial depth of anaesthesia monitors up to now. The aim of the study (**Publication V**) was to show that *Approximate Entropy* generally corresponds better to the visual impression of signal regularity as it takes into account the phase information in the EEG signal while *Spectral Entropy* relies solely on power spectrum of the signal.

To compare behaviour of two signal entropy estimation methods a set of surrogate signals was generated as follows.

The sawtooth waveform of 9995 samples was selected as the original signal corresponding to a 19.99s sample with sampled at rate 500Hz. The signal samples of identical *Spectral Entropy* were derived from original signal by

1. randomising the phase values of the Fourier transform of the original signal and applying inverse Fourier transform

2. relocating the amplitude values of the Fourier transform of the original signal around a dominant frequency and applying inverse Fourier transform

3. randomising the amplitude values of the Fourier transform of the original signal and applying inverse Fourier transform

4. relocating the amplitude values of the Fourier transform of the original signal in the same rank order as in the case of amplitude spectrum of an EEG signal segment recorded in deep propofol anaesthesia and applying inverse Fourier transform

The both *Spectral Entropy* and *Approximate Entropy* of all the signals was calculated. As the *Spectral Entropy* algorithm (3.1) does not consider phase information nor the exact location of the spectral values on the frequency axis of Fourier transform the resulting spectral entropy value for all generated signals was 0.24. *Approximate Entropy* on the other hand was calculated to have values ranging from 0.04 for sawtooth waveform to 2.02 for surrogate signals with randomised spectral components. The experiment shows that the waveforms characterised by the same *Spectral Entropy* value may look visually very different with the *Approximate Entropy* of the waveforms ranging from about 0 to above 2 being close to the value previously obtained for white noise of nearly uniform amplitude distribution (**Publication III**).

CONCLUSIONS

Monitoring brain function in the ICU by means of the EEG is becoming more feasible with advancements in the recording equipment as well as in the signal processing methods used for feature extraction and automated interpretation of the signal. The large variety of algorithms and methods proposed for this application in the literature or applied in commercial monitoring systems makes it difficult to evaluate the reliability of the results obtained.

The aim of this thesis was to study the impact of the mathematical background of selected algorithms of signal complexity and entropy on the capability of these algorithms to follow the change in patient condition in the ICU. Two main approaches were taken: firstly, the preprocessing settings and calculation paradigms of the algorithms were varied to describe how these changes affect the ability of the algorihtms to follow the outcome of clinical assessments of the patient state and secondly, surrogate analysis was applied to study the relevance of certain signal properties with respect to clinically significant changes in either the state of the patient or the visual appearance of the EEG.
The main findings of the research include:

- Prefilter settings (i.e., the bandwith of the signal) have significant impact on the performance of the entropy/complexity as measures of the depth of sedation; cutting off the high frequencies and extending the bandwitdth towards lower frequencies tends to reverse the relation between sedation depth and EEG entropy at light levels of sedation.

- Calculation paradigms like, for example, the windowing scheme and the method used for power spectrum estimation have significant impact on the spectral entropy measure.

- By calculating phase randomised surrogates it was shown that certain measures of signal complexity (*Permutation Entropy*, for example) are significantly more sensitive to the phase information (and thus the nonlinearities) in the signal than others (*Higuchi Fractal Dimension*, for example) in their ability to track the changes in the transition to burst suppression; by its definition the *Spectral Entropy* measure in insensitive to the phase information.

- Measures of signal complexity based on different mathematical backgrounds can behave in a contradictory manner; for example, *Spectral Entropy* and *Approximate Entropy* can change in different directions when alpha rhythm becomes dominant at certain level of anaesthesia.

- Signal Complexity measures do not necessarily correlate with the visual assessment of signal regularity; for example, the same *Spectral Entropy* value

can be obtained for almost regular and for a noise-like signal by manipulating the phase information in the signal.

The results of the thesis help clinicians to understand the background and the limits of the tools they are using on daily basis.

REFERENCES

[1] Aantaa, R., Kanto, J., Scheinin, M., Kallio, A., and Scheinin, H. Dexmedetomidine, an [alpha] 2-adrenoceptor agonist, reduces anesthetic requirements for patients undergoing minor gynecologic surgery. *Anesthesiology*, 73(2), pp. 230–235, 1990.

[2] Accardo, A., Affinito, M., Carrozzi, M., and Bouquet, F. Use of the fractal dimension for the analysis of electroencephalographic time series. *Biological Cybernetics*, 77(5), pp. 339–350, 1997.

[3] Agarwal, R., Gotman, J., Flanagan, D., and Rosenblatt, B. Automatic eeg analysis during long-term monitoring in the icu. *Electroencephalography and clinical Neurophysiology*, 107(1), pp. 44–58, 1998.

[4] Aitken, L. M., Marshall, A. P., Elliott, R., and McKinley, S. Critical care nurses' decision making: sedation assessment and management in intensive care. *Journal of clinical nursing*, 18(1), pp. 36–45, 2009.

[5] Amrein, R., Hetzel, W., Hartmann, D., and Lorscheid, T. Clinical pharmacology of flumazenil. *European journal of anaesthesiology. Supplement*, 2, pp. 65–80, 1987.

[6] Baldesi, O., Bruder, N., Velly, L., and Gouin, F. Spurious bispectral index values due to electromyographic activity. *European journal of anaesthesiology*, 21(04), pp. 324–325, 2004.

[7] Bandt, C. and Pompe, B. Permutation entropy: a natural complexity measure for time series. *Physical Review Letters*, 88(17), pp. 174102, 2002.

[8] Beers, R. and Camporesi, E. Remifentanil update. *CNS drugs*, 18(15), pp. 1085–1104, 2004.

[9] Berton, J., Sargentini, C., Nguyen, J.-L., Belii, A., and Beydon, L. Anaconda® reflection filter: Bench and patient evaluation of safety and volatile anesthetic conservation. *Anesthesia & Analgesia*, 104(1), pp. 130–134, 2007.

[10] Borel, C. and Hanley, D. Neurologic intensive care unit monitoring. *Critical care clinics*, 1(2), pp. 223, 1985.

[11] Breen, D., Karabinis, A., Malbrain, M., Morais, R., Albrecht, S., Jarnvig, I.-L., Parkinson, P., and Kirkham, A. Decreased duration of mechanical ventilation when comparing analgesia-based sedation using remifentanil with standard hypnotic-based sedation for up to 10 days in intensive care unit patients: a randomised trial [isrctn47583497]. *Critical care*, 9(3), pp. R200, 2005.

[12] Brook, A. D., Ahrens, T. S., Schaiff, R., Prentice, D., Sherman, G., Shannon, W., and Kollef, M. H. Effect of a nursing-implemented sedation protocol on the duration of mechanical ventilation. *Critical care medicine*, 27(12), pp. 2609–2615, 1999.

[13] Bruhn, J., Bouillon, T. W., and Shafer, S. L. Electromyographic activity falsely elevates the bispectral index. *Anesthesiology*, 92(5), pp. 1485, 2000.

[14] Carpenter, R. L., Eger, E. I., Johnson, B. H., Unadkat, J. D., Sheiner, L. B., et al. The extent of metabolism of inhaled anesthetics in humans. *Anesthesiology*, 65(2), pp. 201–205, 1986.

[15] Chamoun, N. G. An introduction to bispectral analysis for the electroencephalogram. *Journal of clinical monitoring*, 10(6), pp. 392–404, 1994.

[16] Clark, D., Hosick, E., Adam, N., Castro, A., Rosner, B., and Neigh, J. Neural effects of isoflurane (forane) in man. *Anesthesiology*, 39(3), pp. 261–270, 1973.

[17] Cohen, I. L., Gallagher, T. J., Pohlman, A. S., Dasta, J. F., Abraham, E., and Papadokos, P. J. Management of the agitated intensive care unit patient. *Critical Care Medicine*, 30(1), pp. S97–S123, 2002.

[18] Consales, G., Chelazzi, C., Rinaldi, S., and De Gaudio, A. Bispectral index compared to ramsay score for sedation monitoring in intensive care units. *Minerva anestesiologica*, 72(5), pp. 329, 2006.

[19] Dahaba, A. A., Mattweber, M., Fuchs, A., Zenz, W., Rehak, P. H., List, W. F., and Metzler, H. The effect of different stages of neuromuscular block on the bispectral index and the bispectral index-xp under remifentanil/propofol anesthesia. *Anesthesia & Analgesia*, 99(3), pp. 781–787, 2004.

[20] Dasgupta, M. and Dumbrell, A. C. Preoperative risk assessment for delirium after noncardiac surgery: a systematic review. *Journal of the American Geriatrics Society*, 54(10), pp. 1578–1589, 2006.

[21] De Deyne, C., Struys, M., Decruyenaere, J., Creupelandt, J., Hoste, E., and Colardyn, F. Use of continuous bispectral eeg monitoring to assess depth of sedation in icu patients. *Intensive care medicine*, 24(12), pp. 1294–1298, 1998.

[22] Dellinger, R. P., Levy, M. M., Carlet, J. M., Bion, J., Parker, M. M., Jaeschke, R., Reinhart, K., Angus, D. C., Brun-Buisson, C., Beale, R., et al. Surviving sepsis campaign: international guidelines for management of severe sepsis and septic shock: 2008. *Intensive care medicine*, 34(1), pp. 17–60, 2008.

[23] Detsch, O., Schneider, G., Kochs, E., Hapfelmeier, G., and Werner, C. Increasing isoflurane concentration may cause paradoxical increases in the eeg bispectral index in surgical patients. *British journal of anaesthesia*, 84(1), pp. 33–37, 2000.

[24] Devlin, J. W., Boleski, G., Mlynarek, M., Nerenz, D. R., Peterson, E., Jankowski, M., Horst, H. M., and Zarowitz, B. J. Motor activity assessment scale: a valid and reliable sedation scale for use with mechanically ventilated patients in an adult surgical intensive care unit. *Critical care medicine*, 27(7), pp. 1271–1275, 1999.

[25] Fàbregas, N., Gambús, P. L., Valero, R., Carrero, E. J., Salvador, L., Zavala, E., and Ferrer, E. Can bispectral index monitoring predict recovery of consciousness in patients with severe brain injury? *Anesthesiology*, 101(1), pp. 43–51, 2004.

[26] Frenzel, D., Greim, C.-A., Sommer, C., Bauerle, K., and Roewer, N. Is the bispectral index appropriate for monitoring the sedation level of mechanically ventilated surgical icu patients? *Intensive care medicine*, 28(2), pp. 178–183, 2002.

[27] Freye, E. Cerebral monitoring in the operating room and the intensive care unit—an introductory for the clinician and a guide for the novice wanting to open a window to the brain. *Cerebral Monitoring in the OR and ICU*, pp. 77–168, 2005.

[28] Girard, T. D., Kress, J. P., Fuchs, B. D., Thomason, J. W., Schweickert, W. D., Pun, B. T., Taichman, D. B., Dunn, J. G., Pohlman, A. S., Kinniry, P. A., et al. Efficacy and safety of a paired sedation and ventilator weaning protocol for mechanically ventilated patients in intensive care (awakening and breathing controlled trial): a randomised controlled trial. *The Lancet*, 371(9607), pp. 126–134, 2008.

[29] Glass, P. S., Bloom, M., Kearse, L., Rosow, C., Sebel, P., and Manberg, P. Bispectral analysis measures sedation and memory effects of propofol, midazolam, isoflurane, and alfentanil in healthy volunteers. *Anesthesiology*, 86(4), pp. 836–847, 1997.

[30] Gommers, D. and Bakker, J. Medications for analgesia and sedation in the intensive care unit: an overview. *Critical Care*, 12(Suppl 3), pp. S4, 2008.

[31] Greif, R., Greenwald, S., Schweitzer, E., Laciny, S., Rajek, A., Caldwell, J. E., and Sessler, D. I. Muscle relaxation does not alter hypnotic level during propofol anesthesia. *Anesthesia & Analgesia*, 94(3), pp. 604–608, 2002.

[32] Guérit, J.-M., Amantini, a., Amodio, P., Andersen, K. V., Butler, S., de Weerd, a., Facco, E., Fischer, C., Hantson, P., Jäntti, V., Lamblin, M.-D., Litscher, G., and Péréon, Y. Consensus on the use of neurophysiological tests in the intensive care unit (ICU): electroencephalogram (EEG), evoked potentials (EP), and electroneuromyography (ENMG). *Neurophysiologie clinique = Clinical neurophysiology*, 39(2), pp. 71–83, 2009.

[33] Gugino, L., Chabot, R., Prichep, L., John, E., Formanek, V., and Aglio, L. Quantitative eeg changes associated with loss and return of consciousness in healthy adult volunteers anaesthetized with propofol or sevoflurane. *British Journal of Anaesthesia*, 87(3), pp. 421–428, 2001.

[34] Haenggi, M., Ypparila-Wolters, H., Bieri, C., Steiner, C., Takala, J., Korhonen, I., and Jakob, S. Entropy and bispectral index for assessment of sedation, analgesia and the effects of unpleasant stimuli in critically ill patients: an observational study. *Critical Care*, 12(5), pp. R119, 2008.

[35] Haenggi, M., Ypparila-Wolters, H., Hauser, K., Caviezel, C., Takala, J., Korhonen, I., and Jakob, S. M. Intra-and inter-individual variation of bis-index® and entropy® during controlled sedation with midazolam/remifentanil and dexmedetomidine/remifentanil in healthy volunteers: an interventional study. *Critical Care*, 13(1), pp. R20, 2009.

[36] Hall, J. E., Uhrich, T. D., Barney, J. A., Arain, S. R., and Ebert, T. J. Sedative, amnestic, and analgesic properties of small-dose dexmedetomidine infusions. *Anesthesia & Analgesia*, 90(3), pp. 699–705, 2000.

[37] Henrie, J. R., Parkhouse, J., and Bickford, R. G. Alteration of human consciousness by nitrous oxide as assessed by electroencephalography and psychological tests. *Anesthesiology*, 22(2), pp. 247–259, 1961.

[38] Hering, W., Geisslinger, G., Kamp, H., Dinkel, M., Tschaikowsky, K., Rugheimer, E., and Brune, K. Changes in the eeg power spectrum after midazolam anaesthesia combined with racemic or s–(+) ketamine. *Acta anaesthesiologica scandinavica*, 38(7), pp. 719–723, 1994.

[39] Hernández-Gancedo, C., Pérez-Chrzanowska, H., and Martinez-Casanova, E. Comparing entropy and the bispectral index with the ramsay score in sedated icu patients. *Journal of clinical monitoring and computing*, 21(5), pp. 295–302, 2007.

[40] Higuchi, T. Approach to an irregular time series on the basis of the fractal theory. *Physica D: Nonlinear Phenomena*, 31(2), pp. 277–283, 1988.

[41] Hirota, K., Kubota, T., Ishihara, H., Matsuki, A., et al. The effects of nitrous oxide and ketamine on the bispectral index and 95% spectral edge frequency during propofol–fentanyl anaesthesia. *European journal of anaesthesiology*, 16(11), pp. 779, 1999.

[42] Hirsch, L. J. Brain monitoring: the next frontier of ICU monitoring. *Journal of clinical neurophysiology : official publication of the American Electroencephalographic Society*, 21(5), pp. 305–6, 2004.

[43] Hirsch, L. J. Continuous EEG monitoring in the intensive care unit: an overview. *Journal of clinical neurophysiology : official publication of the American Electroencephalographic Society*, 21(5), pp. 332–40, 2004.

[44] Hirsch, L. J., Brenner, R. P., Drislane, F. W., So, E., Kaplan, P. W., Jordan, K. G., Herman, S. T., LaRoche, S. M., Young, B., Bleck, T. P., Scheuer, M. L., and Emerson, R. G. The ACNS subcommittee on research terminology for continuous EEG

monitoring: proposed standardized terminology for rhythmic and periodic EEG patterns encountered in critically ill patients. *Journal of clinical neurophysiology : official publication of the American Electroencephalographic Society*, 22(2), pp. 128–35, 2005.

[45] Jacobi, J., Fraser, G. L., Coursin, D. B., Riker, R. R., Fontaine, D., Wittbrodt, E. T., Chalfin, D. B., Masica, M. F., Bjerke, H. S., Coplin, W. M., and Others. Clinical practice guidelines for the sustained use of sedatives and analgesics in the critically ill adult. *Critical care medicine*, 30(1), pp. 119–141, 2002.

[46] Jeleazcov, C., Fechner, J., and Schwilden, H. Electroencephalogram monitoring during anesthesia with propofol and alfentanil: the impact of second order spectral analysis. *Anesthesia & Analgesia*, 100(5), pp. 1365–1369, 2005.

[47] Jones, C., Griffiths, R. D., Humphris, G., and Skirrow, P. M. Memory, delusions, and the development of acute posttraumatic stress disorder-related symptoms after intensive care. *Critical care medicine*, 29(3), pp. 573–580, 2001.

[48] Jordan, D., Stockmanns, G., Kochs, E. F., Pilge, S., and Schneider, G. Electroencephalographic order pattern analysis for the separation of consciousness and unconsciousness: an analysis of approximate entropy, permutation entropy, recurrence rate, and phase coupling of order recurrence plots. *Anesthesiology*, 109(6), pp. 1014–22, 2008.

[49] Karabinis, A., Mandragos, K., Stergiopoulos, S., Komnos, A., Soukup, J., Speelberg, B., and Kirkham, A. J. Safety and efficacy of analgesia-based sedation with remifentanil versus standard hypnotic-based regimens in intensive care unit patients with brain injuries: a randomised, controlled trial [isrctn50308308]. *Critical Care*, 8(4), pp. R268, 2004.

[50] Kollef, M. H., Levy, N. T., Ahrens, T. S., Schaiff, R., Prentice, D., and Sherman, G. The use of continuous iv sedation is associated with prolongation of mechanical ventilation. *CHEST Journal*, 114(2), pp. 541–548, 1998.

[51] Kong, K. L., Willatts, S. M., and Prys-Roberts, C. Isoflurane compared with midazolam for sedation in the intensive care unit. *BMJ: British Medical Journal*, 298(6683), pp. 1277, 1989.

[52] Kress, J. P., Pohlman, A. S., O'Connor, M. F., and Hall, J. B. Daily interruption of sedative infusions in critically ill patients undergoing mechanical ventilation. *New England Journal of Medicine*, 342(20), pp. 1471–1477, 2000.

[53] Kwon, M.-Y., Lee, S.-Y., Kim, T.-Y., Kim, D. K., Lee, K.-M., Woo, N.-S., Chang, Y.-J., and Lee, M. Spectral entropy for assessing the depth of propofol sedation. *Korean journal of anesthesiology*, 62(3), pp. 234–239, 2012.

[54] LeBlanc, J. M., Dasta, J. F., and Kane-Gill, S. L. Role of the bispectral index in sedation monitoring in the icu. *The Annals of pharmacotherapy*, 40(3), pp. 490–500, 2006.

[55] Lehnertz, K., Andrzejak, R. G., Arnhold, J., Kreuz, T., Mormann, F., Rieke, C., Widman, G., and Elger, C. E. Nonlinear eeg analysis in epilepsy: Its possible use for interictal focus localization, seizure anticipation, and. *Journal of Clinical Neurophysiology*, 18(3), pp. 209–222, 2001.

[56] Lempel, A. and Ziv, J. On the complexity of finite sequences. *Information Theory, IEEE Transactions on*, 22(1), pp. 75–81, 1976.

[57] Leslie, K., Sessler, D. I., Schroeder, M., and Walters, K. Propofol blood concentration and the bispectral index predict suppression of learning during propofol/epidural anesthesia in volunteers. *Anesthesia & Analgesia*, 81(6), pp. 1269–1274, 1995.

[58] Li, X., Cui, S., and Voss, L. J. Using permutation entropy to measure the electroencephalographic effects of sevoflurane. *Anesthesiology*, 109(3), pp. 448–456, 2008.

[59] Lipping, T. and Anier, A. System for analysis of polygraphic recordings of physiological signals in european data format. *Engineering. Proceedings of the Estonian Academy of Sciences*, 4, pp. 304 – 311, 1999.

[60] Liu, J., Singh, H., and White, P. F. Electroencephalogram bispectral analysis predicts the depth of midazolam-induced sedation. *Anesthesiology*, 84(1), pp. 64–69, 1996.

[61] Maksimow, A., Snapir, A., Särkelä, M., Kentala, E., Koskenvuo, J., Posti, J., Jääskeläinen, S., Hinkka-Yli-Salomäki, S., Scheinin, M., and Scheinin, H. Assessing the depth of dexmedetomidine-induced sedation with electroencephalogram (eeg)-based spectral entropy. *Acta anaesthesiologica scandinavica*, 51(1), pp. 22–30, 2007.

[62] Martin, E., Ramsay, G., Mantz, J., and Sum-Ping, S. J. The role of the α2-adrenoceptor agonist dexmedetomidine in postsurgical sedation in the intensive care unit. *Journal of intensive care medicine*, 18(1), pp. 29–41, 2003.

[63] Martin, J., Parsch, A., Franck, M., Wernecke, K. D., Fischer, M., and Spies, C. Practice of sedation and analgesia in german intensive care units: results of a national survey. *Critical Care*, 9(2), pp. R117, 2005.

[64] McArdle, P. Intravenous analgesia. *Critical care clinics*, 15(1), pp. 89–104, 1999.

[65] Mehta, S., Burry, L., Fischer, S., Martinez-Motta, J. C., Hallett, D., Bowman, D., Wong, C., Meade, M. O., Stewart, T. E., Cook, D. J., et al. Canadian survey of the use of sedatives, analgesics, and neuromuscular blocking agents in critically ill patients*. *Critical care medicine*, 34(2), pp. 374–380, 2006.

[66] Millane, T., Bennett, E., and Grounds, R. Isoflurane and propofol for long-term sedation in the intensive care unit. *Anaesthesia*, 47(9), pp. 768–774, 1992.

[67] Nasraway Jr, S. A., Wu, E. C., Kelleher, R. M., Yasuda, C. M., and Donnelly, A. M. How reliable is the bispectral index in critically ill patients? a prospective, comparative, single-blinded observer study*. *Critical care medicine*, 30(7), pp. 1483–1487, 2002.

[68] Olson, D. M., Zomorodi, M. G., James, M. L., Cox, C. E., Moretti, E. W., Riemen, K. E., and Graffagnino, C. Exploring the impact of augmenting sedation assessment with physiologic monitors. *Australian Critical Care*, 2013.

[69] Paluš, M. Testing for nonlinearity using redundancies: Quantitative and qualitative aspects. *Physica D: Nonlinear Phenomena*, 80, pp. 186–205, 1995.

[70] Park, G., Lane, M., Rogers, S., and Bassett, P. A comparison of hypnotic and analgesic based sedation in a general intensive care unit. *British journal of anaesthesia*, 98(1), pp. 76–82, 2007.

[71] Petty, T. Suspended life or extending death? *Chest*, 114, pp. 360–1, 1998.

[72] Pincus, S. M. Approximate entropy as a measure of system complexity. *Proceedings of the National Academy of Sciences*, 88(6), pp. 2297–2301, 1991.

[73] Plaschke, K., Hill, H., Engelhardt, R., Thomas, C., Von Haken, R., Scholz, M., Kopitz, J., Bardenheuer, H., Weisbrod, M., and Weigand, M. Eeg changes and serum anticholinergic activity measured in patients with delirium in the intensive care unit. *Anaesthesia*, 62(12), pp. 1217–1223, 2007.

[74] Plum, F. and Posner, J. B. *The Diagnosis Of Stupor & Coma*, volume 19. Oxford University Press, 1982.

[75] Prien, T. and Reinhardt, C. History of the development of intensive care medicine in germany. general considerations. 14. vegetative blockade and analgesic sedation]. *Der Anaesthesist*, 49(2), pp. 130, 2000.

[76] Puri, G. Paradoxical changes in bispectral index during nitrous oxide administration. *British journal of anaesthesia*, 86(1), pp. 141–142, 2001.

[77] Rampil, I. J., Kim, J.-S., Lenhardt, R., Negishi, C., and Sessler, D. I. Bispectral eeg index during nitrous oxide administration. *Anesthesiology*, 89(3), pp. 671–677, 1998.

[78] Ramsay, M., Savege, T., Simpson, B., and Goodwin, R. Controlled sedation with alphaxalone-alphadolone. *British medical journal*, 2(5920), pp. 656, 1974.

[79] Rautee, R., Sampson, T., Sarkela, M., Melto, S., Hovilehto, S., and van Gils, M. Application of spectral entropy to eeg and facial emg frequency bands for the assessment of level of sedation in icu. In *Engineering in Medicine and Biology Society, 2004. IEMBS'04. 26th Annual International Conference of the IEEE*, volume 2, IEEE, pp. 3481–3484, 2004.

[80] Richards, G., Schock, P., and Haefely, W. Benzodiazepine receptors: new vistas. *Seminars in Neuroscience*, 3(3), pp. 191 – 203. <ce:title>GABA and Inhibitory Synaptic Transmission in the Brain</ce:title>, 1991.

[81] Riker, R. R., Picard, J. T., and Fraser, G. L. Prospective evaluation of the sedation-agitation scale for adult critically ill patients. *Critical care medicine*, 27(7), pp. 1325–1329, 1999.

[82] Rowe, K. and Fletcher, S. Sedation in the intensive care unit. *Continuing Education in Anaesthesia, Critical Care and Pain*, 8(2), pp. 50–55, 2008.

[83] Rozendaal, F. W., Spronk, P. E., Snellen, F. F., Schoen, A., van Zanten, A. R., Foudraine, N. A., Mulder, P. G., and Bakker, J. Remifentanil-propofol analgo-sedation shortens duration of ventilation and length of icu stay compared to a conventional regimen: a centre randomised, cross-over, open-label study in the netherlands. *Intensive care medicine*, 35(2), pp. 291–298, 2009.

[84] Sackey, P., Radell, P., Granath, F., and Martling, C. Bispectral index as a predictor of sedation depth during isoflurane or midazolam sedation in icu patients. *Anaesthesia and intensive care*, 35(3), pp. 348–356, 2007.

[85] Sackey, P. V. et al. Frontal eeg for intensive care unit sedation: treating numbers or patients? *Crit Care*, 12(5), pp. R119, 2008.

[86] Sackey, P. V., Martling, C.-R., Granath, F., and Radell, P. J. Prolonged isoflurane sedation of intensive care unit patients with the anesthetic conserving device. *Critical care medicine*, 32(11), pp. 2241–2246, 2004.

[87] Schreiber, T. and Schmitz, A. Improved Surrogate Data for Nonlinearity Tests. *Physical Review Letters*, 77(4), pp. 635–638, 1996.

[88] Schreiber, T. and Schmitz, A. Surrogate time series. *Physica D: Nonlinear Phenomena*, 142(3-4), pp. 346–382, 2000.

[89] Sessler, C. N. Sedation scales in the icu. *Chest Journal*, 126(6), pp. 1727–1730, 2004.

[90] Sessler, C. N., Gosnell, M. S., Grap, M. J., Brophy, G. M., O'Neal, P. V., Keane, K. A., Tesoro, E. P., and Elswick, R. The richmond agitation–sedation scale: validity and reliability in adult intensive care unit patients. *American journal of respiratory and critical care medicine*, 166(10), pp. 1338–1344, 2002.

[91] Sessler, C. N., Grap, M. J., Brophy, G. M., and Others. Multidisciplinary management of sedation and analgesia in critical care. In *Seminars in respiratory and critical care medicine*, volume 22, pp. 211–226, 2001.

[92] Sessler, C. N., Grap, M. J., and Ramsay, M. A. Evaluating and monitoring analgesia and sedation in the intensive care unit. *Critical Care*, 12 Suppl 3, pp. S2, 2008.

[93] Shapiro, B. A., Warren, J., Egol, A. B., Greenbaum, D. M., Jacobi, J., Nasraway, S. A., Schein, R. M., Spevetz, A., and Stone, J. R. Practice parameters for intravenous analgesia and sedation for adult patients in the intensive care unit: an executive summary. *Critical care medicine*, 23(9), pp. 1596–1600, 1995.

[94] Sharma, A., Singh, P. M., Trikha, A., Rewari, V., et al. Entropy correlates with richmond agitation sedation scale in mechanically ventilated critically ill patients. *Journal of clinical monitoring and computing*, pp. 1–9, 2013.

[95] Simmons, L. E., Riker, R. R., Prato, B. S., and Fraser, G. L. Assessing sedation during intensive care unit mechanical ventilation with the bispectral index and the sedation-agitation scale. *Critical care medicine*, 27(8), pp. 1499–1504, 1999.

[96] Singh, H. Bispectral index (bis) monitoring during propofol-induced sedation and anaesthesia. *European journal of anaesthesiology*, 16(01), pp. 31–36, 1999.

[97] Sleigh, J. W., Steyn-Ross, D. A., Steyn-Ross, M. L., Williams, M., and Smith, P. Comparison of changes in electroencephalographic measures during induction of general anaesthesia: influence of the gamma frequency band and electromyogram signal. *British journal of anaesthesia*, 86(1), pp. 50–58, 2001.

[98] Soliman, H., Melot, C., and Vincent, J.-L. Sedative and analgesic practice in the intensive care unit: the results of a european survey. *British Journal of Anaesthesia*, 87(2), pp. 186–192, 2001.

[99] Soukup, J., Schärff, K., Kubosch, K., Pohl, C., Bomplitz, M., and Kompardt, J. State of the art: sedation concepts with volatile anesthetics in critically ill patients. *Journal of critical care*, 24(4), pp. 535–544, 2009.

[100] Soukup, J., Selle, A., Wienke, A., Steighardt, J., Wagner, N.-M., and Kellner, P. Efficiency and safety of inhalative sedation with sevoflurane in comparison to an intravenous sedation concept with propofol in intensive care patients: study protocol for a randomized controlled trial. *Trials*, 13(1), pp. 135, 2012.

[101] Spencer, E. and Willatts, S. Isoflurane for prolonged sedation in the intensive care unit; efficacy and safety. *Intensive care medicine*, 18(7), pp. 415–421, 1992.

[102] Stêpieñ, R. A. Testing for non-linearity in eeg signal of healthy subjects. *Acta neurobiologiae experimentalis*, 62(4), pp. 277–282, 2002.

[103] Strøm, T. and Toft, P. Time to wake up the patients in the icu: a crazy idea or common sense? *Minerva anestesiologica*, 77(1), pp. 59, 2011.

[104] Struys, M., Versichelen, L., Byttebier, G., Mortier, E., Moerman, A., and Rolly, G. Clinical usefulness of the bispectral index for titrating propofol target effect-site concentration. *Anaesthesia*, 53(1), pp. 4–12, 1998.

[105] Szumita, P. M., Baroletti, S. A., Anger, K. E., and Wechsler, M. E. Sedation and analgesia in the intensive care unit: evaluating the role of dexmedetomidine. *American journal of health-system pharmacy*, 64(1), pp. 37–44, 2007.

[106] Takamatsu, I., Ozaki, M., and Kazama, T. Entropy indices vs the bispectral index™ for estimating nociception during sevoflurane anaesthesia. *British journal of anaesthesia*, 96(5), pp. 620–626, 2006.

[107] Tanios, M. A., de Wit, M., Epstein, S. K., and Devlin, J. W. Perceived barriers to the use of sedation protocols and daily sedation interruption: a multidisciplinary survey. *Journal of critical care*, 24(1), pp. 66–73, 2009.

[108] Tipps, L. B., Coplin, W. M., Murry, K. R., and Rhoney, D. H. Safety and feasibility of continuous infusion of remifentanil in the neurosurgical intensive care unit. *Neurosurgery*, 46(3), pp. 596–602, 2000.

[109] Tonner, P. H., Paris, A., and Scholz, J. Monitoring consciousness in intensive care medicine. *Best Practice & Research Clinical Anaesthesiology*, 20(1), pp. 191–200, 2006.

[110] Tribl, G., Howorka, K., Heger, G., Anderer, P., Thoma, H., and Zeitlhofer, J. Eeg topography during insulin-induced hypoglycemia in patients with insulin-dependent diabetes mellitus. *European neurology*, 36(5), pp. 303–309, 1996.

[111] Venn, R., Bryant, A., Hall, G., and Grounds, R. Effects of dexmedetomidine on adrenocortical function, and the cardiovascular, endocrine and inflammatory responses in post-operative patients needing sedation in the intensive care unit. *British journal of anaesthesia*, 86(5), pp. 650–656, 2001.

[112] Venn, R., Newman, P., and Grounds, R. A phase ii study to evaluate the efficacy of dexmedetomidine for sedation in the medical intensive care unit. *Intensive care medicine*, 29(2), pp. 201–207, 2003.

[113] Venn, R. M., Hell, J., and Grounds, R. M. Respiratory effects of dexmedetomidine in the surgical patient requiring intensive care. *Critical Care*, 4(5), pp. 302, 2000.

[114] Vereecke, H., Struys, M., and Mortier, E. A comparison of bispectral index and arx-derived auditory evoked potential index in measuring the clinical interaction between ketamine and propofol anaesthesia. *Anaesthesia*, 58(10), pp. 957–961, 2003.

[115] Viertiö-Oja, H., Maja, V., Särkelä, M., Talja, P., Tenkanen, N., Tolvanen-Laakso, H., Paloheimo, M., Vakkuri, A., Yli-Hankala, A., and Meriläinen, P. Description of the entropy™ algorithm as applied in the datex-ohmeda s/5™ entropy module. *Acta Anaesthesiologica Scandinavica*, 48(2), pp. 154–161, 2004.

[116] Vivien, B., Di Maria, S., Ouattara, A., Langeron, O., Coriat, P., and Riou, B. Overestimation of bispectral index in sedated intensive care unit patients revealed by administration of muscle relaxant. *Anesthesiology*, 99(1), pp. 9–17, 2003.

[117] Vivien, B., Langeron, O., and Riou, B. Increase in bispectral index (bis) while correcting a severe hypoglycemia. *Anesthesia & Analgesia*, 95(6), pp. 1824–1825, 2002.

[118] Vivien, B., Paqueron, X., Le Cosquer, P., Langeron, O., Coriat, P., and Riou, B. Detection of brain death onset using the bispectral index in severely comatose patients. *Intensive care medicine*, 28(4), pp. 419–425, 2002.

[119] Wacker, P., Nunes, P. V., Cabrita, H., and Forlenza, O. V. Post-operative delirium is associated with poor cognitive outcome and dementia. *Dementia and geriatric cognitive disorders*, 21(4), pp. 221–227, 2006.

[120] Walsh, T. S., Ramsay, P., and Kinnunen, R. Monitoring sedation in the intensive care unit: can "black boxes" help us? *Intensive care medicine*, 30(8), pp. 1511–1513, 2004.

[121] Walsh, T. S., Ramsay, P., Lapinlampi, T. P., Särkelä, M. O., Viertiö-Oja, H. E., and Meriläinen, P. T. An assessment of the validity of spectral entropy as a measure of sedation statein mechanically ventilated critically ill patients. *Intensive care medicine*, 34(2), pp. 308–315, 2008.

[122] Watling, S., Dasta, J., and Seidl, E. Sedatives, analgesics, and paralytics in the icu. *The Annals of pharmacotherapy*, 31(2), pp. 148–153, 1997.

[123] Wu, C.-C., Lin, C.-S., and Mok, M. S. Bispectral index monitoring during hypoglycemic coma. *Journal of clinical anesthesia*, 14(4), pp. 305–306, 2002.

[124] Yaman, F., Ozcan, N., Ozcan, A., Kaymak, C., and Basar, H. Assesment of correlation between bispectral index and four common sedation scales used in

mechanically ventilated patients in icu. *Eur Rev Med Pharmacol Sci*, 16(5), pp. 660–666, 2012.

4.3 Author's publications

I **Anier, A**., Lipping, T., Melto, S. and Hovilehto, S. Higuchi Fractal Dimension and Spectral Entropy as Measures of Depth of Sedation in Intensive Care Unit. *Engineering in Medicine and Biology Society, 2004. IEMBS'04. 26th Annual International Conference of the IEEE,* 1, pp. 526-529, 2004.

II Lipping, T., Ferenets, R., **Anier, A**., Melto, S. and Hovilehto, S. Power spectrum estimation in the calculation of spectral entropy to assess depth of sedation. *IFMBE Proc,* 11(1), 4p, 2005.

III Ferenets, R., Lipping, T., **Anier, A**., Jäntti, V., Melto, S. and Hovilehto, S. Comparison of Entropy and Complexity Measures for the Assessment of Depth of Sedation. *IEEE Transactions on Biomedical Engineering,* 53(6), pp. 1067-1077, 2006.

IV **Anier, A**., Lipping, T., Jäntti, V., Puumala, P. and Huotari, A-M. Entropy of the EEG in transition to burst suppression in deep anaesthesia: surrogate analysis. *Engineering in Medicine and Biology Society (EMBC), 2010 Annual International Conference of the IEEE,* pp. 2790-2793, 2010.

V **Anier, A**., Lipping, T., Ferenets, R., Puumala, P., Sonkajärvi, E., Rätsep, I. and Jäntti, V. Relationship between approximate entropy and visual inspection of irregularity in the EEG signal, a comparison with spectral entropy. *British journal of anaesthesia,* 109(6), pp. 928-934, 2012.

4.4 List of author's publications related to the thesis

1. Lipping, T. and **Anier, A**. System For Analysis Of Polygraphic Recordings Of Physiological Signals In European Data Format. *Engineering. Proceedings of the Estonian Academy of Sciences,* 4, pp. 304 - 311, 1999.

2. Lipping, T., **Anier, A.**, Ratsep, I., Kleemann, P., Toome, V. and Jantti, V. Tracking rhythm in long-term EEG recordings using empirical mode calculation. *Engineering in Medicine and Biology Society, 2008. EMBS 2008. 30th Annual International Conference of the IEEE,* pp. 3604-3607, 2008.

KOKKUVÕTE

Elektroentsefalogrammi komplekssuse hindamine aju monitooringul intensiivravis

Esitatud uurimistöö põhiliseks eesmärgiks oli uurida valitud EEG signaali komplekssuse ja entroopia algoritmide matemaatilise tausta mõju nende võimele järgida intensiivravi patsientide seisundi muutuseid. Tulemuse saamiseks kasutati kahte lähenemisviisi: esiteks uuriti signaali eeltöötluse ja algoritmide realiseerimise paradigmade mõju algoritmide võimele järgida patsiendi seisundi kliinilise hindamise tulemusi; teiseks kasutati surrogaatanalüüsi uurimaks EEG signaali teatud omaduste (näiteks faasiinformatsioon) olulisust kliiniliselt oluliste muutuste tuvastamisel või signaali visuaalse kuju hindamisel.

Töö esimeses osas käsitleti anesteesia sügavuse hindamise põhiprintsiipe. Kirjeldati peamistest anesteetikumidest tingitud muutusi inimese EEG-s ning kuidas kommertsiaalsetes anesteesia sügavuse hindamise seadmetes kasutusele võetud algoritmid kasutavad neid muutusi hindamaks anesteesia sügavust.

Töö teises osas keskenduti EEG signaali komplekssuse hindamisel põhinevatele meetoditele. Esitati tööde tulemused, mis uurisid EEG signaali võimsusspektri hindamiseks kasutatava meetodi mõju arvutatud spektraalentroopia väärtusele, signaalile rakendatavate digitaalsete filtrite parameetrite mõju komplekssuse ja entroopia algoritmidele ning osutati, et spektraalentroopia ja aproksimaatne entroopia käituvad vastandlikult alfa-rütmi osakaalu muutumisel EEG signaalis.

Töö kolmandas osas esitati entroopia / komplekssuse algoritmide oluliste parameetrite surrogaatanalüüsi tulemusi.

Töö peamised tulemused on järgmised:

- Eelfiltri määrangud mõjutavad oluliselt entroopia / komplekssuse algoritmide võimet järgida anesteesia sügavuse muutumist; kõrgemate sageduste eemaldamine ja madalamate sageduste kaasamine põhjustab EEG signaali entroopia / komplekssuse ja anesteesia sügavuse vahelise seose inversiooni.

- Algoritmide realiseerimise paradigmad nagu akna-funktsiooni kasutamine ja EEG signaali võimsusspektri hindamiseks kasutatava algoritmi valik mõjutavad oluliselt arvutatud spektraalentroopia väärtust.

- Faas-randomiseeritud surrogaatide abil näidati, et mõned signaali komplekssuse hindamise algoritmid (näiteks permutatsioonientroopia) on oluliselt tundlikumad signaalis sisalduvale faasiinformatsioonile (ja seega mittelineaarsustele) kui teised (näiteks Higuchi fraktaaldimensioon) ning annavad sellest tulenevalt teatud anesteesia sügavustel EEG signaali komplekssuse hindamisel erinevaid tulemusi.

- Erinevatele matemaatilistele alustele toetuvad signaali komplekssuse hindamise algoritmid võivad teatud tingimustel anda vasturääkivaid tulemusi, näiteks muutuvad spektraalentroopia ja approksimaatne entroopia α-rütmi domineerimise korral teatud anesteesia sügavusel erinevates suundades.
- Signaali komplekssuse algoritmilise hindamise tulemused ei pruugi korreleeruda signaali komplekssuse visuaalsete hinnangutega. Manipuleerides faasiinformatsiooniga on võimalik saavutada visuaalselt väga erinevaid signaale sama spektraalentroopia mõõduga.

ABSTRACT

Estimation of the Complexity of the Electroencephalogram for Brain Monitoring in Intensive Care

The main goal of the research presented in this thesis was to study the impact of the mathematical background of selected algorithms of signal complexity and entropy on the capability of these algorithms to follow the changes in patient condition in the ICU. Two main approaches were taken: firstly, the preprocessing settings and calculation paradigms of the algorithms were varied to describe how these changes affect the ability of the algorihtms to follow the outcome of clinical assessments of the patient state and secondly, surrogate analysis was applied to study the relevance of certain signal properties with respect to clinically significant changes in either the state of the patient or the visual appearance of the EEG.

In the first part of the thesis the basic principles of assessing the level of sedation are discussed. The effect of common anaesthetic agents to human EEG are explained followed by an explanation of the methods applied in commercial anaesthesia monitors to detect these changes and estimate the level of sedation as a result.

In the second part of the thesis EEG signal complexity based methods are studied in-depth. Three studies are presented explaining the effect of the method used for power spectrum calculation on the spectral entropy measure, indicating the influence of the prefilter settings on the behavior of the entropy/complexity measures and showing the opposite behaviour of the spectral entropy and approximate entropy measures in the case of developing alpha rhythm.

In the third part entropy/complexity measures are studied further in their limits using surrogate analysis.

The main findings of the research include:

- Prefilter settings (i.e., the bandwith of the signal) has significant impact on the performance of the entropy/complexity as measures of the depth of sedation; cutting off the high frequencies and extending the bandwitdth towards lower frequencies tends to reverse the relation between sedation depth and EEG entropy at light levels of sedation.

- Calculation paradigms like, for example, the windowing scheme and the method used for power spectrum estimation have significant impact on the spectral entropy measure.

- By calculating phase randomised surrogates it was shown that certain measures of signal complexity (permutation entropy, for example) are significantly more sensitive to the phase information (and thus the nonlinearities)

in the signal than others (Higuchi fractal dimension, for example) and differ in their ability to track the changes in the transition to burst suppression; by its definition the spectral entropy measure in insensitive to the phase information.

- Measures of signal complexity based on different mathematical backgrounds can behave in a contradictory manner; for example, spectral entropy and approximate entropy change in different directions when alpha rhythm becomes dominant at certain level of anaesthesia.
- Signal complexity measures do not necessarily correlate with the visual assessment of signal regularity; for example, the same spectral entropy value can be obtained for almost regular and for a noise-like signal by manipulating the phase information in the signal.

PUBLICATONS

Publication I

Anier, A., Lipping, T., Melto, S. and Hovilehto, S. Higuchi Fractal Dimension and Spectral Entropy as Measures of Depth of Sedation in Intensive Care Unit. *Engineering in Medicine and Biology Society, 2004. IEMBS'04. 26th Annual International Conference of the IEEE,* 1, pp. 526-529, 2004.

Higuchi Fractal Dimension and Spectral Entropy as Measures of Depth of Sedation in Intensive Care Unit

A. Anier[1], T. Lipping[2], S. Melto[3], S. Hovilehto[3]
[1]Centre for Biomedical Engineering, Tallinn Technical University, Tallinn, Estonia
[2]Department of Information Technology, Tampere University of Technology, Pori, Finland
[3]Department of Intensive Care Unit, South Karelia Central Hospital, Lappeenranta, Finland

Abstract—**The ability of two easy-to-calculate nonlinear parameters, the Higuchi fractal dimension (HD_f) and spectral entropy, to follow the depth of sedation in the Intensive Care Unit is assessed. For comparison, the relative beta ratio is calculated. The results are evaluated using clinical assessment of the Ramsay score. The results show that the HD_f discriminates well between Ramsay scores 2-4 while beta ratio is superior for deeper levels of sedation. The value of the HD_f correlates highly with the cutoff frequency of the low-pass prefilter while spectral entropy is sensitive to the length of the analysis window.**

Keywords—**Higuchi fractal dimension, spectral entropy, beta ratio, depth of sedation**

I. Introduction

The assessment of the depth of anesthesia using the EEG signal has been an active research area for the last decade. Several systems and methods like the Bispectral Index Score, the Patient State Index, the Spectral Entropy Measure, the Narcotrend system etc. have been developed [1-4]. Each method has certain advantages and drawbacks, however, all of them seem to work in a satisfactory manner in most cases if surgical anesthesia levels are considered.

The situation is much more complicated in the Intensive Care Unit (ICU). In addition to the sedative drugs several other factors like various medication and the condition of the patient have influence on the EEG signal. Also, the environment in the ICU is hostile from the point of view of EEG measurement. Various kinds of equipment are used causing artifacts in the signal and patients might be agitated. Due to these reasons the measures of the depth of anesthesia used in the operating room often fail in the ICU.

The aim of this paper is to evaluate the ability of the Higuchi fractal dimension (HD_f) calculated from the EEG signal to follow the depth of sedation in ICU environment. We compare the performance of the HD_f with that of spectral entropy and beta ratio. The influence of the cutoff frequency of the low-pass prefilter and the window length on the behavior of the parameters is also assessed.

The algorithm of the Higuchi fractal dimension was proposed in [5]. Its applicability to EEG signal analysis has been thoroughly studied in [6]. In contrast to conventional methods for the estimation of fractal dimension in state space, the HD_f can be calculated directly in time domain and is therefore simple and fast. It has also been found to give reliable estimates for samples as short as 150-500 data points. Our results confirm that the HD_f is independent of the length of the signal segment. The application of the HD_f for the assessment of the depth of sedation is based on the hypothesis that the signal complexity decreases with deepening level of sedation.

The concept of spectral entropy based on the peaks of the Fourier spectrum as a measure of regularity was introduced by Powell and Percival in 1979 [7]. For the purpose of anesthesia monitoring spectral entropy was introduced by Viertiö-Oja et. al. [3]. The method has been applied in the Entropy module of the Datex-Ohmeda S/5 anesthesia monitor.

For comparison, the relative beta ratio is calculated. Beta ratio is calculated in spectral domain and is part of the Bispectral Index Score developed for the assessment of anesthetic depth by Aspect Medical Systems Inc. [1]. The correlation of all the mentioned parameters with the Ramsay score, the most widely used score for the clinical assessment of depth of hypnosis is studied [8].

II. Material

The results presented in this paper are based on EEG recordings from 12 ICU patients (age from 29 to 83 with the mean 63 years). Patients with known neurological disorders and patients admitted to the ICU after drug overdose were excluded from the study. The study was approved by the Ethics Committee of the South Karelia Central Hospital. The EEG signal was measured from the forehead, just below the hairline, and sampled with 400 Hz frequency.

The methods were applied to signal segments chosen manually according to the following rules (see figure 1):

- the segments have to precede the Ramsay score assessment
- all the calculated parameters (HD_f, spectral entropy, β-ratio) must be stable for at least 5 minutes before the endpoint of the segment
- the segments have to be as close to the Ramsay score assessment as possible
- if no stable period can be found or if burst-suppression pattern is seen in the EEG, the Ramsay score assessment is discarded.

The number of segments incorporated into the study together with corresponding Ramsay scores is presented in table 1.

The points of the Ramsay score assessment were determined according to the following protocol (if the status of the patient allowed scoring):

1) during steady state periods:
   - 30 minutes after previous scoring
   - the patient had been in a steady state for at least 10 minutes
2) during interventions
   - immediately after the bolus dose of the anesthetic drug given before the intervention
   - if bolus dose was not given, just before the intervention
   - in addition, 1-2 minutes after the intervention
3) when sedation was stopped:
   - immediately after the sedation was stopped
   - in addition, 10-15 minutes after the sedation was stopped

All the recordings were carefully annotated.

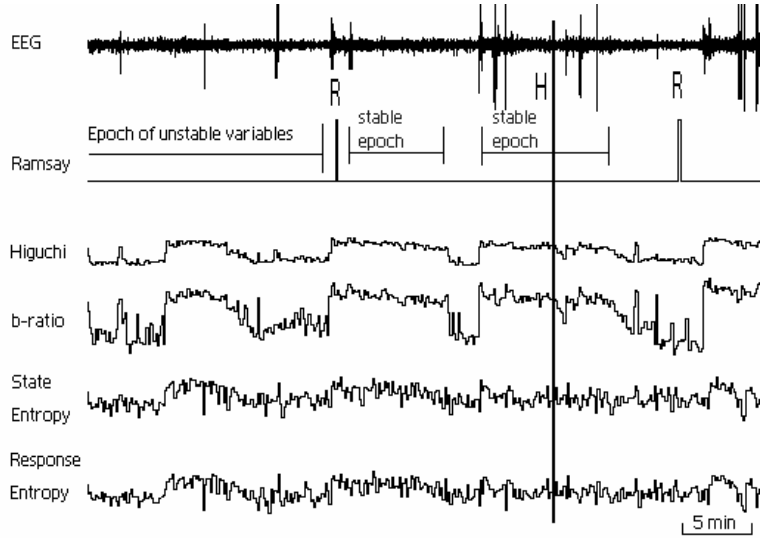

Figure 1. Principles of the selection of signal segments. The parameter values are calculated over 10 sec. window and in the calculation of the Higuchi fractal dimension 37 Hz low-pass prefilter is used.

II. Methods

The Higuchi fractal dimension is calculated as follows. First, from a given time series $x[1], x[2], \ldots, x[N]$ k new time series are constructed for $m = 1, \ldots, k$:

$$X_m^k = \left\{ x[m], x[m+k], \ldots, x\left[m + \left\lfloor \frac{N-m}{k} \right\rfloor k\right] \right\}.$$

The length of X_m^k is defined as:

TABLE I
RAMSAY SCORE ASSESSMENTS INCORPORATED INTO THE STUDY

Rec.	***Ramsay score***					
No.	**1**	**2**	**3**	**4**	**5**	**6**
1				22	2	
2			21	3	5	15
3		2	2			22
4	1	1	4	9	4	4
5		5	9	4		
6	3			8	3	11
7	1		6	19	2	2
8	1	2	8	3	2	2
9					6	19
10	1		9	10	10	1
11						31
12		10	10	4	2	
Sum	**7**	**20**	**69**	**82**	**36**	**107**

$$L_m^k = \frac{1}{k}\left[\sum_{i=1}^{\left\lfloor (N-m)/k \right\rfloor} \left| x[m+ik] - x[m+(i-1)k] \right| \cdot \frac{N-1}{\left\lfloor (N-m)/k \right\rfloor} \right].$$

Thus, L_m^k is proportional to the average difference of consecutive values of X_m^k. Averaging the lengths L_m^k over m and calculating these averages for all k gives us the sequence $L[k]$. The HD_f is defined as the best linear least-squares fit to the equation:

$$\ln(L[k]) = \mathrm{HD_f} \cdot \ln\left(\tfrac{1}{k}\right) + \bar{b}$$

Detailed description of the algorithm can be found in [6]. We applied the HD_f algorithm to prefiltered signal segments. Four prefilter cutoff frequencies were used: 19, 37, 47 and 100 Hz.

Spectral entropy is calculated by the following equation:

$$S_{f_1,f_2} = \sum_{f_i=f_1}^{f_2} P(f_i) \log \frac{1}{P(f_i)},$$

where $P(f)$ is the normalized power spectrum of the signal segment in question. To get entropy values independent of the frequency range, S_{f_1,f_2} is normalized by dividing it by $\log\left(N_{f_1,f_2}\right)$, where N is the number of frequency values in the range $[f_1, f_2]$.

In the entropy module developed by Datex Ohmeda, spectral entropy of two different frequency ranges is used: 0.8-32 Hz (called State Entropy) and 0.8-47 Hz (called Response Entropy). We used these parameters to check for stability when signal segments were picked for the analysis by visual inspection (figure 1). However, in the analysis of the segments we calculated spectral entropy over four frequency ranges: from 0.8 Hz to 19, 37, 47 and 100 Hz, respectively.

The relative β-ratio is calculated in spectral domain as $\log\left(P_{30-47}/P_{11-20}\right)$, where P_{A-B} denotes the sum of the spectral values in the frequency band from A to B Hz [1].

To study the effect of the window length on the parameter values, the described variables were calculated over windows of 5 different lengths: 5, 10, 20, 40 and 80 seconds.

III. Results

The value of the Higuchi fractal dimension was found to be highly dependent on the cutoff frequency of the low-pass prefilter. For example, values in the range of 0.04-0.08 were obtained when 19 Hz filter was used while preserving the frequencies up to 47 Hz gave values in the range of 0.2-0.5. At the same time the window length had no influence on this parameter. Figure 2 shows the Higuchi fractal dimension results in the case of 37 Hz low-pass prefilter for various window lengths while table II presents the p-value calculated pairwise for the measured Ramsay scores. The Wilcoxon rank sum test was used for the calculation of the statistical significance as, according to the Lilliefors hypothesis test, the data could not always be described by normal distribution. The 37 Hz cutoff frequency of the prefilter gave the best discrimination between different Ramsay scores although the results for other cutoff frequencies were similar.

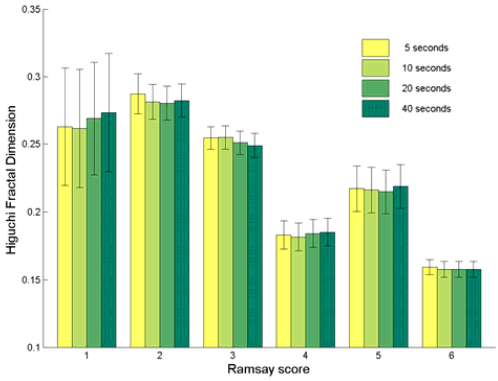

Figure 2. Higuchi fractal dimension (mean ± standard error) of 37 Hz low-pass filtered data for four window lengths

TABLE II
STATISTICAL SIGNIFICANCE (P-VALUES) OF THE DIFFERENCE OF HIGUCHI FRACTAL DIMENSION FOR DIFFERENT RAMSAY SCORES (WINDOW LENGTH 5 SEC.)

	R 1	R 2	R 3	R 4	R 5
R 2	*.9779*				
R 3	.6534	**.0333**			
R 4	.0922	**.0000**	**.0000**		
R 5	.2704	**.0128**	**.0487**	*.1338*	
R 6	**.0130**	**.0000**	**.0000**	**.0132**	**.0004**

In tables II-IV statistically significant differences ($p < 0.05$) are marked in bold. P-values for the pairs of Ramsay scores for which the difference in the variable value deviates from overall monotonic behavior are shown in italics. Outliers were discarded from statistical analysis.

The results for spectral entropy, presented in figure 3 and table III, show that this parameter is highly correlated with the window length – the longer the window the higher the entropy value. Correlation with the cutoff frequency of the prefilter is weak (not presented in the figure). We chose to present the results for 47 Hz cutoff frequency of the prefilter as this gave the best discrimination. However, like in the case of the HD_f, different cutoff frequencies gave similar results.

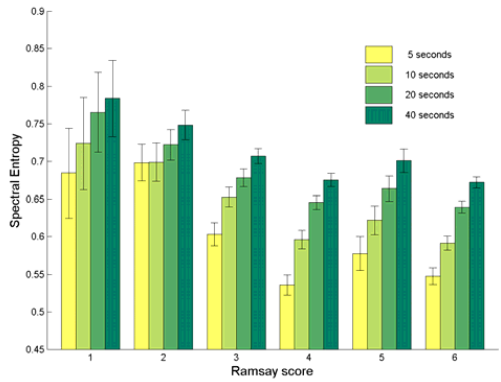

Figure 3. Spectral entropy (mean ± standard error) of 47 Hz low-pass filtered data for four window lengths

TABLE III
STATISTICAL SIGNIFICANCE (P-VALUES) OF THE DIFFERENCE OF SPECTRAL ENTROPY FOR DIFFERENT RAMSAY SCORES (WINDOW LENGTH 5 SEC.)

	R 1	R 2	R 3	R 4	R 5
R 2	*.6782*				
R 3	.1559	**.0020**			
R 4	**.0049**	**.0000**	**.0001**		
R 5	.1344	**.0024**	.5961	***.0251***	
R 6	**.0271**	**.0000**	**.0079**	*.1108*	.1240

The results for the beta ratio are presented in figure 4 and table IV. As this parameter is defined using the frequency band edges, only the window length could be varied. Beta ratio seems not to correlate significantly with the length of the data used in the calculations.

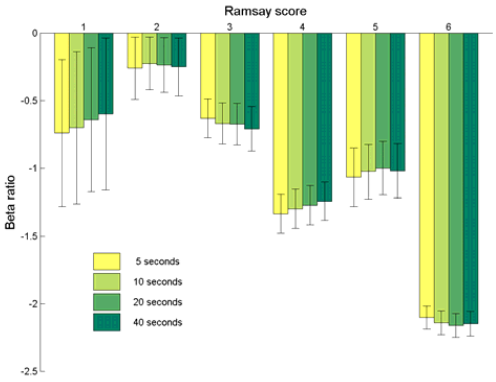

Figure 4. Beta ratio (mean ± standard error) of the EEG data for four window lengths

TABLE IV
STATISTICAL SIGNIFICANCE (P-VALUES) OF THE DIFFERENCE OF BETA RATIO FOR DIFFERENT RAMSAY SCORES (WINDOW LENGTH 5 SEC.)

	R 1	**R 2**	**R 3**	**R 4**	**R 5**
R 2	*.4864*				
R 3	*.9291*	.1326			
R 4	.4103	**.0000**	**.0000**		
R 5	.4202	**.0019**	**.0019**	*.4852*	
R 6	**.0099**	**.0000**	**.0000**	**.0000**	**.0000**

IV. DISCUSSION

The results obtained in this study are preliminary as the number of analyzed data segments is limited. It should also be noted that the data are unbalanced – for example, we had only 7 segments for Ramsay score 1 (see table I). This is reflected by high standard error. However, several important observations can be made based on the results.

In general, the behavior of all the tested parameters is similar. Ramsay scores 2 and 5 do not follow the 'ideal' monotonic relationship between the score and the parameter value. For Ramsay score 2 the explanation could be in increasing beta activity at very light levels of sedation. It seems that all the algorithms have trouble in discriminating Ramsay scores 4 and 5. One reason might be the limited amount of data. Spectral entropy tends to increase when sedation level increases from Ramsay score 4, which is opposite to the overall trend. Beta ratio gives the best behavior in deep sedation.

V. CONCLUSION

The following observations can be made based on our study:

- all the analyzed parameters are in general capable of discriminating between different Ramsay scores in ICU environment
- based on our analysis, the HD_f gives the best discrimination between the Ramsay scores 2 – 4 while beta ratio is superior for deep sedation (Ramsay score 6). Spectral entropy has reverse behavior for the sedation levels deeper than Ramsay score 4
- incorporating higher frequencies into the analysis changes the value of HD_f significantly while spectral entropy is not very sensitive to the frequency content. On the other hand, the HD_f is insensitive to the window length while spectral entropy correlates highly with the length of data. However, this observation might depend on several factors as, for example, the noise level and muscle activity in the recordings.

Although the presented results were found to be statistically significant and in most cases confirm our initial assumptions, a lot of work needs to be done to develop a clinically acceptable parameter to assess the depth of sedation in ICU environment.

ACKNOWLEDGMENT

This work was partly supported by Estonian Science Foundation grant No. 5625

REFERENCES

[1] I. J. Rampil. "A primer for EEG signal processing in anesthesia," *Anesthesiology,* vol. 89, pp. 980-1002, 1998.
[2] D. R. Drover, H. J. Lemmens, E. T. Pierce, G. Plourde, G. Loyd, E. Ornstein, L. S. Prichep, R. J. Chabot, and L. Gugino. "Patient state index: Titration of delivery and recovery from propofol, alfentanil, and nitrous oxide anesthesia," *Anesthesiology,* vol. 97, pp. 82-9, 2002.
[3] H. Viertiö-Oja, V. Maja, M. Särkelä, P. Talja, N. Tenkanen, H. Tolvanen-Laakso, M. Paloheimo, A. Vakkuri, A. Yli-Hankala, and P. Meriläinen. "Description of the Entropy™ algorithm as applied in the Datex-Ohmeda S/5™ entropy module," *Acta Anaesthesiol Scand,* vol.48, pp. 154-61, 2004.
[4] S. Kreuer, A. Biedler, R. Larsen, S. Altmann, and W. Wilhelm. "Narcotrend monitoring allows faster emergence and a reduction of drug consumption in propofol-remifentanil anesthesia," *Anesthesiology,* vol. 99, pp. 34-41, 2003.
[5] T. Higuchi. "Approach to an irregular time series on the basis of the fractal theory," *Physica D*, vol. 31, pp. 277-83, 1988.
[6] A. Accardo, M. Affinito, M. Carrozzi, and F. Bouquet. "Use of fractal dimension for the analysis of electroencephalographic time series," *Biol Cybern,* vol. 77, pp. 339-50, 1997.
[7] G. E. Powell, and I. C. Percival. "A spectral entropy method for distinguishing regular and irregular motion of Hamiltonian systems," *J Phys A: Math Gen,* vol. 12, pp. 2053-71, 1979.
[8] M. Ramsay, T. Savege, and B. Simpson. "Controlled sedation with alphaxolene/alphadalone," *Br J Med*, vol. 2, pp. 656-9, 1974.

PUBLICATONS

Publication II

Lipping, T., Ferenets, R., **Anier, A**., Melto, S. and Hovilehto, S. Power spectrum estimation in the calculation of spectral entropy to assess depth of sedation. *IFMBE Proc,* 11(1), 4p, 2005.

POWER SPECTRUM ESTIMATION IN THE CALCULATION OF SPECTRAL ENTROPY TO ASSESS DEPTH OF SEDATION

T. Lipping*, R. Ferenets*, A. Anier**, S. Melto*** and S. Hovilehto***

* Tampere University of Technology/Information Technology, Pori, Finland
** Tallinn University of Technology/Biomedical Engineering Centre, Tallinn, Estonia
*** South Karelia Central Hospital/Intensive Care Unit, Lappeenranta, Finland

tarmo.lipping@tut.fi

Abstract: The problem of the dependence of spectral entropy on data length is addressed. The EEG data recorded from 12 ICU patients is analyzed using four different schemes of power spectrum estimation for obtaining spectral entropy. Two of the schemes comprise the Welch periodogram averaging method, one scheme is based on the estimation of the autocorrelation function and one on the autoregressive modelling. The results show that spectral entropy values depend highly on the smoothness of the power spectrum estimate. Spectral entropy correlates significantly with data length only if FFT is used for power spectrum estimation and the FFT size varies together with the data length.

Introduction

Developing an objective measure for anesthetic depth has been a subject of great interest during the past decade. Although EEG-based devices for anesthesia monitoring were available already in 1970s [1], a breakthrough took place in 1997 when Aspect Medical Systems Inc., USA, introduced the Bispectral Index Score (BIS). This scalar index is a combination of three parameters calculated from the EEG signal: 1) the Beta Ratio, based on the power spectrum, 2) the SynchFastSlow measure, calculated in the bispectral domain, and 3) the burst-suppression ratio [2]. BIS gained much popularity and is currently widely used by anesthesiologists. It is often referred as the 'golden standard' in anesthesia monitoring.

Since the introduction of BIS, many companies have developed their own algorithms for the assessment of depth of anesthesia. The following commercially available methods can be mentioned as examples: the Patient State Index (PSI) by Physiometrix Inc., USA [3], the Narcotrend index by MonitorTechnik, Germany [4], the Entropy index by Datex-Ohmeda, Finland [5], the cAAI Index by Danmeter, Denmark (the algorithm is partly described in [6]). The performance of these indices has been discussed in numerous papers. However, comparison of the methods is difficult as the studies differ in various aspects like the anesthetic drug used, medication, patient condition etc.

Besides the various commercially available systems several new measures have recently been proposed for the assessment of anesthetic depth. This has mainly been motivated by the complexity of the problem – the available methods are far from being exhaustively studied while at the same time the field of application of depth-of-anesthesia/sedation measures is getting wider comprising the Intensive Care Unit (ICU) as well as Emergency. Main interest has been in measures quantifying the entropy and/or complexity of the EEG signal like approximate entropy [7], Shannon entropy [8], Lempel-Ziv complexity [9], Higuchi fractal dimension [10], spectral entropy [5].

Our interest has recently been to compare the behavior of the various entropy/complexity measures at different levels of sedation in the ICU. We have found that the various ways of quantifying signal entropy/complexity depend on different signal properties causing sometimes their contradictory behavior. For example, while all the other entropy measures decrease with deepening sedation, Shannon entropy tends to increase. Shannon entropy depends purely on the amplitude distribution of the signal regardless of the information about the time order of the samples. Another important observation is the sensitivity of the results on the EEG frequency band incorporated into the analysis. For example, cutting off the high frequencies and incorporating the delta frequency band tends to reverse the relation between sedation depth and EEG entropy at light levels of sedation.

This paper addresses a problem we met in comparing the entropy/complexity measures of the EEG signal – the dependence of spectral entropy on the length of the signal window. Our aim was to test if this dependence was due to added information when incorporating more data or if it was due to the algorithm.

Material

The results presented in this paper are based on EEG recordings from 12 ICU patients (age from 29 to 83 with the mean 63 years). Patients with known neurological disorders and patients admitted to the ICU after drug overdose were excluded from the study. The study was approved by the Ethics Committee of the South Karelia Central Hospital. The EEG electrodes were placed bilaterally to the forehead, below the hairline, approximately 5 cm above the eyebrows. The

ISSN: 1727-1983

distance of the electrodes from the midline was about 4 cm to either direction. The EEG signal was sampled with 400 Hz frequency.

Ramsay score assessments were performed by the ICU nurse during the course of the recordings according to predefined protocol. The Ramsay score uses 6 stages to evaluate the level of consciousness with score 1 indicating the subject being fully awake and score 6 indicating full unconsciousness, i.e., the lack of response to slightly painful stimulus [11]. The time instants of Ramsay score assessment were determined according to the following protocol (if the status of the patient allowed scoring):

1) during steady state periods:
   - 30 minutes after previous scoring
   - the patient had been in a steady state for at least 10 minutes
2) during interventions
   - immediately after the bolus dose of the anesthetic drug given before the intervention
   - if bolus dose was not given, just before the intervention
   - in addition, 1-2 minutes after the intervention
3) when sedation was stopped:
   - immediately after the sedation was stopped
   - in addition, 10-15 minutes after the sedation was stopped

All the recordings were carefully annotated.

Spectral entropy was calculated of manually selected signal segments. The segments were extracted according to the following rules:

- the segments had to precede the Ramsay score assessment
- the segments had to be as close to the Ramsay score assessment as possible
- if burst-suppression pattern was seen in the EEG or if the signal was too noisy the corresponding Ramsay score assessment was discarded.

Valid signal segments obtained from the data were distributed according to the Ramsay score values as follows:

Ramsay score	1	2	3	4	5	6
Number of segments	7	20	69	82	36	107

Methods

Spectral entropy is defined as:

$$S[f_1, f_2] = \sum_{f_i=f_1}^{f_2} P_n(f_i) \log \frac{1}{P_n(f_i)},$$

where $P_n(f)$ is the normalized power spectrum (normalization here means that $\sum_i P(f_i) = 1$) and spectral entropy is estimated in the frequency range $f_1 \ldots f_2$. Usually the result is also normalized to give entropy values between 0 and 1:

$$S_N[f_1, f_2] = \frac{S[f_1, f_2]}{\log(N[f_1, f_2])},$$

with $N[f_1, f_2]$ being the number of frequency values in the considered frequency range. Thus, spectral entropy is a measure of 'flatness' of the power spectrum with pure sine wave and white noise giving the entropy values 0 and 1, respectively.

In the calculation of spectral entropy usually periodogram is used to estimate the power spectrum. However, it is well known that periodogram is an unconsistent estimate of power spectrum - in other words, the estimate does not converge to the true power spectrum as more data becomes available.

In order to study the cause of the dependence of spectral entropy on data length, the selected 20 second segments of the EEG signal were processed using four different schemes of the estimation of power spectrum:

1) Welch periodogram averaging method I; the signal segment was divided into subsegments with 50% overlap. The subsegments were windowed using the hamming window and the FFT was taken. The estimate of the power spectrum was obtained as the average of the FFTs of the subsegments. We used four subsegment lengths: 1.25 sec., 2.5 sec., 5 sec. and 10 sec. - the shorter the subsegment the more subsegments were incorporated into the average. The FFT size was increased together with the subsegment length.
2) Welch periodogram averaging method II; this scheme was similar to the previous one except that the FFT size was kept constant - 4096 data points. The signal subsegments were zero-padded before taking the FFT.
3) Autocorrelation method; the autocorrelation function was estimated and power spectrum was obtained as the FFT of the hamming-windowed middle part of the autocorrelation function. Four different window lengths were used for cutting the middle part of the autocorrelation function: 5 sec., 10 sec., 20 sec. and 40 sec. The FFT size was equal to the window length.
4) Autoregressive modeling; power spectrum was estimated based on the coefficients of the autoregressive model. Model orders of 16, 32, 48 and 64 were used.

Results

The results are shown in figures 1…4 for the different schemes of power spectrum estimation. Figure 1 shows that if the FFT size is varied, the obtained spectral entropy is highly dependent on the signal subsegment length over which the FFT is calculated. Figure 2 shows that this dependence is actually reversed if the segmentation scheme remains the same but the FFT length is kept constant – in our case 4096 data points. The dependence is not as severe as in the case of scheme 1. Figure 3 shows that using the autocorrelation function for power spectrum estimation did not eliminate the dependence of the results on the window

ISSN: 1727-1983

length as far as the FFT size changes together with the window length.

In the case of AR modelling, the behaviour of the power spectrum depends on the model order rather than the length of the signal window. Therefore, the coefficients were estimated over the whole 20 sec. signal segment. Figure 4 shows that if sufficient AR-model order is used, the obtained spectral entropy is fairly stable, not depending on the choice of the model order.

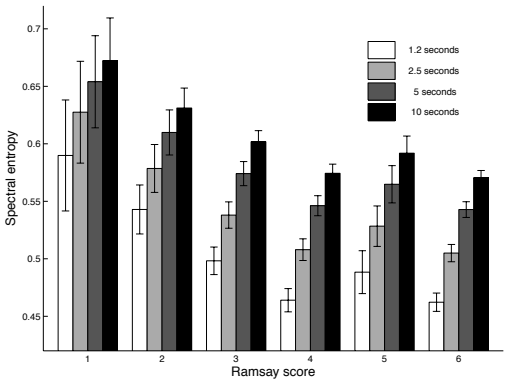

Figure 1: Correlation of spectral entropy with the Ramsay score. Power spectrum is estimated using the Welch periodogram averaging method I. The window lengths of 1.2 sec., 2.5 sec., 5 sec. and 10 sec. are used; the length of the FFT is increased together with the window length.

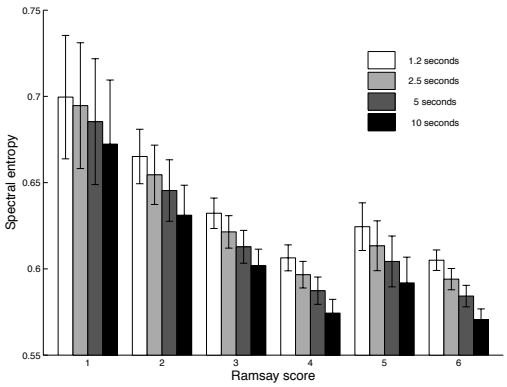

Figure 2: Correlation of spectral entropy with the Ramsay score. Power spectrum is estimated using the Welch periodogram averaging method II. The window lengths of 1.2 sec., 2.5 sec., 5 sec. and 10 sec. are used; the signal subsegment is zero-padded to give the FFT length of 4096 samples for all window lengths.

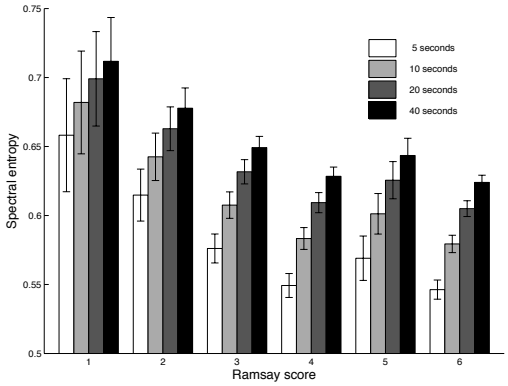

Figure 3: Correlation of spectral entropy with the Ramsay score. Power spectrum is estimated using the autocorrelation method. FFT is taken over the middle 5 sec., 10 sec., 20 sec. and 40 sec. part of the autocorrelation function.

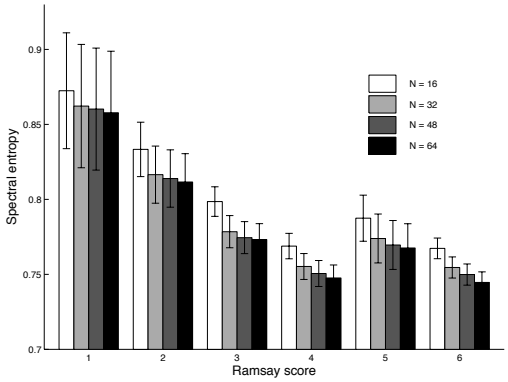

Figure 4: Correlation of spectral entropy with the Ramsay score. Power spectrum is estimated using autoregressive model coefficients. The order of the AR model of 16, 32, 48 and 64 is used.

An important result based on the figures is the correlation between the smoothness of the power spectrum and the value of spectral entropy. AR-model gives generally smoother power spectrum compared to the Welch periodogram averaging method. The figures show that the entropy values obtained using AR-model coefficients are in the range of 0.75…0.87 while the other schemes give values in the range approximately 0.5…0.7. Also, if constant FFT size is used (fig. 2), the entropy value is higher for shorter subsegment length, corresponding to smoother power spectrum (shorter subsegments mean averaging over larger number of subsegment spectra). In figure 1 this does not hold due to the effect of varying FFT size.

ISSN: 1727-1983

Discussion

The results presented in this paper show that the dependence of spectral entropy values on the length of the signal window is not caused by the variable amount of information available but rather the properties of the periodogram as the estimate of the power spectrum. The amount of data available was equal – 8000 samples – for all the calculation schemes. Both schemes using varying FFT size (schemes 1 and 3) caused severe correlation between the FFT size and the spectral entropy value.

Based on the results we suggest that the AR-model based calculation scheme for spectral entropy is the most stable with respect to data size. Model order 16 seems to be too low to capture the behaviour of the true power spectrum. Model of order 32…48 can be suggested.

It is important to note that although the different schemes for power spectrum estimation gave different values of spectral entropy, the correlation of the entropy with depth of sedation was not affected. This implies that as far as equal window lengths are used, the choice of the power spectrum estimation method is not critical.

Conclusions

The following conclusions can be drawn from the analysis presented in this paper:

- the ability of the estimate of EEG spectral entropy to differentiate between various levels of sedation does not depend on the method used for power spectrum estimation in general. However, spectral entropy values achieved using different methods for power spectrum estimation are not comparable with each other
- in the case of periodogram averaging, higher spectral entropy estimates for longer data windows are not due to the additional information contained in the data but rather comes from high variance of the power spectrum estimate typical to this method
- in general, smoother power spectrum estimates (using AR-model coefficients, for example) give higher values of spectral entropy.

References

[1] MAYNARD D., PRIOR P. (1969): 'Device for Continuous Monitoring of Cerebral Activity in Resuscitated Patients', *Br. Med. J.*, **4**, pp. 545-546

[2] RAMPIL I. J. (1998): 'A Primer for EEG Signal Processing in Anesthesia', *Anesthesiology*, **89**, pp. 980-1002

[3] DROVER D. R., LEMMENS H. J., PIERCE E. T., PLOURDE G., LOYD G., ORNSTEIN E., PRICHEP L. S., CHABOT R. J., GUGINO L. (2002): 'Patient State Index: Titration of Delivery and Recovery from Propofol, Alfentanil, and Nitrous Oxide Anesthesia', *Anesthesiology*, **97**, pp. 82-89

[4] SCHULTZ, B., SCHULTZ A., GROUVEN U. (2000): 'Sleeping Stage Based Systems (Narcotrend®)', in BRUCH, H.-P. ET. AL (Eds): 'New Aspects of High Technology in Medicine 2000', (Monduzzi Editore, Bologna), pp. 285-291

[5] VIERTIÖ-OJA H., MAJA V., SÄRKELÄ M., TALJA P., TENKANEN N., TOLVANEN-LAAKSO H., PALOHEIMO M., VAKKURI A., YLI-HANKALA A., MERILÄINEN P. (2004): 'Description of the Entropy™ Algorithm as Applied in the Datex-Ohmeda S/5™ Entropy Module', *Acta Anaesthesiol Scand.*, **48**, pp. 154-161

[6] JENSEN E. W., LINDHOLM P., HENNEBERG S. W. (1996): 'Autoregressive Modeling with Exogenous Input of Middle Latency Auditory-Evoked Potentials to Measure Rapid Changes in Depth of Anesthesia', *Methods of Information in Medicine*, **35**, pp. 256-260

[7] BRUHN J., RÖPCKE H., HOEFT A. (2000): 'Approximate Entropy as an Electroencephalographic Measure of Anestetic Drug Effect during Desflurane Anesthesia', *Anesthesiology*, **92**, pp. 715-726

[8] BRUHN J., LEHMANN L. E., RÖPCKE H., BOUILLON T. W., HOEFT A. (2001): 'Shannon Entropy Applied to the Measurement of the Electroencephalographic Effects of Desflurane', *Anesthesiology*, **95**, pp. 30-35

[9] ZHANG X.-S., ROY R. J., JENSEN E. W. (2001): 'EEG Complexity as a Measure of Depth of Anesthesia for Patients', *IEEE Trans on Biomed Eng*, **48**, pp. 1424-1433

[10] ANIER A., LIPPING T., MELTO S., HOVILEHTO S. (2004): 'Higuchi Fractal Dimension and Spectral Entropy as Measures of Depth of Sedation in Intensive Care Unit', Proc. of 26th IEEE EMBS Annual International Conference (EMBC'04), San Francisco, USA, 2004, pp. 526-529

[11] RAMSAY M., SAVEGE T., SIMPSON B. (1974): 'Controlled Sedation with Alphaxolene/ Alphadalone', *Br. J. Med.*, **2**, pp. 656- 659

ISSN: 1727-1983

PUBLICATONS

Publication III

Ferenets, R., Lipping, T., **Anier, A**., Jäntti, V., Melto, S. and Hovilehto, S. Comparison of Entropy and Complexity Measures for the Assessment of Depth of Sedation. *IEEE Transactions on Biomedical Engineering,* 53(6), pp. 1067-1077, 2006.

Comparison of Entropy and Complexity Measures for the Assessment of Depth of Sedation

Rain Ferenets, *Student Member, IEEE*, Tarmo Lipping*, *Senior Member, IEEE*, Andres Anier, *Student Member, IEEE*, Ville Jäntti, Sari Melto, and Seppo Hovilehto

***Abstract*—Entropy and complexity of the electroencephalogram (EEG) have recently been proposed as measures of depth of anesthesia and sedation. Using surrogate data of predefined spectrum and probability distribution we show that the various algorithms used for the calculation of entropy and complexity actually measure different properties of the signal. The tested methods, Shannon entropy (ShEn), spectral entropy, approximate entropy (ApEn), Lempel-Ziv complexity (LZC), and Higuchi fractal dimension (HFD) are then applied to the EEG signal recorded during sedation in the intensive care unit (ICU). It is shown that the applied measures behave in a different manner when compared to clinical depth of sedation score—the Ramsay score. ShEn tends to increase while the other tested measures decrease with deepening sedation. ApEn, LZC, and HFD are highly sensitive to the presence of high-frequency components in the EEG signal.**

***Index Terms*—Complexity, depth of anesthesia, depth of sedation, EEG, entropy, Ramsay score, surrogate data.**

I. Introduction

ANESTHESIA monitoring based on parameters calculated from the electroencephalogram (EEG) signal has been an active research topic during the past decade. After some earlier attempts to develop anesthesia monitors, a breakthrough was achieved in 1997 when Aspect Medical Systems Inc. developed the bispectral index (BIS)—a method incorporating bispectral analysis for the calculation of a scalar "depth-of-anesthesia" measure [1]. Since then, several algorithms have been developed and commercialized for the assessment of depth of anesthesia. As examples, the Patient State Index (PSI, Physiometrix Inc.), the Narcotrend index (MonitorTechnik, Germany), the Entropy index (Datex Ohmeda, Finland) can be mentioned. An overview and a reference list can be found in [2].

Manuscript received March 18, 2005; revised December 4, 2005. This work was supported in part by the Estonian Science Foundation under Grant 5625. *Asterisk indicates corresponding author.*

R. Ferenets is with the Department of Information Technology, FIN-28101 Pori, Tampere University of Technology, Pori, Finland, and also with the Biomedical Engineering Center, Tallinn University of Technology, 19086 Tallinn, Estonia.

*T. Lipping is with the Department of Information Technology, Pori, Tampere University of Technology, FIN-28101 Pori, Finland (tarmo.lipping@tut.fi).

A. Anier is with the Biomedical Engineering Center, Tallinn University of Technology, 19086 Tallinn, Estonia.

V. Jäntti is with the Department of Clinical Neurophysiology, Tampere University Hospital, FIN-33014 Tampere, Finland.

S. Melto and S. Hovilehto are with the Intensive Care Unit, South Karelia Central Hospital, FIN-53100 Lappeenranta, Finland.

Digital Object Identifier 10.1109/TBME.2006.873543

Despite the various methods available, the research aiming at enhanced EEG-based anesthesia/brain monitoring methods is still very active mostly due to the following reasons. First, the available methods have certain drawbacks causing them to fail in certain situations (like, e.g., halothane anesthesia in children) and second, EEG and brain monitoring are becoming feasible in several other areas (e.g., in intensive care, emergency) and the methods developed for monitoring surgical anesthesia are not suitable for these applications. They must either be tuned or new algorithms must be applied.

Two trends can be observed in the development of anesthesia monitoring methods. Some of the algorithms (PSI, Narcotrend) combine well-known time- and frequency domain parameters and feed them to a classification algorithm trained using extensive databases. Other algorithms put more emphasis on some advanced parameters like bispectrum (BIS) or entropy (the Entropy monitor).

It is generally known that the EEG signal slows down becoming more regular and less complex as the subject becomes unconscious. However, there are many different ways of defining complexity and entropy, and even more ways of calculating it. Like J. von Neumann put it for Claude Shannon: "No one knows what entropy really is, so in a debate you will always have the advantage" [3]. This statement is very true in the EEG analysis today—different properties of the signal are used to estimate entropy and the results are compared with one another in the literature.

The purpose of this paper is to investigate the actual properties of the signal quantified by several common entropy/complexity measures. The following algorithms were chosen: Shannon entropy (ShEn), approximate entropy (ApEn), spectral entropy, Lempel-Ziv complexity (LZC), and Higuchi fractal dimension (HFD). There are mainly the following three reasons for this choice:

1) these measures have been proposed as the indicators of depth of anesthesia/sedation in several recently published papers ([4]–[8] can be mentioned as some examples);
2) the calculation of these measures is straightforward and computationally efficient;
3) the algorithms give reliable results in the case of short signal segments thus being applicable in real-time patient monitoring.

We are especially interested in the sensitivity of the mentioned measures to the bandwidth of the signal spectrum and the shape of the probability density function (PDF). In part II of the paper a short description of the algorithms is given. After that we

apply the methods to test signals of various probability density and spectral bandwidth. The test signals are generated using the iterative algorithm proposed by Schreiber and Schmitz [9]. We also apply the algorithms to a data set measured in the intensive care unit (ICU) and compare the results to the Ramsay score, a clinical depth of sedation score. The results of this comparison are presented in part IV of the paper. In addition, the Beta Ratio, a simple frequency domain parameter used in the BIS algorithm is calculated of the ICU data for comparison.

II. Methods for Estimating Signal Entropy and Complexity

A. Shannon Entropy

The concept of entropy in the context of information theory was first introduced by Shannon [10], and it can be viewed as a measure of order in the signal. Shannon entropy, H_{Sh}, quantifies the PDF of the signal and it can be calculated as

$$H_{\mathrm{Sh}} = -\sum_i p_i \log p_i \tag{1}$$

where i goes over all amplitude values of the signal and p_i is the probability that amplitude value a_i occurs anywhere in the signal.

However, in the case of measured signals the PDF is not known and should be estimated. Also, it is generally not reasonable to take into account all amplitude values a_i. The easiest way to estimate the PDF is to use the histogram method where the amplitude range of the signal is linearly divided into k bins so that the ratio k/N is constant (N is the number of signal samples). The ratio k/N characterizes the average filling of the histogram.

In order to get normalized values, H_{Sh} should be divided by $\log k$

$$\mathrm{ShEn} = \frac{H_{\mathrm{Sh}}}{\log k}. \tag{2}$$

B. Spectral Entropy

The idea of spectral entropy, H_{Sp}, is straightforward in the sense that the PDF in (1) is simply replaced by the power density P from the signal's spectrum (normalized so that $\sum P_n = 1$)

$$H_{Sp} = -\sum_{i=f_l}^{f_h} P_i \log P_i \tag{3}$$

where f_l and f_h define the frequency band we are interested in [6], [11]–[13].

Usually spectral entropy is normalized to the range of values between 0 and 1

$$\mathrm{SpEn} = \frac{H_{\mathrm{Sp}}}{\log N_f} \tag{4}$$

where N_f is the number of frequency components in the range $[f_l, f_h]$ [6].

C. Approximate Entropy

ApEn, introduced by Pincus [14], is a measure quantifying the unpredictability or randomness of the signal. ApEn is originated from nonlinear dynamics. It is an approximation of the Kolmogorov entropy in the sense that the limits ($r_f \to 0$, $N \to \infty$, $m \to \infty$) can be relaxed. Therefore, it can be applied to signals of finite length [5], [12], [14]–[16].

The calculation of ApEn of signal s of finite length N is performed as follows. First, fix a positive integer m and a positive real number r_f. Next, from the signal s the $N-m+1$ vectors $\mathbf{x}_m(i) = \{s(i), s(i+1), \ldots, s(i+m-1)\}$ are formed. After that, for each i, $1 \leqslant i \leqslant N-m+1$, the quantity $C_i^m(r_f)$ is calculated using

$$C_i^m(r_f) = \frac{\text{number of such } j \text{ that } d[\mathbf{x}_m(i), \mathbf{x}_m(j)] \leqslant r_f}{N-m+1} \tag{5}$$

where the distance d between the vectors $\mathbf{x}_m(i)$ and $\mathbf{x}_m(j)$ is defined as:

$$d[\mathbf{x}_m(i), \mathbf{x}_m(j)] = \max_{k=1,2,\ldots,m} \left(|s(i+k-1) - s(j+k-1)|\right). \tag{6}$$

Next, the quantity $\Phi^m(r_f)$ is calculated as

$$\Phi^m(r_f) = \frac{1}{N-m+1} \sum_{i=1}^{N-m+1} \log C_i^m(r_f). \tag{7}$$

Finally, the ApEn is defined as follows:

$$\mathrm{ApEn}(m, r_f, N) = \Phi^m(r_f) - \Phi^{m+1}(r_f). \tag{8}$$

The parameter r_f corresponds to an *a priori* fixed distance between the neighboring trajectory points; therefore, r_f can be viewed as a filtering level and the parameter m is the embedding dimension determining the dimension of the phase space.

Frequently, r_f is chosen according to the signal's standard deviation (SD); in this paper we use the values $r_f = 0.2$ SD and $m = 2$ with SD taken over the signal segment under consideration [5], [15].

D. Lempel-Ziv complexity

The normalized complexity, C_α, as introduced by Lempel and Ziv [17], is a measure reflecting the rate of new pattern generation along given sequence of symbols. In other words, C_α characterizes the structure or, as the name implicates, the complexity of the signal—whether the signal is predictable (has simple structure) or nonpredictable (has complex, random structure) [7], [18].

The calculation algorithm of C_α for the sequence of symbols $\mathbf{x}_1^N = x_1, x_2, x_3, \ldots, x_N$ of length N is defined as follows. A block B of length l ($1 \leqslant l \leqslant N$) is a subsequence of l

consecutive symbols, $B = \mathbf{x}_{i+1}^{i+l} = x_{i+1}, x_{i+2}, \ldots, x_{i+l}$ $(0 \leqslant i \leqslant N-l)$. The first block, B_1, is set equal to the first symbol of the sequence $\mathbf{x}_1^N$, i.e. $B_1 = \mathbf{x}_1^1 = x_1$. Next

$$B_{k+1} = \mathbf{x}_{n_k+1}^{n_{k+1}} \qquad (n_k + 1 \leqslant n_{k+1} \leqslant N) \tag{9}$$

is defined to be the following consecutive block of minimal length such that it does not occur in the sequence $\mathbf{x}_1^{n_{k+1}-1}$. Therefore, by continuing this recursive procedure until the last symbol of $\mathbf{x}_1^N$ is reached it is possible to obtain the decomposition of $\mathbf{x}_1^N$ into minimal blocks

$$\mathbf{x}_1^N = B_1, B_2, \ldots, B_n. \tag{10}$$

The complexity c_α of $\mathbf{x}_1^N$ is defined as the number of blocks in the decomposition, n (10)

$$c_\alpha \equiv n = n(\alpha) \tag{11}$$

where α is the number of possible different symbols in $\mathbf{x}_1^N$. The normalized complexity, C_α, is defined as

$$C_\alpha = \frac{c_\alpha\left(\mathbf{x}_1^N\right)}{N/\log_\alpha N} = \frac{n(\alpha)}{N}\log_\alpha N. \tag{12}$$

Prior to applying the above described algorithm the signal s has to be converted into a sequence of symbols, which can be done as follows. Depending on the number of different symbols α, $\alpha - 1$ thresholds T_i have to be selected within the signal range $s_{\min} < \cdots < T_i < \cdots < s_{\max}$, where $s_{\min}$ and $s_{\max}$ are the minimum and maximum values of the signal s, respectively. For instance, if $\alpha = 2$, i.e. two symbols, "0" and "1" are used, there is only one threshold T_1 and by comparing the samples of s with this threshold the signal is converted into the sequence of symbols: if $s(i) < T_1$ then $x_i = 0$, otherwise $x_i = 1$. For larger α the conversion procedure is analogous.

E. Higuchi Fractal Dimension

Fractal dimension is another measure of signal complexity, generally evaluated in phase space by means of correlation dimension. Higuchi proposed an algorithm for the estimation of fractal dimension directly in the time domain without reconstructing the strange attractor [19]. This method gives reasonable estimate of the fractal dimension in the case of short signal segments and is computationally fast [19], [20].

Higuchi's algorithm is based on the following scheme: from a given signal $s = \{s(1), s(2), \ldots, s(N)\}$, k new curves s_m^k are constructed as follows:

$$s_m^k = \{s(m), s(m+k), \ldots, s\left(m + \lfloor (N-m)/k \rfloor \cdot k\right)\} \qquad m = 1, 2, \ldots, k \tag{13}$$

TABLE I
SUMMARY OF THE SELECTED PARAMETER VALUES

Method	Parameter	Value
$ShEn$	Average filling of the histogram, k/N	0.01
$SpEn$	Lowest frequency, f_l	0
	Highest frequency, f_h	$f_{Nyquist}$
$ApEn$	Embedding dimension, m	2
	Filtering level, r_f	0.2·SD
LZC	Number of symbols, α	2
	Threshold, T	mean of s
HFD	Max interval time, $k_{\max}$	8

where both m and k are integers and they indicate the initial time and the time interval, respectively. The length, $L_m(k)$, of each curve s_m^k is calculated as

$$L_m(k) = \left[\left(\sum_{i=1}^{\lfloor \frac{N-m}{k} \rfloor} |s(m+ik) - s\left(m+(i-1)k\right)|\right) \cdot \frac{N-1}{\lfloor \frac{N-m}{k} \rfloor k}\right] \Big/ k. \tag{14}$$

The length of the curve for time interval k, $L(k)$, is calculated as the average of the m curves $L_m(k)$ for $m = 1, \ldots, k$. If $L(k) \propto k^{-D}$, the signal is fractal-like with the dimension D. Therefore, if $L(k)$ is plotted against $1/k$, where $k = 1, \ldots, k_{\max}$, in double logarithmic plot, the data points should fall into straight line with the slope D. Finally, linear fitting by the means of least-squares is applied to the pairs $(\log 1/k, \log L(k))$, $k = 1, \ldots, k_{\max}$ and the slope of the obtained line is calculated giving the estimate of the fractal dimension D.

For a summary of the selected parameter values, for each measure considered herein, see Table I.

III. DEPENDENCE OF ENTROPY/COMPLEXITY MEASURES ON SIGNAL PROPERTIES

A. Generation of Signals of Predefined Probability Density and Spectrum

Generation of reference signals of fixed power spectrum and probability density, the so-called surrogates, is widely used, for instance, for detecting nonlinearities in a given signal. A common way of generating surrogates is to use the amplitude adjusted Fourier transform (AAFT) algorithm, which basically contains rank-ordering and phase randomizing as the main processing steps.

Schreiber and Schmitz have found, however, that more accurate surrogates can be obtained by iteratively changing the probability distribution and the power spectrum of the surrogate until the required precision or the maximum number of iterations is obtained [9], [21]. The iterative algorithm was originally used for generating surrogates with properties similar to a given signal. In our study we are interested in test signals of predefined power spectrum and probability distribution. Our approach is to generate a signal s with given probability distribution and to

use the iterative algorithm for shaping the power spectrum as desired.

Let P be the desired power spectrum for the surrogate and c a copy of the signal s sorted in ascending order. At each iteration stage (i) there is a sequence $r^{(i)}$, which has the correct probability distribution given by s and a sequence $s^{(i)}$, which has the correct power spectrum given by P. The process starts by assigning $r^{(0)}$ the random shuffle of s. Each following iteration contains two consecutive steps.

In the first step, $r^{(i)} \rightarrow s^{(i)}$, the Fourier transform, $R^{(i)}$, of $r^{(i)}$ is obtained, $R^{(i)} = \mathcal{DFT}\{r^{(i)}\}$, where $\mathcal{DFT}$ denotes the discrete Fourier transform (DFT) operator. Next, the amplitude $|R^{(i)}|$ is replaced by the desired one, i.e. with $\sqrt{P}$, and the complex phase of $R^{(i)}$, $e^{j\psi^{(i)}} = R^{(i)}/|R^{(i)}|$, is kept. Hereafter, the inverse Fourier transform is taken and $s^{(i)}$ is obtained, $s^{(i)} = \mathcal{IDFT}\{\sqrt{P}e^{j\psi^{(i)}}\}$, where $\mathcal{IDFT}$ denotes the Inverse DFT operator.

In the second step, $s^{(i)} \rightarrow r^{(i+1)}$, rank-ordering is performed: $r^{(i+1)}(n) = c_{\mathrm{rank}\{s^{(i)}(n)\}}$, $n = 1, \ldots, N$, where N is the length of the given signal s. Here $\mathrm{rank}\{s^{(i)}(n)\}$ denotes the ascending rank of $s^{(i)}(n)$, i.e. $\mathrm{rank}\{s^{(i)}(n)\} = 1$ if $s^{(i)}(n)$ is the smallest element of $s^{(i)}$, $\mathrm{rank}\{s^{(i)}(n)\} = 2$ if $s^{(i)}(n)$ is the 2nd smallest element of $s^{(i)}$ and so forth.

The first step enforces the correct power spectrum but it alters the probability distribution. The second step, on the other hand, guarantees the correct probability distribution but power spectrum is changed. Therefore, these two steps have to be iterated several times.

At each iteration the relative error, $\varepsilon^{(i)}$, between the desired power spectrum, P, and the obtained one, $|R^{(i)}|^2$, is calculated as

$$\varepsilon^{(i)} = \frac{\sum \left(|R^{(i)}|^2 - P \right)^2}{\sum P^2}. \tag{15}$$

This error was used in making the decision on stopping the iterative algorithm and accepting the generated surrogate according the criteria presented in Table II.

In order to generate surrogate data sets, first the random signal s of predetermined probability density p_s was generated. p_s was determined by the following function [22]:

$$p_s = \eta \cdot e^{-\frac{|s|^\nu}{\nu}} \tag{16}$$

where the positive-valued parameter ν is used for controlling the sharpness/flatness of the probability distribution and η is the normalizing parameter to assure that $\int_{-\infty}^{\infty} p_s(x)dx = 1$. For small ν values ($\nu < 0.1$) p_s takes sharp shapes, on the other hand, $\nu \rightarrow \infty$ gives uniform distribution. If $\nu = 1$ or $\nu = 2$, Laplace (double exponential) or Gaussian distribution is obtained, respectively.

Random signals of predefined probability distributions were generated using the rejection method. This method constitutes a technique for generating random numbers whose probability distribution function p is known and computable. First, a comparison function f of finite area is chosen such that p is everywhere less than f. f is chosen so that it is possible to generate random numbers in two dimensions, uniformly distributed over the area covered by f. If such a random number falls into the area covered by f but not by p it is rejected, otherwise it is accepted. The x coordinate of the resulting two-dimensional random numbers is distributed according to p. More detailed description of the rejection method can be found in [23].

TABLE II
CRITERIA FOR SURROGATE DATA GENERATION

Action	Criterion
Stopping surrogate generation	Error, $\varepsilon < 10^{-6}$
	Number of iterations, $(i) > 50$
Acceptance of the surrogate, s	Error, $\varepsilon < 10^{-2}$

In our study the sharpness/flatness controlling parameter of the PDF, ν, was selected to have the following values:

$$\nu = 2^{-2}, 2^{-1.5}, 2^{-1}, \ldots, 2^{6}. \tag{17}$$

Hence, in total, test signals of 17 probability distributions of varying shapes were obtained. Fig. 1 illustrates every other generated distribution between the sharpest and the flattest one.

The power spectrum, P, was selected to have rectangular shape centered at $\omega = 0.5$, where ω is the normalized frequency ranging from 0 to 1, corresponding to the DC component and the Nyquist frequency, respectively. Test signals of the following normalized bandwidth r were generated:

$$r = 10^{-2}, 10^{-1.5}, 10^{-1}, 10^{-0.5}, 10^{0}. \tag{18}$$

For example, the value $r = 10^{-1}$ means that the bandwidth of the corresponding signal covers 10% of the whole bandwidth. All used power spectra are illustrated in Fig. 2.

B. Dependence of Entropy/Complexity Measures on Signal Amplitude Distribution and Signal Bandwidth

In order to estimate the dependence of entropy/complexity measures on signal properties, 85 signals with 17 predefined PDF shapes and 5 power spectrum bandwidths were generated and the methods described throughout Sections II-Ato II-E were applied. This procedure was repeated 20 times and the results were averaged. The whole process of test signal generation was performed for three different signal lengths: 1024, 4096, and 16 384 data points. Fig. 3 summarizes the obtained results. The first row reveals that ShEn does not depend on signal bandwidth as could be expected from the definition of this measure. Slight divergence of the curves corresponding to similar PDF but different spectra at small ν values (sharp PDFs) is due to the fact that the PDF is no longer independent of the spectrum here and the iterative algorithm for surrogate generation did not converge well.

The second row illustrates the behavior of SpEn which, in contrary to ShEn, does not depend on the shape of the signal's

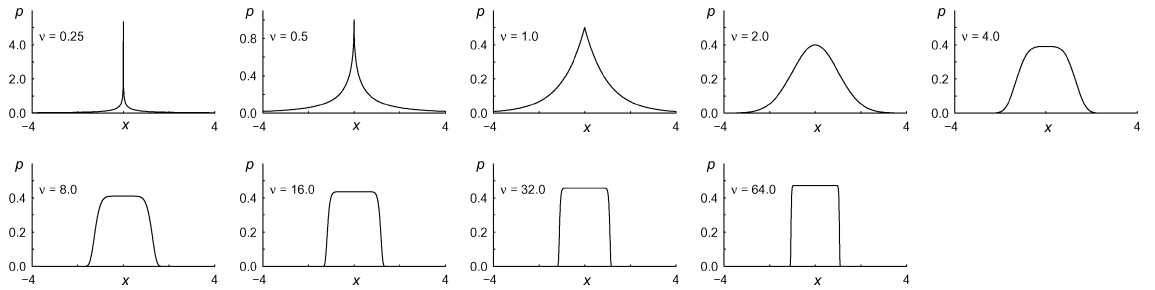

Fig. 1. PDFs of different sharpness/flatness controlled by the parameter ν. In the figure we show every other PDF used in the test signal generation. Note that the scale of the y-axis of the first two PDFs ($\nu = 0.25$ and $\nu = 0.5$) is different compared to that of the other plots.

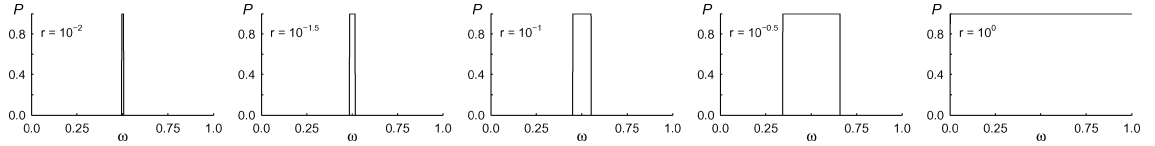

Fig. 2. Power spectra of different bandwidth controlled by the parameter r.

PDF (the lines are almost parallel to the x-axis). Here, analogously to the case of ShEn, the divergence of the curves corresponding to similar spectra but different PDFs at small ν values and especially in the case of short signals is due to the inaccuracy of the properties of the test signals. SpEn is also dependent on signal length; therefore, for short signals, SpEn tends to be smaller than for longer signals.

The third row shows that ApEn depends on both the shape of the PDF as well as the spectral bandwidth of the signal. At sharp PDFs, ApEn behaves similarly to ShEn with respect to the shape of the PDF (given that the bandwidth is large enough). As the signal amplitude becomes more uniformly distributed, ApEn values stay constant, depending only on the spectral bandwidth. Also, the ApEn values slightly increase with increasing signal length.

The behavior of LZC, and HFD, illustrated in the last two rows of Fig. 3, looks similar. Both parameters depend mainly on the bandwidth of the signal spectrum while slight dependence on the PDF can be observed mostly when ν is small.

The theory underlying ApEn and HFD comprises embedding of the data onto the phase space. As it is not feasible to generate signals of predefined phase space embedding, PDF and power spectrum were used in our analysis as the starting point for the test signal generation. Decreasing the spectral bandwidth causes the signals to become more regular. In order to follow the changes in signal dynamics we plotted the phase space representation of the test data in the cases of Laplace, Gaussian and uniform distributions for the five bandwidths of (18). The results in Fig. 4 show that as the bandwidth decreases from that defined by $r = 10^{-1.5}$, the phase space is no more uniformly covered by the data points but certain patterns start to form. Comparison with Fig. 3 shows that ApEn, HFD, and LZC values change most rapidly when the signal bandwidth decreases from $r = 10^{-0.5}$ to $r = 10^{-1.5}$, detecting regularity in the signal before it can be seen visually in phase space.

IV. Entropy/Complexity of EEG During Sedation in Intensive Care Unit

The results presented in part III were tested using EEG recordings from 12 ICU patients (age from 29 to 83 with the mean 63 years), sedated with propofol. Patients having known neurological disorders were excluded from the study. The EEG electrodes were placed bilaterally to the forehead, below the hairline, approximately 5 cm above the eyebrows. The distance of the electrodes from the midline was about 4 cm to either direction. The EEG signal was sampled at 400 Hz. Ramsay score assessments were performed by the ICU nurse during the course of the recording according to predefined protocol. The Ramsay score uses 6 stages to evaluate the level of consciousness with score 1 indicating the subject being fully awake and score 6 indicating full unconsciousness, i.e., the lack of response to slightly painful stimulus [24].

To evaluate the algorithms, segments of the EEG signal corresponding to the Ramsay score assessments were extracted. Preliminary calculation of HFD and SpEn was performed to the whole data and the segments to be analyzed were chosen according to the following rules:

- the segment had to precede the Ramsay score assessment
- the segment had to locate as close in time to the Ramsay score assessment as possible. A short margin, however, was left between the end of the segment and the Ramsay score assessment to ensure that the assessment procedure would not alter the patient's level of consciousness
- the segment corresponding to a certain Ramsay score assessment was discarded if the burst-suppression pattern was detected, if the signal was hidden by noise, or if the preliminary calculations gave unstable values.

Valid signal segments obtained from the data were distributed according to the Ramsay score values as follows.

Ramsay score:	1	2	3	4	5	6
Number of segments:	7	20	69	82	36	107.

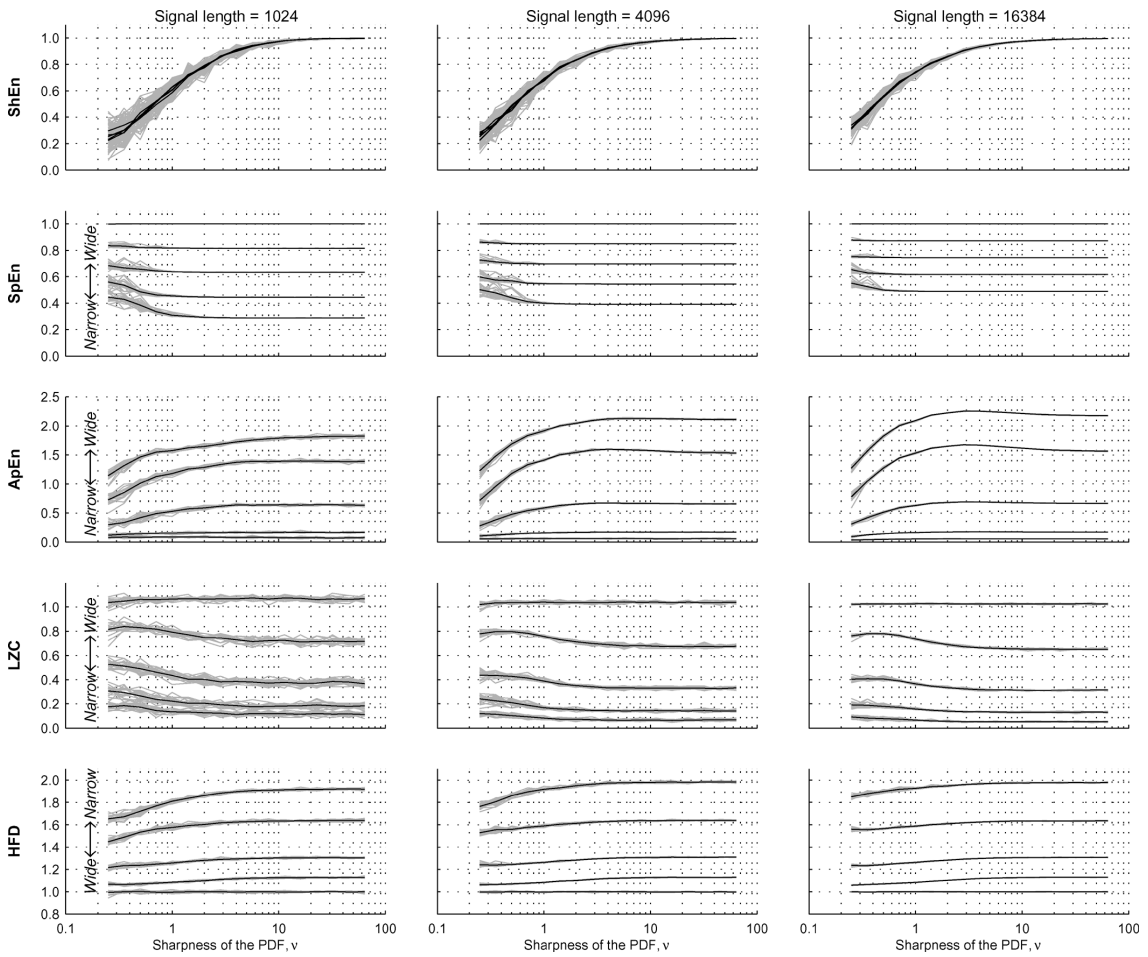

Fig. 3. Entropy/complexity of the generated test signals. The rows correspond to the measures described in Sections II-Ato II-E (from top to bottom: ShEn, SpEn, ApEn, LZC, and HFD). Columns from left to right represent the length of test signals: 1024, 4094, and, 16 384, respectively. 20 surrogates were generated for every ν of (17) and every r of (18). The measure values for individual surrogates and the averages over the surrogates are represented by gray and black lines, respectively. On all the plots the x-axis represents the PDF's sharpness/flatness controlling parameter ν and the y-axis shows the value of the corresponding entropy/complexity measure. Different curves on the plots correspond to different spectral bandwidth. The dependence of the parameter values on spectral bandwidth is indicated by the arrows at the left side of each row (except for ShEn, which does not depend on spectral bandwidth). For example, on the SpEn plots the upper curve corresponds to the widest spectrum ($r = 1$) and the lowest one corresponds to the narrowest spectrum ($r = 0.01$).

More detailed description of the data and the segment selection procedure can be found in [8].

Before calculating the measures the extracted signal segments were prefiltered. We used bandpass linear phase equiripple filter with high-pass cutoff frequency of 2 Hz, transition band width of 2 Hz and passband and stopband attenuation of 0.01. The high-frequency component of the measured signal during sedation has twofold meaning—on one hand, the frequency band of the EEG can extend up to 40 Hz or even higher; on the other hand, at high frequencies the signal can be contaminated by the muscle activity, especially as the patient wakes up from sedation. In [25] the effective border frequency between the EEG and the muscle activity for depth of sedation analysis was found to be about 20 Hz. Although noise from the EEG point of view, the muscle activity can be useful in the early detection of arousal from sedation. Due to this dual interpretation of high-frequency components we performed the calculations using three low-pass cutoff frequencies: 19, 37, and 47 Hz (columns of Fig. 5 in which the results are presented). Comparing the scales of the y-axis in the figure shows that the values of ApEn, LZC, and HFD greatly depend on the cutoff frequency while SpEn and ShEn are relatively insensitive to the high-frequency components.

Another feature of the analysis influencing the results is the window length. In Fig. 5, the results are presented for windows of 5, 20, and 60 s. The windows are extended backward from the endpoint of the selected segments. It can be seen that while ApEn, LZC, and HFD are relatively independent of the amount of data, SpEn and, in some cases also ShEn, show significant trend. This comes from the fact that ShEn and SpEn both use

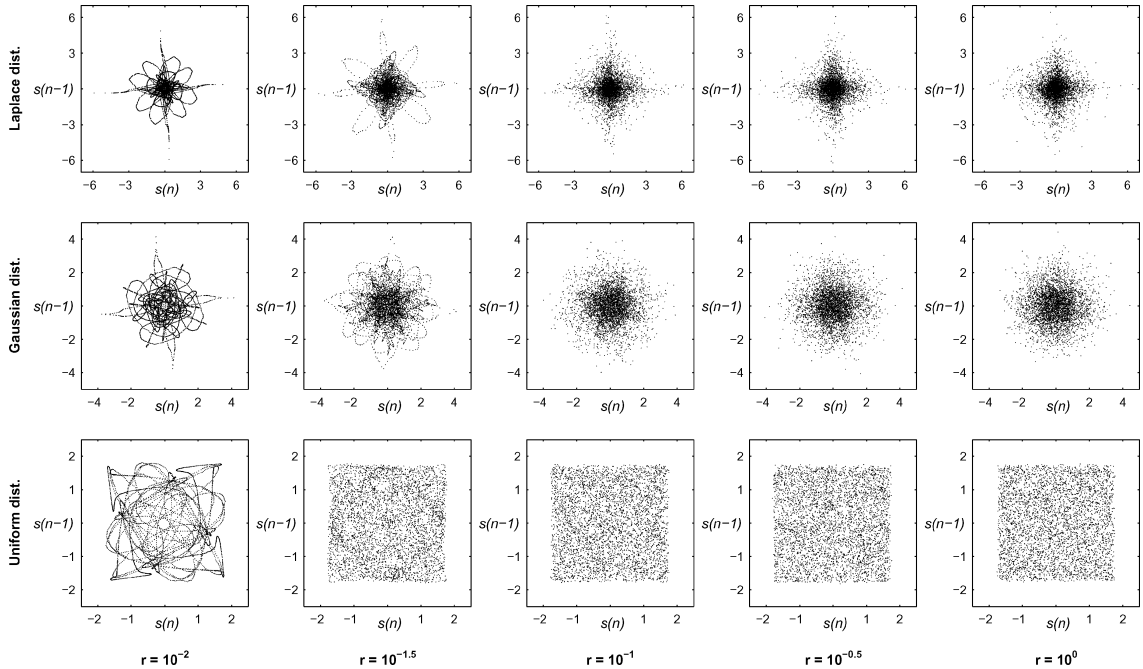

Fig. 4. Phase space representation of the test data of Laplace, Gaussian and uniform distribution and of spectral bandwidth corresponding to all values of r given by (18).

transformation over the Shannon function. In the case of SpEn, for example, it is well known that the fast Fourier transform (FFT) algorithm used for the calculation of this measure gives an inconsistent estimate of the power spectrum and thus increasing the window length increases the relative (per constant frequency range) variability of the spectrum estimate. This influences significantly the acquired SpEn values. The same principle affects the values of ShEn if the filling of the histogram varies for different data lengths. In the considered application, however, the dependence of the measures on the window length does not restrain the interpretation of the analysis results as far as we compare the values achieved using similar windows.

Statistical analysis was performed using the Wilcoxon ranksum test. This test does not assume Gaussian distribution of the data and allows the amount of data to vary from class to class. The tables in Fig. 5 show the p-values calculated pairwise for the six Ramsay scores in the case of 20 second window. The cases when the entropy/complexity increased with increasing level of sedation (higher Ramsay score) are marked in italics and those giving p-value lower that 0.05 are marked in bold. Although the amount of data used in the current study is too small for any final conclusions the methods based on the phase space background (ApEn and HFD) or pattern recurrence (LZC) seem to have slight advantage in discriminating the EEG corresponding to different Ramsay scores. All the methods seem to have difficulty in discriminating Ramsay score 5. Our preliminary analysis using other data sets shows that this phenomenon is not related to the particular data set but is more general, indicating the need for further study.

For comparison, we processed our data with the Beta Ratio (BRt) measure applied as one of the three components in the Aspect Medical Inc. Bispectral Index monitor. BRt is calculated as

$$BRt = \log \frac{P_{30-47}}{P_{11-20}} \tag{19}$$

where P_{30-47} and P_{11-20} denote the power in the frequency bands 30–47 Hz and 11–20 Hz, respectively. It has been argued that BRt is the main component in BIS and that the bispectral analysis actually does not add much value from the monitoring point of view [26]. It might even be more so in the case of sedation as in BIS BRt has higher weight in light anesthesia and in sedation the level of unconsciousness is usually lighter compared to surgical anesthesia. The BRt for our data is shown in Fig. 6.

V. Discussion

Assessment of depth of anesthesia and sedation is a research area of great theoretical and practical interest. Although several new methods for brain function analysis like functional magnetic resonance imaging, magnetoencephalography, various kinds of evoked potentials, etc. have emerged, EEG is still the most suitable parameter for long term monitoring. Assessment of depth of anesthesia and sedation is closely related to brain monitoring in broader range of situations like, e.g., the detection of hypoxia and ischemia.

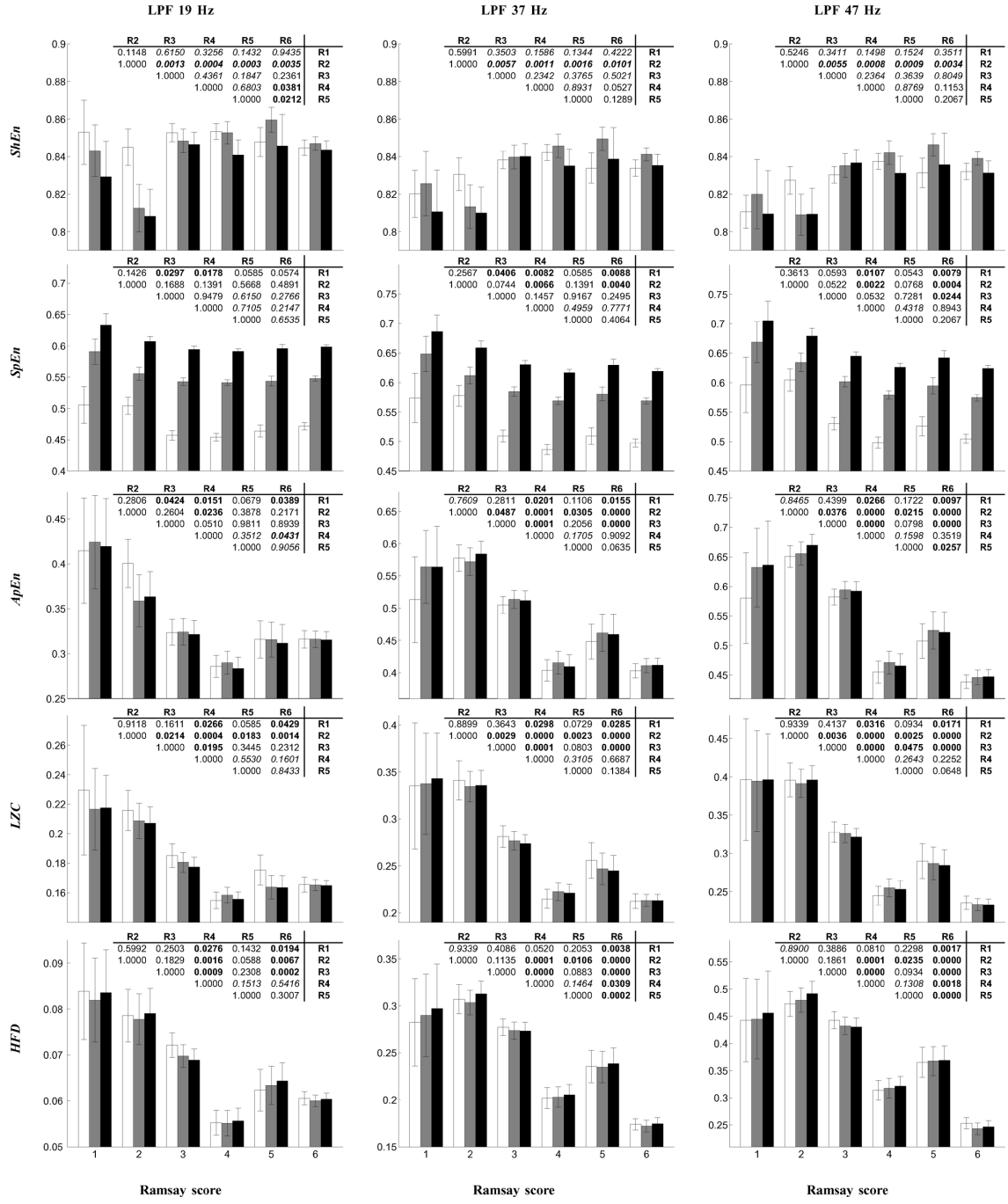

Fig. 5. Mean and standard error of ShEn, SpEn, ApEn, LZC, and HFD (rows from top to bottom, respectively) calculated from the EEG segments corresponding to Ramsay scores 1 to 6. The columns in the figure from left to right correspond to the cutoff frequency of the prefilter of 19, 37 and 47 Hz, respectively. The white bars correspond to 5 s, gray bars to 20 s, and black bars to 60 s window length. The tables indicate the p-value calculated pairwise for the signal segments corresponding to different Ramsay scores using the Wilcoxon ranksum test. The p-values are calculated for window length 20 s. The cases when the entropy/complexity increased with increasing level of sedation (higher Ramsay score) are marked in italics and those giving p-value lower that 0.05 are marked in bold.

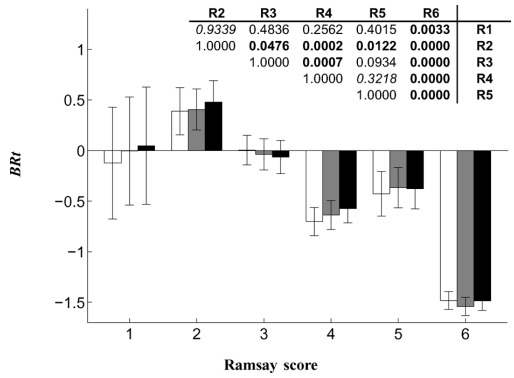

Fig. 6. Beta ratio of the EEG data. For detailed explanation refer to the caption of Fig. 5.

Our approach in this paper has been to study the sensitivity of various entropy and complexity measures to the change in signal properties like spectral bandwidth and amplitude distribution. The results clearly show that the various parameters called entropy actually measure different properties of the signal. ShEn, the "classical" entropy measure, does not depend on signal spectrum while spectral entropy is insensitive to the amplitude distribution. This is easy to predict from the mathematical formulas defining these parameters. The other tested methods, ApEn, LZC and HFD, are sensitive to both spectral bandwidth as well as amplitude distribution, however, the dependence on bandwidth dominates.

The last decade has seen the presentation of a large number of EEG measures for anesthesia monitoring. However, no algorithm significantly better than the others has been developed. Fig. 5 shows that while all the other tested entropy and complexity measures decrease with deepening sedation, the "classical" ShEn actually tends to behave in the opposite manner (see also [4]). ShEn is the only tested measure depending solely on the amplitude distribution being thus indifferent to the time order of the signal samples. When compared to the results in Fig. 3 the cautious conclusion that the amplitude distribution of the EEG signal gets wider with deepening sedation, especially when there is a transition from Ramsay score 2 to Ramsay score 3 can be made. The results also show that the frequency content of the EEG signal is generally a better indicator of the sedation depth compared to the amplitude distribution. Actually, the more sensitive the algorithm is to the changes in bandwidth, the better it seems to discriminate the levels of sedation.

Comparison of the performance of different measures is difficult due to the following reasons.

1) Each measure can be calculated using various algorithms. A good example here is the choice of the method for the power spectrum estimation in the calculation of SpEn. Our recent studies show that if, instead of the FFT, autoregressive modeling is used for estimating the power spectrum, the SpEn values no more depend on the window length. Using other methods than the FFT for spectrum estimation, however, did not improve the SpEn as a measure of depth of sedation. A detailed study on the influence of the spectrum estimation method on SpEn will be published elsewhere. In this paper, however, we used the FFT for comparability reasons as this algorithm is also employed in the Datex Ohmeda Entropy module and thus applied in all the studies performed using this device.
2) For each algorithm certain parameter values should be fixed. The parameter values used in this paper are presented in Table I. They were chosen according to the values used in the literature for similar applications. Probably the most questionable is the choice of the embedding dimension m and the filtering level r_f for the ApEn measure. We made the calculations for $m = 2 \cdots 6$ and $r_f = 0.1$ SD, 0.2 SD both in the case of the surrogates as well as the real EEG signal. The analysis employing the surrogates showed that if the filtering level was decreased and/or the embedding dimension was increased, the monotonic trend of increasing entropy with increasing bandwidth was lost. In the case of higher dimensions the results for the surrogates of similar properties did not necessarily converge. This effect was more severe for shorter window lengths. The EEG analysis showed that increasing the embedding dimension did not improve the performance of the ApEn measure in discriminating between different Ramsay scores. In the case of short data segments (5 s) the behavior of ApEn was reversed at higher embedding dimensions—deeper sedation gave higher ApEn values.
3) Window length has an influence on the results. This can be caused by two reasons. First, the algorithm may be sensitive to the window length like, for example, in the case of the SpEn. Second, some algorithms may not give reliable results in the case of short data windows. In real-time monitoring systems relatively short data windows should be used to react quickly to alterations in the condition of the patient. Commercial depth-of-anesthesia monitors use a wide range of window lengths starting from a couple of seconds up to 60-s windows. In the Entropy module, for example, a carefully tuned windowing scheme is used where the window length varies with frequency. Our analysis indicates that in some cases 5-s window might be too short to get reliable results (see, for example, the ApEn results for LPF 37 or 47 and Ramsay score 1 in Fig. 5) whereas 20 s seems to be sufficient.
4) The frequency band of the signal is a crucial factor in the assessment of the depth of sedation. While most commercial algorithms employ EEG frequencies starting from 0.5 Hz, the lower cutoff frequency of the Danmeter Cerebral State Index (Danmeter A/S, Denmark), for example, is set at 6 Hz, neglecting the delta frequency band of the EEG signal. The key point in the choice of the upper cutoff frequency is the incorporation of the muscle activity into the depth of sedation index. Several commercial anesthesia monitoring systems display the EMG activity, obtained usually from the same electrodes as the EEG but using frequencies from 60–80 Hz, separately. Our recent analysis of the influence of the EEG frequency band on the various entropy/complexity measures shows that the behavior of several measures (SpEn and ApEn, for example) can actually be reversed, especially in the region of lighter sedation,

if high frequencies are cut off and the delta frequency band is fully incorporated. We have also found that remifentanil, an opioid often used together with sedative drugs, greatly influences the entropy measures when low frequencies are preserved (lower cutoff frequency at 0.5 Hz).

Although due to the arguments presented above it is not feasible to point out "the best" EEG measure for the assessment of the depth of sedation, our results indicate that the measures sensitive to both the power spectrum as well as the amplitude distribution, i.e., the ApEn, LZC and HFD, perform slightly better than the other two tested measures. In the case of the tested measures, window length of 20 s can be recommended. The dependence of the measures on the frequency content of the signal should be studied more systematically in the future. Comparison with the simple spectrum-based measure BRt, an important component of the BIS monitor, shows that BRt is superior in discriminating the Ramsay score 6 (i.e., deep sedation) while the tested entropy/complexity measures may have advantage in following the depth of sedation at lighter scales.

A serious obstacle to applying entropy/complexity measures in commercial monitoring systems is the difficulty in interpreting the results. The experience of neurophysiologists in classifying the EEG signal is based on visual analysis. By looking at the curve it is easy to detect beta activity or large delta waves, however, there is no experience on how the EEG of different ApEn, for example, looks like. This can be studied by generating surrogates of the real EEG signal with different entropy/complexity. We plan to address this problem in our future work.

In clinical practice an easy-to-use anesthesia/sedation monitor, performing well in a wide range of situations and for all anesthetic drugs would be needed. On the other hand, physiologically, anesthesia is not a well defined phenomenon as every anesthetic has somewhat different way of action [27]. Anesthesia can be viewed as a mixed state of unconsciousness, analgesia, muscle relaxation, amnesia. Even some of these components—unconsciousness, for example—are physiologically very difficult to define. As a solution to these contradictory points of view on anesthesia/sedation monitoring we suggest that a more specific approach to data analysis could increase the value of long-term brain monitoring. This contains the following features:

- recognition of drug specific patterns and events related to the condition of the patient;
- using more EEG channels in studies where the clinical setup affords;
- model based approach—the results of signal analysis could be fitted to models in known correspondence with the physiological state of the patient;
- more detailed analysis of the variation of EEG signal properties, linear as well as nonlinear, during anesthesia and sedation.

VI. Conclusion

In this paper, we have shown that the broad set of measures usually referred to as "entropy" and/or "complexity" actually reveal different properties of signals. While "classical" ShEn is sensitive to the amplitude distribution, spectral entropy depends purely on signal spectrum and the methods based on phase space and recurrence analysis are sensitive to both mentioned properties. This indicates that it is not correct to speak generally about EEG entropy but the term should be more specifically defined.

Analysis of the EEG signal during sedation in the ICU showed that the various entropy/complexity measures behave in a different manner when related to the clinical assessment of the Ramsay score. While ShEn increases or remains constant with deepening sedation, the other measures tend to decrease, although, there are exceptions like the case of Ramsay score 5, for example. Spectral properties seem to be more discriminative between different levels of sedation compared to amplitude distribution. Spectral entropy, calculated using the FFT for power spectrum estimation is more sensitive to the length of the data segment compared to the other measures. The values of ApEn, LZC, and HFD depend highly on the presence of high frequencies (19–47 Hz). This emphasizes the importance of the prefilter settings and window length when comparing the results achieved using different methods.

The results achieved by a simple spectral measure, the beta ratio, show its advantage in discriminating the Ramsay score 6 over the tested entropy/complexity measures. We suggest that combining different measures can increase the reliability of the overall index. It should also be noted that the analysis described in Section IV were performed on raw data. Preprocessing the data using various kinds of artifact removal algorithms, for example, could change the performance of different algorithms.

References

[1] I. J. Rampil, "A primer for EEG signal processing in anesthesia," *Anesthesiology*, vol. 89, pp. 980–1002, 1998.

[2] T. Lipping and V. Jäntti, "EEG signal in monitoring brain function in anesthesia and intensive care: a review," *Proc. Estonian Acad. Sci.: Eng.*, vol. 10, no. 2, pp. 95–109, 2004.

[3] M. Tribus and E. C. McIrvine, "Energy and information," *Scientif. Am.*, vol. 225, no. 3, pp. 179–188, 1971.

[4] J. Bruhn, L. E. Lehmann, H. Röpcke, T. W. Bouillon, and A. Hoeft, "Shannon entropy applied to the measurement of the electroencephalographic effects of desflurane," *Anesthesiology*, vol. 95, pp. 30–35, 2001.

[5] J. Bruhn, H. Röpcke, and A. Hoeft, "Approximate entropy as an electroencephalographic measure of anestetic drug effect during desflurane anesthesia," *Anesthesiology*, vol. 92, pp. 715–726, 2000.

[6] H. Viertiö-Oja, V. Maja, M. Särkelä, P. Talja, N. Tenkanen, H. Tolvanen-Laakso, M. Paloheimo, A. Vakkuri, A. Yli-Hankala, and P. Meriläinen, "Description of the entropy algorithm as applied in the datex—ohmeda S/5 entropy module," *Acta Anaesthesiol. Scand.*, vol. 48, pp. 154–161, 2004.

[7] X.-S. Zhang, R. J. Roy, and E. W. Jensen, "EEG Complexity as a measure of depth of anesthesia for patients," *IEEE Trans. Biomed. Eng.*, vol. 48, no. 12, pp. 1424–1433, Dec. 2001.

[8] A. Anier, T. Lipping, S. Melto, and S. Hovilehto, "Higuchi fractal dimension and spectral entropy as measures of depth of sedation in intensive care unit," in *Proc. 26th IEEE EMBS Annu. Int. Conf. (EMBC'04)*, San Francisco, CA, Sep. 2004, pp. 526–529.

[9] T. Schreiber and A. Schmitz, "Improved surrogate data for nonlinearity tests," *Phys. Rev. Lett.*, vol. 77, pp. 635–638, 1996.

[10] C. E. Shannon, "A mathematical theory of communication," *Bell Syst. Tech. J.*, vol. 27, pp. 379–423, July, October 1948, 623-656.

[11] T. Inouye, K. Shinosaki, H. Sakamoto, S. Toi, S. Ukai, A. Iyama, Y. Katsuda, and M. Hirano, "Quantification of EEG irregularity by use of the entropy of the power spectrum," *Electroencephalogr. Clin. Neurophysiol.*, vol. 79, pp. 204–210, 1990.

[12] I. A. Rezek and S. J. Roberts, "Stochastic complexity measures for physiological signal analysis," *IEEE Trans. Biomed. Eng.*, vol. 45, no. 9, pp. 1186–1191, Sep. 1998.

[13] A. Vakkuri, A. Yli-Hankala, S. Mustola, H. Tolvanen-Laakso, T. Sampson, and H. Viertiö-Oja, "Time-frequency balanced spectral entropy as a measure of anesthetic drug effect in central nervous system during sevoflurane, propofol, and thiopental anesthesia," *Acta Anaesthesiol. Scand.*, vol. 48, pp. 145–143, 2004, P. T..

[14] S. M. Pincus, "Approximate entropy as a measure of system complexity," *Proc. Nat. Acad. Sci.*, vol. 88, pp. 2297–2301, Mar. 1991.

[15] J. S. Richman and J. R. Moorman, "Physiological time-series analysis using approximate entropy and sample entropy," *Am. J. Physiol. Heart Circ. Physiol.*, vol. 278, pp. 2039–2049, 2000.

[16] K. K. Ho, G. B. Moody, C. K. Peng, J. E. Mietus, M. G. Larson, D. Levy, and A. L. Goldberger, "Predicting survival in heart failure case and control subjects by use of fully automated methods for deriving nonlinear and conventional indices of heart rate dynamics," *Circulation*, vol. 96, no. 3, pp. 842–848, 1997.

[17] A. Lempel and J. Ziv, "On the complexity of finite sequences," *IEEE Trans. Inf. Theory*, vol. IT-22, pp. 75–81, 1976.

[18] J. Szczepański, J. M. Amigó, E. Wajnryb, and M. V. Sanches-Vives, "Application of Lempel-Ziv complexity to the analysis of neural discharges," *Network: Computation Neural Syst.*, vol. 14, pp. 335–350, 2003.

[19] T. Higuchi, "Approach to an irregular time series on the basis of the fractal theory," *Physica D*, vol. 31, pp. 277–283, 1988.

[20] A. Accardo, M. Affinito, M. Carrozzi, and F. Bouquet, "Use of the fractal dimension for the analysis of electroenchepalographic time series," *Biol. Cybern.*, vol. 1997, pp. 339–350, 1997.

[21] T. Schreiber and A. Schmitz, "Surrogate time series," *Physica D*, vol. 142, pp. 346–382, 2000.

[22] A. Hyvärinen, J. Karhunen, and E. Oja, *Independent Component Analysis*. New York: Wiley, 2001.

[23] W. H. Press, S. A. Teukolsky, W. T. Vetterling, and B. P. Flannery, *Numerical Recipes in C: The Art of Scientific Computing*, 2nd ed. Cambridge, U.K.: Cambridge Univ. Press, 1992.

[24] M. Ramsay, T. Savege, and B. Simpson, "Controlled sedation with alphaxolene/alphadalone," *Br. J. Med.*, vol. 2, pp. 656–659, 1974.

[25] R. Rautee, T. Sampson, M. Särkelä, S. Melto, S. Hovilehto, and M. van Gils, "Application of spectral entropy to EEG and facial EMG frequency bands for the assessment of level of sedation in ICU," in *Proc. 26th IEEE EMBS Annu. Int. Conf. (EMBC'04)*, San Francisco, CA, Sept. 2004, pp. 3481–3484.

[26] A. Miller, J. W. Sleigh, J. Barnard, and D. A. Steyn-Ross, "Does bispectral analysis of the electroencephalogram add anything but complexity?," *Br. J. Anaesth.*, vol. 92, pp. 8–13, 2004.

[27] I. Kissin, "General anesthetic action: an obsolete notion?," *Anesth. Analg.*, vol. 76, pp. 215–218, 1993.

Rain Ferenets (S'00) was born in 1976 in Rapla, Estonia. He received the M.Sc. degree in electronics and biomedical engineering in 2002, from the Tallinn University of Technology, Tallinn, Estonia. He is currently working toward the Ph.D. degree in signal processing in Tampere University of Technology, Tampere, Finland.

His research field includes biomedical signal processing in general and processing anesthesia EEG signals in particular.

Tarmo Lipping (M'03–SM'06) was born in 1967 in Tallinn, Estonia. He received the M.Sc. and Ph.D. degrees in 1995 and 2001, respectively, from the Department of Information Technology, Tampere University of Technology, Tampere, Finland.

During 2001–2002 he spent one year as a post doc at Dartmouth College, NH. In 2002 and 2003, he held a professorship in the Biomedical Engineering Centre at Tallinn University of Technology, Estonia, serving as the head of the Centre. Since 2004 he is Professor of Signal Processing in the Pori Unit of Tampere University of Technology. His main research interest is in biomedical signal analysis, especially in brain monitoring during anesthesia and in the Intensive Care Unit.

Andres Anier (S'04) received the M.Sc. degree from the faculty of information Technology, Tallinn University of Technology, Tallinn, Estonia, in 2002. During 1996 to 2002 his research topic was multiresolution time-frequency analysis of polygraphic records of physiological signals. Since 2003, he is working towards the Ph.D. degree in the Biomedical Engineering Centre, Tallinn University of Technology.

His current research interests include development of automatic system for the assessment of depth of anesthesia using EEG signal, and transesophageal ventricular PES.

Ville Jäntti was born in 1950 in Helsinki, Finland. He studied at the University of Turku, Finland and received the M.D. and Ph.D. degrees in 1974 and 1982, respectively.

Dr. Jäntti is specialized in clinical neurophysiology in 1981.

He has lectured regularly in Universities of Turku and Tampere, as well as Tampere Technical University. He is senior lecturer (docent) in clinical neurophysiology in universities of Tampere and Oulu, Finland. He has published over 100 papers and chapters in textbooks on clinical neurophysiology, and the balance physiology and neurophysiology of anesthesia, especially cognitive anesthesiology.

Sari Melto was born in 1966. She graduated as Registered Nurse in 1990, and has specialized in medicine and surgery.

Since graduation she has worked in the Intensive Care Unit of South Karelia Central Hospital, Lappeenranta, Finland.

Seppo Hovilehto was born in 1954 in Astola, Finland. He received the M.D. degree in 1979 and specialized in anesthesiology at University of Helsinki, Helsinki, Finland, in 1986.

He is the Head of the Intensive Care Unit of South Karelia Central Hospital, Lappeenranta, Finland.

PUBLICATONS

Publication IV

Anier, A., Lipping, T., Jäntti, V., Puumala, P. and Huotari, A-M. Entropy of the EEG in transition to burst suppression in deep anaesthesia: surrogate analysis. *Engineering in Medicine and Biology Society (EMBC), 2010 Annual International Conference of the IEEE,* pp. 2790-2793, 2010.

32nd Annual International Conference of the IEEE EMBS
Buenos Aires, Argentina, August 31 - September 4, 2010

Entropy of the EEG in transition to burst suppression in deep anesthesia: surrogate analysis.

Andres Anier *Student Member, IEEE*, Tarmo Lipping *Senior Member, IEEE*, Ville Jäntti, Pasi Puumala and Ari-Matti Huotari

***Abstract*— In this paper 5 methods for the assessment of signal entropy are compared in their capability to follow the changes in the EEG signal during transition from continuous EEG to burst suppression in deep anesthesia. To study the sensitivity of the measures to phase information in the signal, phase randomization as well as amplitude adjusted surrogates are also analyzed. We show that the selection of algorithm parameters and the use of normalization are important issues in interpretation and comparison of the results. We also show that permutation entropy is the most sensitive to phase information among the studied measures and that the EEG signal during high amplitude delta activity in deep anesthesia is of highly nonlinear nature.**

I. INTRODUCTION

Entropy of the electroencephalographic signal (EEG) has been considered by many research groups as a promising measure of the level of consciousness [1], [2]. EEG entropy has also been found as an indicator of ischemia and hypoxia in the Intensive Care Unit (ICU) as well as of neurological recovery after cardiac arrest [3]. A measure of signal entropy based on the power spectrum, the spectral entropy measure (SpEn), is the main feature underlying the commercial M-Entropy® index of anesthetic depth available by GE Healthcare Finland [4].

The term 'entropy' was introduced in the field of information technology by Claude Shannon in his classic paper on communication theory [5]. This measure, widely known as Shannon entropy, is calculated by applying the Shannon equation to the probability distribution of the variable under consideration. Another entropy measure, the Spectral entropy (SpEn), is obtained in a similar way except that the probability distribution is replaced by the normalized power spectrum of the variable. Still other measures of signal entropy, Approximate entropy (ApEn) and Sample entropy (SmpEn), are based on the phase space representation of the time series. Permutation entropy (PrmEn), on the other hand, quantifies the occurrences of patterns in the time series. Comparison of different measures of EEG signal entropy in anesthesia has resulted in a boom of scientific papers. Comparison is, however difficult, as each study uses different montages, filters, and different sets of analysis parameters.

In this paper we approach the problem of time domain patterns with surrogate signals. In surrogate analysis some signal properties are fixed while others are varied to obtain a set of surrogate signals. If the response of an algorithm to the surrogates is similar to the response to the original signal it can be concluded that the algorithm is not sensitive to the properties of the signal varied in the surrogate generation process. A common way to generate surrogates is to calculate the Fourier' transform of the signal segment, randomize the phase response and apply the inverse Fourier' transform. Phase randomization modifies the amplitude distribution of the time series towards Gaussian distribution with the consequence that the surrogate can be fully described by first and second order statistics. More realistic surrogates can be obtained by iteratively modifying the properties of a surrogate so that both the power spectrum as well as the amplitude distribution resemble that of the original signal as well as possible [6], [7].

The aim of this paper is to test the ability of various entropy algorithms to follow the changes in the EEG signal during the transition from continuous EEG to burst suppression in deep anesthesia. The algorithms are applied to the original signal as well as surrogates to evaluate their sensitivity to nonlinearities in the signal.

II. MATERIAL AND METHODS

A. Patient data

The test data used in the analysis was obtained from a 40 years old male patient undergoing a routine surgery. Propofol was used as the anesthetic agent. The signal was obtained from channel Cz-M2. The signal was prefiltered using a bandpass FIR filter with lower and upper cutoff frequencies of 0.5 and 35 Hz, respectively. As the study protocol involved somatosensory evoked responses (not present in the signal segment used in this analysis), the original sampling frequency was 20 kHz. Before applying the entropy algorithms the signal was downsampled to 100 Hz, however, using appropriate anti-aliasing filtering.

B. Entropy measures

1) Spectral entropy: The underlying principle of spectral entropy, $SpEn$, is straightforward – the Shannon function:

$$y = -\sum_i x_i \log x_i, \tag{1}$$

A. Anier is with ELIKO Competence Centre, Estonia anier@girf.ee
T. Lipping is with Pori unit of Tampere University of Technology, Pori, Finalnd tarmo.lipping@tut.fi
V. Jäntti is with Seinäjoki Central Hospital, Seinäjoki, Finalnd ville.jantti@uta.fi
P. Puumala is with Department of Clinical Neurophysiology, Jorvi Hospital, University Hospital of Helsinki, Helsinki, Finland ppuumala@pp.sonera.net
A-M. Huotari is with Department of Anesthesiology, Oulu University Hospital, Oulu, Finalnd

is applied to the normalized power spectrum P_n (normalized in the sense: $\sum P_n = 1$) of the given signal:

$$SpEn = -\sum_{i=f_l}^{f_h} P_i \log P_i, \tag{2}$$

where f_l and f_h define the frequency band we are interested in [8].

Usually spectral entropy is normalized so that its values are guaranteed to lie between 0 and 1:

$$SpEn_n = \frac{SpEn}{\log N}, \tag{3}$$

where N is the number of frequency components in the range $[f_l, f_h]$

2) Approximate entropy: Approximate entropy, $ApEn$, introduced by Pincus [9], is a measure quantifying the unpredictability or randomness of the signal. $ApEn$ is originated from nonlinear dynamics but unlike most measures coming from this field it does not require the use of limits ($t \to \infty$, $r \to 0$, $N \to \infty$, $m \to \infty$). Therefore, it is more suitable for signals of finite length.

The calculation of $ApEn$ of the signal s of the finite length N is performed as follows. First, fix a positive integer m and a positive real number r. Next, from the signal s the $N-m+1$ vectors $\mathbf{x}_m(i) = \{s(i), s(i+1)..., s(i+m-1)\}$ are formed. After that, for each $i, 1 \leqslant i \leqslant N-m+1$, the quantity $C_i^m(r)$ is calculated using:

$$C_i^m(r) = \frac{\text{number of such } j \text{ that } d[\mathbf{x}_m(i), \mathbf{x}_m(j)] \leqslant r}{N-m+1}, \tag{4}$$

where the distance d between the vectors $\mathbf{x}_m(i)$ and $\mathbf{x}_m(j)$ is defined as:

$$d[\mathbf{x}_m(i), \mathbf{x}_m(j)] = \max_{k=1,2,...,m} (|s(i+k-1) - s(j+k-1)|) \tag{5}$$

Next, the quantity $\Phi^m(r)$ is calculated as:

$$\Phi^m(r) = \frac{1}{N-m+1} \sum_{i=1}^{N-m+1} \log C_i^m(r) \tag{6}$$

Finally, the approximate entropy is defined as follows:

$$ApEn(m, r, N) = \Phi^m(r) - \Phi^{m+1}(r) \tag{7}$$

The parameter r corresponds to the maximum allowable distance between the neighboring trajectory points; therefore, r can be viewed as a filtering level. The parameter m is the embedding dimension and it determines the dimension of the phase space.

Frequently, r is chosen according to the signal's standard deviation (SD); it has been suggested that the initial value for r be 0.2 SD. A common value for m in EEG signal analysis is 2.

3) Sample entropy: Similarly to ApEn, Sample entropy (SampEn) is also based on phase space representation of the time series. There are several differences between the two algorithms, however. Firstly, in calculating the number of similar sequences (i.e., close data points in phase space) self-matches ($i = j$ in equation 4) are excluded. Secondly, equations 6 and 7 are replaced by the following operations:

$$C^m(r) = \frac{1}{N-m} \sum_{i=1}^{N-m} C_i^m(r) \tag{8}$$

and

$$SampEn(m, r, N) = -\ln \frac{C^{m+1}(r)}{C^m(r)} \tag{9}$$

4) Permutation entropy: Permutation entropy (PermEn) measures the randomness of the occurrence of symbols in a time series [10], [11]. The symbols are obtained by considering the rank order of signal samples in a fixed length sequence. Let the symbol length be 4. As an example, a sequence of signal values $\mathbf{x}_4(t) = 5973$ gives the symbol 3021 as in this case $x(t+3) < x(t) < x(t+2) < x(t+1)$. All possible sequences of length 4 are considered and the probabilities of occurrence of each of the 4! symbols are found. PermEn is calculated based on these probabilities according to the Shannon equation (equation 1).

5) Higuchi fractal dimension: Fractal dimension is another measure of signal complexity, generally evaluated in phase space by means of correlation dimension. Higuchi proposed an algorithm for the estimation of fractal dimension directly in time domain without reconstructing the strange attractor [12]. This method gives reasonable estimate of fractal dimension in case of short signals and is computationally fast. The reason for including Higuchi fractal dimension in this comparison was our previous experience with this measure.

Higuchi's algorithm is based on the following scheme: from a given signal $s = \{s(1), s(2), ..., s(N)\}$, k new curves s_m^k are constructed as follows:

$$\begin{aligned} s_m^k &= \{s(m), s(m+k), ..., s(\lfloor (N-m)/k \rfloor \cdot k)\} \\ &\quad m = 1, 2, ..., k, \end{aligned} \tag{10}$$

where both m and k are integers and they indicate the initial time and the time interval, respectively. The length, $L_m(k)$, of each curve s_m^k is calculated as

$$L_m(k) = \left[\left(\sum_{i=1}^{\lfloor \frac{N-m}{k} \rfloor} |s(m+ik) - s(m+(i-1)k)| \right) \cdot \frac{N-1}{\lfloor \frac{N-m}{k} \rfloor k} \right] \Big/ k \tag{11}$$

The length of the curve for time interval k, $L(k)$, is calculated as the average of the m curves $L_m(k)$ for $m = 1, ..., k$. If $L(k) \propto k^{-D}$, the signal is fractal-like with the dimension D. Therefore, if $L(k)$ is plotted against $1/k$, where $k = 1, ..., k_{\max}$, in double logarithmic plot, the data

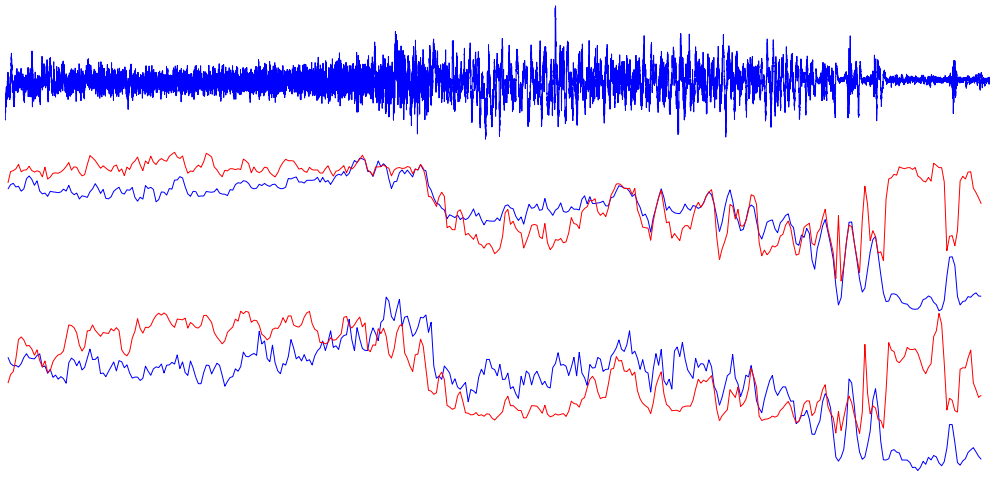

Fig. 1. The original EEG signal (upper curve), approximate entropy and sample entropy. The entropy measures are calculated using segment-by-segment normalization (red curves) as well as in a non-normalized manner (blue curves)

points should fall into straight line with the slope D. Finally, linear fitting by the means of least-squares is applied to the pairs $(\log 1/k, \log L(k))$, $k = 1, ..., k_{\max}$ and the slope of the obtained line is calculated giving the estimate of the fractal dimension D.

C. IAAFT algorithm for surrogate generation

Let P be the power spectrum of the original signal s and c a copy of the signal sorted in ascending order. At each iteration stage (i) there is a sequence $r^{(i)}$, which has the correct probability distribution given by s and a sequence $s^{(i)}$, which has the correct power spectrum given by P. The process starts by assigning $r^{(0)}$ the random shuffle of s. Each following iteration contains two consecutive steps.

In the first step, $r^{(i)} \rightarrow s^{(i)}$, the Fourier transform, $R^{(i)}$, of $r^{(i)}$ is obtained, $R^{(i)} = \mathcal{DFT}\{r^{(i)}\}$, where $\mathcal{DFT}$ denotes the Discrete Fourier Transform operator. Next, the amplitude $|R^{(i)}|$ is replaced by the desired one, i.e. with $\sqrt{P}$, and the complex phase of $R^{(i)}$, $e^{j\psi^{(i)}} = R^{(i)}/|R^{(i)}|$, is kept. Hereafter, the inverse Fourier transform is taken and $s^{(i)}$ is obtained, $s^{(i)} = \mathcal{IDFT}\{\sqrt{P}e^{j\psi^{(i)}}\}$, where $\mathcal{IDFT}$ denotes the Inverse Discrete Fourier Transform operator.

In the second step, $s^{(i)} \rightarrow r^{(i+1)}$, rank-ordering is performed: $r^{(i+1)}(n) = c_{\mathrm{rank}\{s^{(i)}(n)\}}$, $n = 1, ..., N$, where N is the length of the given signal s. Here $\mathrm{rank}\{s^{(i)}(n)\}$ denotes the ascending rank of $s^{(i)}(n)$, i.e. $\mathrm{rank}\{s^{(i)}(n)\} = 1$ if $s^{(i)}(n)$ is the smallest element of $s^{(i)}$, $\mathrm{rank}\{s^{(i)}(n)\} = 2$ if $s^{(i)}(n)$ is the 2nd smallest element of $s^{(i)}$ and so forth.

The first step enforces the correct power spectrum but it alters the probability distribution. The second step, on the other hand, guarantees the correct probability distribution but power spectrum is changed. Therefore, these two steps have to be iterated several times until the error between the original power spectrum and the obtained one falls below a predefined value.

III. RESULTS

To show the influence of the algorithm parameters on the results normalized as well as non-normalized versions of ApEn and SampEn algorithms were applied to the signal segment. The selected segment marks the transition from continuous EEG to burst suppression with a period of high amplitude delta-frequency ($0.5 \ldots 4$ Hz) activity in the middle (figure 1). This is a typical pattern seen in deep anesthesia. The entropy measures were calculated in a stepping window of length 4 s and the step size was 1 s. The value $m = 2$ was used for both algorithms. For ApEn the value of the filtering parameter r_f was 0.2 SD, however, in the case of the blue curve the standard deviation was calculated over the whole signal while in the case of the red curve standard deviation was obtained window-by-window. For SampEn the red curve was obtained using variance normalization window-by-window while the blue curve marks the behavior of the measure without normalization. In figure 2 the behavior of all the above presented entropy measures is shown for the original signal as well as for the phase randomized and amplitude adjusted surrogates. No window-by-window normalization is used. The symbol length parameter was set to 4 in the calculation of PermEn and the parameter value $k = 8$ was used in Higuchi fractal dimension.

IV. DISCUSSION AND CONCLUSIONS

It has been suggested that Approximate entropy classifies correctly anesthetic depth also during burst suppression [13]. The results presented in figure 1 indicate that this property depends on normalization. More specifically, if the filtering parameter is adjusted according to the standard deviation of the signal window-by-window, ApEn, like SpEn for example, scales up the noisy signal during suppression yielding high entropy values.

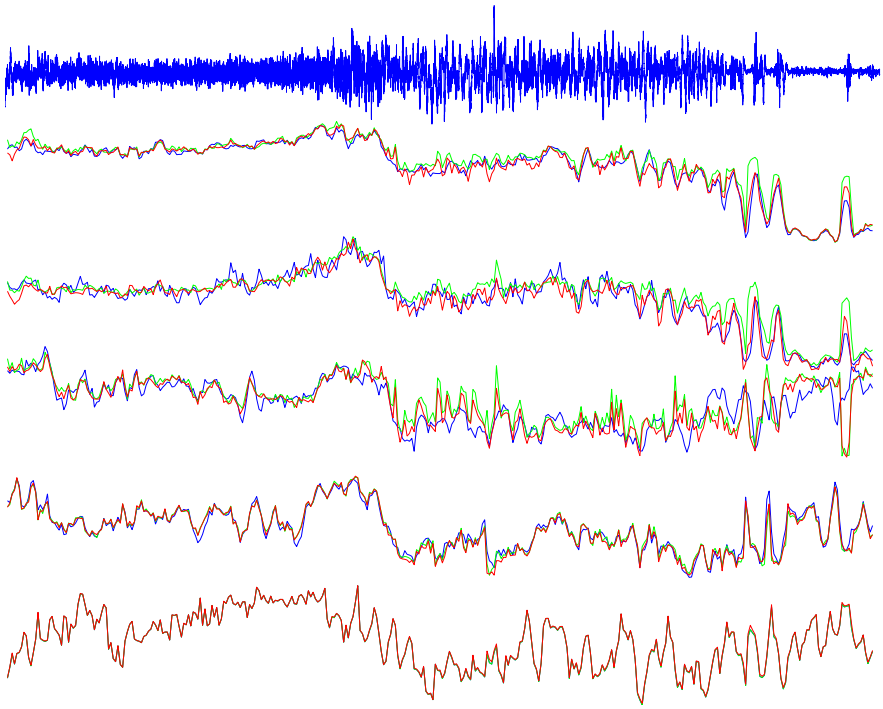

Fig. 2. The original signal and the entropy measures (from top to bottom): Approximate entropy, Sample entropy, Permutation entropy, Higuchi fractal dimension, and Spectral entropy. For each entropy measure the entropy of the original signal (blue curves), the average entropy of 10 phase-randomized surrogates (green curves), and the average entropy of 10 amplitude adjusted surrogates (red curves) are shown

The results presented in figure 2 show that permutation entropy is highly sensitive while Higuchi fractal dimension is almost insensitive to phase information and nonlinearities in the signal. As power spectrum does not contain phase information, the three curves of SpEn are almost identical. Quite naturally, for segments when the results for surrogates differ from those for the original signal, the IAAFT-surrogates give values between those for the the original signal and those for the phase randomization surrogates (red curve lies between blue and green curves). The three curves disagree to greater extent during the period of high delta waves indicating higher degree of nonlinearities.

V. ACKNOWLEDGMENTS

This research has been partly supported by European Regional Development Fund, Competence Centre program of Enterprise of Estonia

REFERENCES

[1] J. Bruhn, T. W. Bouillon, A. Hoeft, and S. L. Shafer, "Artifact robustness, inter- and intraindividual baseline stability, and rational EEG parameter selection," *Anesthesiology*, vol. 96, no. 1, 2002.

[2] R. Ferenets, T. Lipping, A. Anier, V. Jantti, S. Melto, and S. Hovilehto, "Comparison of entropy and complexity measures for the assessment of depth of sedation," *Biomedical Engineering, IEEE Transactions on*, vol. 53, no. 6, pp. 1067–1077, June 2006.

[3] X. Kang, X. Jia, R. G. Geocadin, N. V. Thakor, and A. Maybhate, "Multiscale entropy analysis of eeg for assessment of post-cardiac arrest neurological recovery under hypothermia in rats," *Biomedical Engineering, IEEE Transactions on*, vol. 56, no. 4, pp. 1023 –1031, april 2009.

[4] H. Viertiö-Oja, V. Maja, M. Särkelä, P. Talja, N. Tenkanen, H. Tolvanen-Laakso, M. Paloheimo, A. Vakkuri, A. Yli-Hankala, and P. Meriläinen, "Description of the entropy^{tm} algorithm as applied in the Datex-Ohmeda s/5^{tm} entropy module," *Acta Anaesthesiologica Scandinavica*, vol. 48, no. 2, pp. 154–161, 2004.

[5] C. Shannon, "A mathematical theory of communication," *Bell Systen Techn J*, vol. 27, pp. (379–423):623–656, 1948.

[6] T. Schreiber and A. Schmitz, "Improved surrogate data for nonlinearity tests," *Phys. Rev. Lett.*, vol. 77, pp. 635–638, 1996.

[7] ——, "Surrogate time series," *Physica D*, vol. 142, pp. 346–382, 2000.

[8] T. Inouye, K. Shinosaki, H. Sakamoto, S. Toi, S. Ukai, A. Iyama, Y. Katsuda, and M. Hirano, "Quantification of EEG irregularity by use of the entropy of the power spectrum," *Electroencephalography and clinical Neurophysiology*, vol. 79, pp. 204–210, 1990.

[9] S. M. Pincus, "Approximate entropy as a measure of system complexity," *Proc. Natl. Acad. Sci.*, vol. 88, pp. 2297–2301, March 1991.

[10] C. Bandt and B. Pompe, "Permutation entropy: A natural complexity measure for time series," *Phys. Rev. Lett.*, vol. 88, no. 17, p. 174102, Apr 2002.

[11] X. Li, S. Cui, and L. J. Voss, "Using permutation entropy to measure the electroencephalographic effects of sevoflurane," *Anesthesiology*, vol. 109, no. 3, 2008.

[12] T. Higuchi, "Approach to an irregular time series on the basis of the fractal theory," *Physica D*, vol. 31, pp. 277–283, 1998.

[13] J. Bruhn, H. Röpcke, B. Rehberg, T. Bouillon, and A. Hoeft, "Electroencephalogram approximate entropy correctly classifies the occurrence of burst suppression pattern as increasing anesthetic drug effect," *Anesthesiology*, vol. 93, no. 4, pp. 981–985, 2000.

PUBLICATONS

Publication V

Anier, A., Lipping, T., Ferenets, R., Puumala, P., Sonkajärvi, E., Rätsep, I. and Jäntti, V. Relationship between approximate entropy and visual inspection of irregularity in the EEG signal, a comparison with spectral entropy. *British journal of anaesthesia,* 109(6), pp. 928-934, 2012.

BJA Advance Access published August 30, 2012

British Journal of Anaesthesia Page 1 of 7
doi:10.1093/bja/aes312

BJA

Relationship between approximate entropy and visual inspection of irregularity in the EEG signal, a comparison with spectral entropy

A. Anier[1], T. Lipping[2]*, R. Ferenets[1], P. Puumala[3], E. Sonkajärvi[4], I. Rätsep[5] and V. Jäntti[6]

[1] Institute of Biomedical Engineering, Tallinn University of Technology, Tallinn, Estonia
[2] Information Technology, Pori, Tampere University of Technology, Pohjoisranta 11A, PO Box 300, Pori FIN-28101, Finland
[3] Department of Clinical Neurophysiology, Jorvi Hospital, University Hospital of Helsinki, Helsinki, Finland
[4] Department of Anaesthesiology, Oulu University Hospital, Oulu, Finland
[5] North Estonian Regional Hospital, Tallinn, Estonia
[6] Department of Clinical Neurophysiology, Seinäjoki Central Hospital, Seinäjoki, Finland

*Corresponding author. E-mail: tarmo.lipping@tut.fi

Editor's key points

- Using artificial signals, this study compares the spectral and approximate entropy of the EEG to measure the hypnotic component of anaesthesia.
- These measures quantify different features of the signal and may therefore behave in an incomparable way when calculated for standardized EEG patterns.
- Understanding the differences in these measures is essential to use them in clinical practice.

Background. Several measures have been developed to quantify the change in EEG from wakefulness to deep anaesthesia. Measures of signal complexity or entropy have been popular and even applied in commercial monitors. These measures quantify different features of the signal, however, and may therefore behave in an incomparable way when calculated for standardized EEG patterns.

Methods. Two measures widely studied for anaesthesia EEG analysis were considered: spectral entropy and approximate entropy. First, we generated surrogate signals which had the same spectral entropy as a prototype signal, the sawtooth wave. Secondly, EEG samples where rhythmic pattern caused a peak in the power spectrum in the α-frequency band were modified by enhancing or suppressing the corresponding rhythm.

Results. We found that the value of spectral entropy does not, in general, correlate with the visual impression of signal regularity. Also, the two entropy measures interpret a standardized artificially modified EEG signal in opposite directions: spectral peak of increasing amplitude in the α-frequency band causes spectral entropy to increase but decreases approximate entropy when low frequencies are present in the signal.

Conclusions. Spectral entropy and approximate entropy of EEG are two totally different measures. They change similarly in deepening anaesthesia due to an increase in slow activity. In some cases, however, they may change in opposite directions when the EEG signal properties change during anaesthesia. Failure to understand the behaviour of these measures can lead to misinterpretation of the monitor readings or study results if no reference to the raw EEG signal is taken.

Keywords: anaesthesia, depth; EEG; monitoring, electroencephalography

Accepted for publication: 19 June 2012

Several commercial monitors, calculating an estimate of the hypnotic effect of anaesthetic drugs from the EEG, are available. Common to all of them is that they give an estimate of the hypnotic effect if anaesthetics with gabaergic mode of action are used. These drugs cause gradual slowing of the EEG until burst suppression and then continuous suppression. The patterns vary, however, depending on the drug and patient. The features which correlate with consciousness probably originate from the physiological systems controlling sleep and arousal.[1 2] Correspondingly, the indexes are also useful in the assessment of consciousness during sleep.

In addition to the commercial indexes, several other measures of the EEG signal have been proposed for the assessment of anaesthetic depth. Among these, the measures quantifying the complexity or regularity of the signal are especially popular. Many of these measures are called entropies, referring to the information-richness of the EEG. Despite the common name 'entropy', the measures like spectral entropy, approximate entropy, Shannon entropy, permutation entropy, etc. have different mathematical backgrounds and therefore describe different properties in the signal. Probably, the most curious example is the opposite change in Shannon entropy compared with approximate entropy with deepening anesthesia.[3–5] While most of the entropy measures (approximate entropy, spectral entropy) tend to decrease

with deepening anaesthesia, the Shannon entropy tends to increase.

The usefulness of the entropy measures in the assessment of anaesthetic depth is commonly justified by the claims that the EEG becomes more regular with deepening anaesthesia and that these measures correctly quantify this increase in regularity. Several studies have shown, however, that these assumptions do not hold in general. Certain conditions like EMG activity or arousal reactions, for example, can cause at least temporary irregularity in the measured EEG even in very deep anaesthesia.[6 7] On the other hand, in this study, we show that the results obtained by the entropy measures—depending on their mathematical background—may not correspond at all with what we visually consider regularity in the signal.

The increase in EEG regularity (and, consequently, the decrease in entropy) with deepening anaesthesia is often explained by the shift in the frequency content of the signal towards lower frequencies with the appearance of low-frequency rhythmic components.[8] We show that this kind of change does not necessarily affect the different entropy measures in a similar manner.

From the entropy measures, only spectral entropy has been applied in commercial depth-of-anaesthesia monitors up to now. Our aim in this study is to show that approximate entropy generally corresponds better to the visual impression of signal regularity as it takes into account the phase information in the signal. As the various measures of the assessment of depth of anaesthesia may respond in a contradictory manner to changes in the EEG, those who use and study these measures should understand the physiological basis and the principle of calculation of these measures.

Methods

Calculation of the entropy measures

Spectral entropy is calculated by applying the Shannon function to the normalized power spectrum. All the values in the power spectrum are equally used in the calculation of spectral entropy independent of their location on frequency axis. The phase information of the original signal and the frequency information in the power spectrum are thus omitted in the calculation. A description of the calculation algorithm is given by Viertiö-Oja and colleagues.[8] Approximate entropy, introduced by Pincus,[9] originates from non-linear dynamics, but unlike most measures coming from this field, it is calculated in time domain without phase space reconstruction of the signal. Therefore, it is more suitable for relatively short signal segments.[3 10 11] The calculation algorithm of the approximate entropy measure is described by various groups.[4]

Surrogate signals of sawtooth wave

We selected the sawtooth waveform as the original signal, as it presents a regular pattern (Fig. 1A). A sawtooth signal of 9995 data points, corresponding to a 19.99 s sample digitized at 500 Hz, was generated. The property of the spectral entropy of neglecting the phase information and the information about the location of the spectral values on the frequency axis was used in generating surrogate signals of identical spectral entropy. First, the phase values of the Fourier transform of the original signal were randomized (Fig. 1B). Secondly, the amplitude values were relocated on the frequency axis systematically around a dominant frequency (Fig. 1C) or at random (Fig. 1D). In each case, the surrogate signals were produced by applying the inverse Fourier transform of the frequency domain representation of the signal, that is, the modified amplitude spectrum, and randomized phase spectrum. We also calculated the amplitude spectrum of an EEG signal segment recorded in deep propofol anaesthesia and arranged the spectral values of the sawtooth wave signal in the same rank order as the spectral components of the EEG signal were located (Fig. 1E). The relocation in this case was performed according to the magnitude of the spectral components so that the *k*th highest spectral component of the sawtooth wave was shifted to the frequency at which the *k*th highest spectral component of the EEG signal segment occurred. This procedure was repeated from the highest to the lowest frequency component.

We produced 20 different realizations of surrogate signals for each case and calculated the approximate entropy of these signals. The mean and standard deviation of the approximate entropy over the realizations was calculated in each case in order to obtain a more reliable estimate.

Effect of increasingly rhythmic activity on spectral entropy and approximate entropy

In the second part of the analysis, we selected a sample of anaesthesia EEG with regular, rhythmic pattern seen in the power spectrum. Because α-rhythm has been used as an example of regular, rhythmic EEG in anesthesia[8] and is often recorded from frontal montage, we also selected an EEG sample with spectral peak at about 11 Hz. This was recorded from the derivation Fp1–Fp2 in propofol anaesthesia. The EEG sample was prefiltered using a linear-phase filter of passband 0.8, . . . ,45 Hz. The amplitude of the rhythmic component was manipulated using the autoregressive moving average (ARMA) modelling technique to obtain test signals of similar spectral properties as the original EEG signal but of eight different proportions of the rhythmic activity in the α-band (Fig. 2). The ARMASA software package developed by Broersen[12] (Delft University of Technology, The Netherlands) was used. Fifty realizations were calculated for each of the eight test conditions, and the spectral entropy and approximate entropy of these modified signals were presented as a function of their spectral peak height.

Results

Surrogate signals and their entropy

The results of surrogate analysis are presented in Figure 1. In the left column, 2 s samples of the original 19.99 s signal segment and its surrogates are presented, while the right

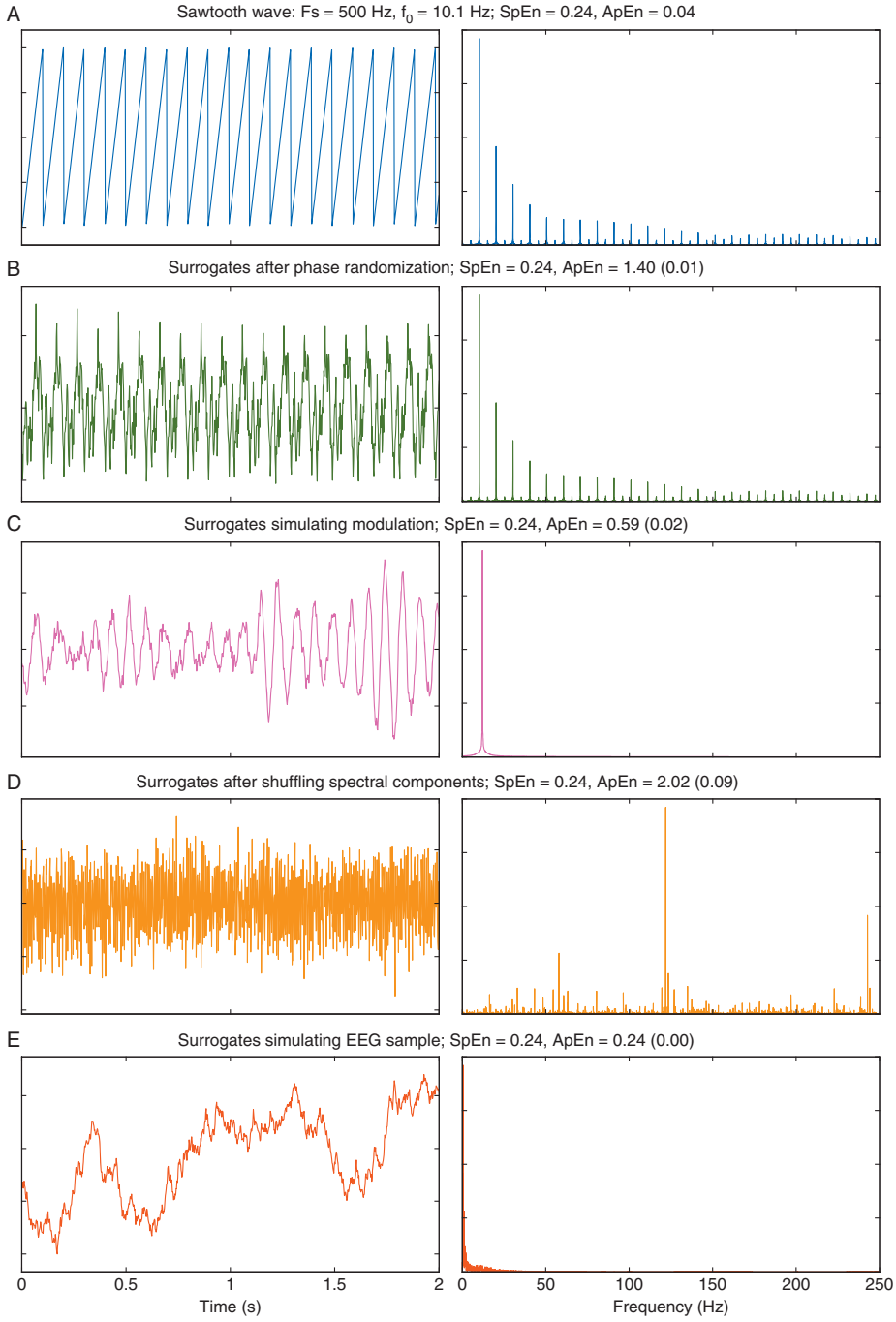

Fig 1 Waveforms (left column) and corresponding amplitude spectra (right column) of signals characterized by fixed spectral entropy (SpEn) of 0.24. In time domain, a 2 s excerpt of the waveforms is shown. The phase spectrum of all the surrogates is randomized. The approximate entropy (ApEn) estimate [mean (SD)] over 20 realizations of the surrogates is indicated above each row of the figure. The characteristic frequency of the original sawtooth wave is 10.1 Hz and the sampling frequency is 500 Hz.

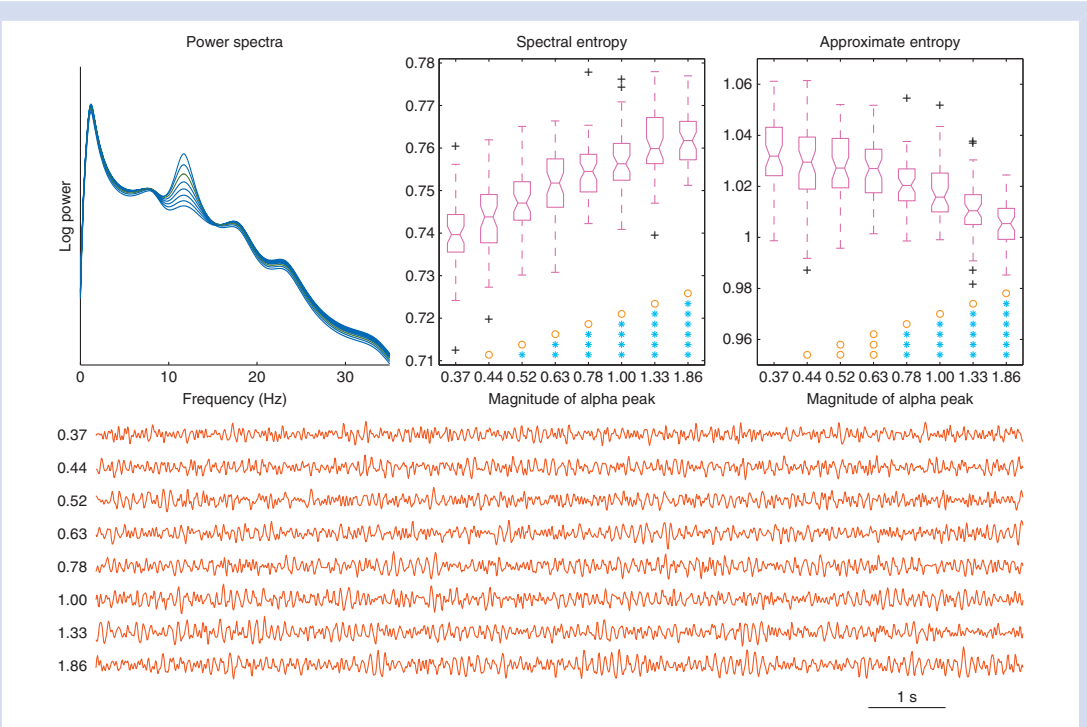

Fig 2 Sensitivity of spectral entropy and approximate entropy to rhythmic activity of the α-frequency band in the EEG. The proportion of the rhythmic activity in the signal is modified in eight steps using the ARMA modelling technique and the corresponding power spectra are plotted (upper left plot). From 50 realizations of the modified signals for each eight levels of the rhythmic activity, the spectral entropy and approximate entropy measures were calculated and presented as box plots (upper middle and right). Statistical significance of the trends of the entropy measures are indicated below the box plots: the bottommost mark indicates the result of comparing the corresponding peak magnitude to the case of maximally flat power spectrum (the leftmost box). A star indicates statistically significant difference. Samples of time domain waveforms of the modified signals are shown in the bottom half of the figure.

column shows the corresponding power spectra. From Figure 1A (the upper row), it can be seen that the power spectrum of the original sawtooth wave contains minor spurious components in addition to the harmonic ones. This is due to digitizing effects and comes from the fact that there is a non-integer number of samples in each sawtooth period. This is also the case with real-life signals: the period of the signal rhythm never exactly matches with the sampling frequency. The approximate entropy of the sawtooth wave is 0.04, indicating very high regularity. All the signals in this figure have spectral entropy of exactly 0.24 as they are spectral entropy surrogates.

When the phase spectrum of the sawtooth wave is randomized leaving the amplitude spectrum as is, a random-looking waveform is obtained (Fig. 1B); however, the periodicity of the waveform can still be well observed. The approximate entropy measure of this waveform is 1.40 (0.01) calculated over the 20 realizations of the random phase spectra. In Figure 1C, the components of the amplitude spectrum of the sawtooth wave are concentrated around a dominant frequency of 10 Hz to simulate the amplitude variation of the EEG α-rhythm. The signal waveform looks quite regular indeed and the approximate entropy of 0.59 (0.02) is obtained over the 20 realizations of the random phase spectra. When both the amplitude spectrum and the phase spectrum are randomized, a highly irregular signal waveform is obtained (Fig. 1D). As the amplitude difference between the highest and the second highest frequency component is quite large in the spectrum of the sawtooth wave, the rhythmicity of the signal waveform depends highly on the location of the highest component after reshuffling. In the case shown in Figure 1, the approximate entropy of 2.02 (0.09) is obtained, indicating very high irregularity. Rearranging the spectral components of the sawtooth wave according to the spectrum of an EEG signal sample resulted in a waveform resembling raw EEG signal (Fig. 1E). The spectral components of the generated surrogate signal decay significantly faster though compared with natural EEG signal. The phases of the frequency components were again randomized and the approximate entropy of 0.24 (0.00) was obtained.

The experiment shows that the waveforms characterized by fixed spectral entropy may look very different with the approximate entropy of the waveforms ranging from 0 to above 2, the latter being close to the value we previously obtained for white noise of nearly uniform amplitude distribution.[4]

Effect of rhythmic activity on spectral entropy and approximate entropy

Figure 2 shows the effect of rhythmic α-frequency pattern of varying amplitude on the entropy measures. In the upper left panel of the figure, the power spectra corresponding to different levels of the rhythmic activity are shown. The corresponding signal waveforms are shown in the lower panel. The increasing proportion of the α-frequency rhythm when moving from the top to bottom signal samples can well be observed from the waveforms. At the left of the curves, the ratio of the maximum power of the rhythmic component relative to that of the underlying EEG signal sample is indicated. The power of the rhythmic activity varies from 0.37 to 1.86 times that of the EEG sample.

The spectral entropy and approximate entropy measures calculated for 50 realizations of each spectral shape are indicated in the upper middle and upper right panels of the figure, respectively. The magnitude of the α-frequency component with respect to that of the original EEG segment is indicated below each boxplot. In the lower part of the panels, the statistical significance of the changes in the entropy measures is indicated. The stars denote statistically significant difference with 95% confidence level (balanced one-way analysis of variance test with multiple comparison correction using the Tukey's honestly significant difference criterion). The bottommost mark indicates the result of comparing the corresponding peak level with the case of maximally flat power spectrum. It can be seen that the spectral entropy measure increases significantly with each two-step increase in the peak level of the rhythmic activity. In the case of the approximate entropy, the first three steps of increase in the α-rhythm peak do not cause a significant change in the entropy. However, the entropy decrease becomes significant with higher proportions of the rhythmic activity. In summary, the results show that in the presence of very low-frequency components (<1.5 Hz), spectral entropy increases significantly (indicating the power spectrum becoming more flat and the signal more irregular), while approximate entropy decreases significantly (indicating the signal becoming more regular) when the EEG becomes more rhythmic.

To illustrate the opposite behaviour of the spectral entropy and approximate entropy measures with the increase in rhythmic activity in the original EEG signal, three consecutive signal segments from the same recording underlying the experiment of Figure 2 are shown in Figure 3. From curve 1 to curve 3 in the figure, the amount of slow activity decreases and rhythmic activity increases causing flattening of the spectrum and increase in spectral entropy. At the same time, the increase in the relative amplitude of the rhythmic activity is reflected by approximate entropy as increasing regularity and hence decreasing entropy value. The two entropy measures change in different directions from 1 to 3.

Discussion

The results of the first part of this study show that a given value of spectral entropy gives no information about the frequency spectrum, waveform, or the visual impression of regularity of the signal. Therefore, contrary to the claims in the literature, spectral entropy does not describe the irregularity, complexity, or unpredictability characteristics of the signal in general.[8] Yet in special cases like deepening anaesthesia, for example, spectral entropy correlates with the EEG changes. This is due to the power spectrum becoming more peaked with increasing low-frequency components and decreasing high-frequency components. This does not necessarily mean that the signal becomes more regular.

The approximate entropy measure, on the other hand, reflects well the visual impression of regular *vs* irregular signal. This can be understood because approximate entropy uses the phase and frequency information in the signal, while in the calculation of spectral entropy, this information is discarded.

As the first application of spectral entropy was quantifying the α-rhythm of the EEG, it has been suggested that spectral entropy is also useful in quantifying rhythmic patterns in the EEG during anaesthesia, that is, patterns which produce a peak in the power spectrum. The second part of our study shows that this is not the case. On the contrary, the appearance of a spectral peak due to the rhythmic pattern in the EEG can make the power spectrum more flat if a high-amplitude very low-frequency activity is present, increasing thus the spectral entropy and suggesting that the EEG becomes more irregular. The presence of this very low activity together with the increase in the α-rhythm in deep anaesthesia is very common. These results contradict with what has been suggested in the literature previously.[8]

The risk of misinterpretation of the results of depth-of-anaesthesia monitors or clinical studies is especially high when unexpected components appear in the EEG signal. One such component frequently affecting the entropy reading during anaesthesia is the muscle activity. It has been suggested that surface EMG may dominate the measured signal in the frequency range from about 30 Hz upwards.[8] During anaesthesia, sometimes, the activity of a single motor unit can be observed in the EEG measurement. It can fire at a very regular frequency of, say, 4 Hz, overriding the EEG contribution to power spectrum.[13] This low-frequency EMG can totally cover the EEG even at burst suppression level of anesthesia.[6] In these cases, it is practically impossible to evaluate the depth of hypnosis from the signal recorded from the forehead: we are not aware of any measures of signal entropy which could quantify EEG which is covered by EMG.

During the last decades, a wide range of signal analysis algorithms have been applied for quantification of

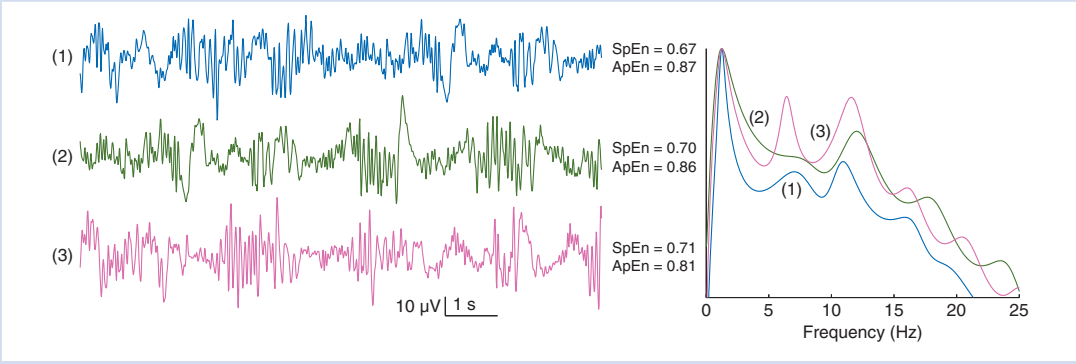

Fig 3 The effect of the relative increase in rhythmic activity on power spectra and the entropy measures. From 1 to 3, the amount of slow activity decreases and rhythmic activity increases. The logarithmic power spectra are scaled according to the maximum of the δ-frequency peak. This illustrates the flattening of the spectrum which causes the increase in spectral entropy. At the same time, the increase in the relative amplitude of rhythmic activity is reflected by approximate entropy as increasing regularity and hence decreasing entropy value. The two entropy measures change in different directions from 1 to 3.

unconsciousness-related EEG patterns during anaesthesia. While older methods like median frequency or spectral edge frequency have been proven useful in measuring the relative increase in slow activity and decrease in fast activity with deepening anesthesia,[14] manufacturers of commercial devices have preferred methods like bispectrum or different measures of the complexity of the signal. These complexity measures all aim at measuring the regularity or predictability of the signal waveform. However, often the terms complexity, entropy, or fractal dimension are used without stressing the corresponding algorithm used in the calculations and measures having similar name can behave in different, even opposite, manner with deepening anaesthesia.[4]

Measuring signal entropy has its roots in Claude Shannon's theory of communication.[15] In information theory, Shannon's formula is applied to the amplitude distribution of the signal, yielding Shannon entropy of the signal. The value of Shannon entropy gives an idea of the amplitude distribution of the signal, and thus the appearance of the signal. It does not, however, give any information about the frequency characteristics of the signal.

The application of Shannon's formula to the power spectrum of the signal yields a measure named spectral entropy. It was first applied to EEG in 1991 to measure the regularity of α-rhythm in posterior regions of the awake brain.[16] This gives an idea of the regularity of the α-rhythm, if lower frequencies are minimal or have been filtered away. Later, spectral entropy has been applied to the quantification of anaesthesia EEG. In deepening anaesthesia, the increase in both irregular, arrhythmic and regular, rhythmic slow activity and the decrease in fast activity leads to the increase in the slope of the logarithmic power spectrum, which is roughly linear. Therefore, the power–frequency distribution of the EEG becomes more uneven or peaked yielding lower spectral entropy values. The same development makes the amplitude distribution of the signal less peaked causing Shannon entropy to increase.[4 5] Consequently, these two measures of EEG entropy, based on the same Shannon formula, change in opposite directions in deepening anaesthesia.

Approximate entropy, calculated in the time domain and based on the phase space analysis of signals, was first introduced for EEG signal analysis in 1998.[11] It has since drawn a lot of attention as a promising measure of the hypnotic drug effect.[3 17] Being calculated in time domain, approximate entropy is easier to relate to the visual appearance of the signal. However, to our knowledge, no commercial anaesthesia monitor currently uses the approximate entropy algorithm.

In conclusion, a value of spectral entropy does not, in general, correlate with the regularity of the signal waveform. Using artificially generated test signals, our analysis showed that approximate entropy values reflected better the visual impression of regularity and predictability. Secondly, appearance of rhythmic activity at frequencies above the lower edge of the spectrum tends to increase spectral entropy but decreases approximate entropy, that is, they may change in opposite directions. We have demonstrated these ideas using artificially generated test signals to keep the signal parameters controlled and, therefore, the results have limited impact on the practical clinical situation. The example shown in Figure 3 and long-term experience in EEG analysis and interpretation suggest that the studied phenomena are also common in the practical situation. It should be noted, however, that these limitations in algorithms do not contradict other evidence of adequate clinical performance of the spectral entropy measure.

If measures of signal entropy or indexes based on them are used clinically or in research, it is obligatory that the principles of these measures are understood. Furthermore, the

raw signal must always be visually checked for artifacts as EMG and arousal reactions may affect different indexes differently due to the mathematical methods used.

Declaration of interest

None declared.

Funding

This work was partly supported by Estonian Science Foundation (grant no. 7225).

References

1 Jäntti V. Unconsciousness and EEG burst suppression. *Br J Anaesth* 2012; **108**: 342–3P

2 Jäntti V, Sloan T. EEG and anesthetic effects. Intraoperative monitoring of neural function. In: Nuwer MR, ed. *Handbook of Clinical Neurophysiology*, Vol. 8. Amsterdam: Elsevier BV, 2008; 77–93

3 Bruhn J, Röpcke H, Rehberg B, Bouillon T, Hoeft A. Electroencephalogram approximate entropy correctly classifies the occurrence of burst suppression pattern as increasing anesthetic drug effect. *Anesthesiology* 2000; **93**: 981–5

4 Ferenets R, Lipping T, Anier A, Jantti V, Melto S, Hovilehto S. Comparison of entropy and complexity measures for the assessment of depth of sedation. *IEEE Trans Biomed Eng* 2006; **53**: 1067–77

5 Bruhn J, Lehmann LE, Röpcke H, Bouillon TW, Hoeft A. Shannon entropy applied to the measurement of the electroencephalographic effects of desflurane. *Anesthesiology* 2001; **95**: 30–5

6 Aho AJ, Yli-Hankala A, Lyytikäinen LP, Jäntti V. Facial muscle activity, Response Entropy, and State Entropy indices during noxious stimuli in propofol–nitrous oxide or propofol–nitrous oxide–remifentanil anaesthesia without neuromuscular block. *Br J Anaesth* 2009; **102**: 227–33

7 Aho AJ, Lyytikäinen LP, Yli-Hankala A, Kamata K, Jäntti V. Explaining Entropy responses after a noxious stimulus, with or without neuromuscular blocking agents, by means of the raw electroencephalographic and electromyographic characteristics. *Br J Anaesth* 2011; **106**: 69–76

8 Viertiö-Oja H, Maja V, Särkelä M, et al. Description of the Entropy™ algorithm as applied in the Datex-Ohmeda S/5™ Entropy Module. *Acta Anaesthesiol Scand* 2004; **48**: 154–61

9 Pincus SM. Approximate entropy as a measure of system complexity. *Proc Natl Acad Sci USA* 1991; **88**: 2297–301

10 Richman JS, Moorman JR. Physiological time-series analysis using approximate entropy and sample entropy. *Am J Physiol Heart Circ Physiol* 2000; **278**: 2039–49

11 Rezek I, Roberts S. Stochastic complexity measures for physiological signal analysis. *IEEE Trans Biomed Eng* 1998; **45**: 1186–91

12 Broersen PM. *Automatic Autocorrelation and Spectral Analysis*. London: Springer-Verlag London Limited, 2006

13 Kamata K, Aho AJ, Hagihira S, Yli-Hankala A, Jäntti V. Frequency band of EMG in anaesthesia monitoring. *Br J Anaesth* 2011; **107**: 822–3

14 Jordan D, Stockmanns G, Kochs E, Schneider G. Median frequency revisited: an approach to improve a classic spectral electroencephalographic parameter for the separation of consciousness from unconsciousness. *Anesthesiology* 2007; **107**: 397–405

15 Shannon C. A mathematical theory of communication. *Bell Systen Techn J* 1948; **27**: 623–56

16 Inouye T, Shinosaki K, Sakamoto H, *et al.* Quantification of EEG irregularity by use of the entropy of the power spectrum. *Electroencephalogr Clin Neurophysiol* 1991; **79**: 204–10

17 Jordan D, Stockmanns G, Kochs EF, Pilge S, Schneider G. Electroencephalographic order pattern analysis for the separation of consciousness and unconsciousness: an analysis of approximate entropy, permutation entropy, recurrence rate, and phase coupling of order recurrence plots. *Anesthesiology* 2008; **109**: 1014–22

ELULOOKIRJELDUS

1. Isikuandmed

Ees- ja perekonnanimi	Andres Anier
Sünniaeg ja -koht	08.12.1972 Jõhvi, Ida-Virumaa, Eesti
Kodakondsus	eestlane
E-posti aadress	andres.anier@mail.ee

2. Hariduskäik

Õppeasutus (nimetus lõpetamise ajal)	Lõpetamise aeg	Haridus (eriala/kraad)
Tallinna Tehnikaülikool	1998	Süsteemitehnika ja informaatika magister
Tallinna Tehnikaülikool	2002	Biomeditsiinitehnika magister
Tallinna Tehnikaülikool		Biomeditsiinitehnika doktoriõpe

3. Keelteoskus (alg-, kesk- või kõrgtase)

Keel	Tase
Eesti	Emakeel
Inglise	Kõrgtase
Vene	Kesktase
Soome	Algtase

4. Teenistuskäik

Töötamise aeg	Tööandja nimetus	Ametikoht
1995-1998	Aetec AS	Tarkvaraarhitekt
1998-2002	Philips Eesti OÜ	Meditsiinitehnika insener
2000-	Girf OÜ	Asutaja, juhatuse liige
2002-2003	Hansapank	Süsteemiintegratsiooni projektijuht
2004-	ELIKO Tehnoloogia Arenduskeskus	eTervise- ja telemeditsiini-tehnoloogiate projektijuht
2013-	EdgeWise OÜ	Asutaja, juhatuse liige

5. Teadustegevus, sh tunnustused ja juhendatud lõputööd

Kala, R., (juh) Anier, A. EEG based assessment of depth of sedation in ICU : bakalaureusetöö. Tallinn, Tallinna Tehnikaülikool, 2008.

Anier, A., Kaik, J., and Meigas, K. Method for Reducing Pacing Current Threshold at Transesophageal Stimulation. *IFMBE Proc*, pp. 554 - 557, 2007.

Anier, A., Kaik, J. and Meigas, K. A Novel Method for Reducing Pain Sensation at Transesopageal Atrial Stimulation. *Engineering in Medicine and Biology Society, 2007. EMBS 2007. 29th Annual International Conference of the IEEE*, pp. 923 - 926, 2007.

Anier, A., Kaik, J., and Meigas, K. Precise Positioning of Electrodes at Transesophagael Atrial Simulation Using Multichannel Transesophagael Pacemaker and Lead. *IFMBE Proc*, pp. 183 - 185, 2008.

Anier, An., Kaik, J., and Meigas, K. Device and Methods for Performing Transesophageal Stimulation at Reduced Pacing Current Threshold. *Estonian Journal of Engineering*, 14(2), pp. 154 – 166, 2008.

Lõõbas, I., Reilent, E., Anier, A., Luberg, A. and Kuusik, A. Towards semantic contextual content-centric assisted living solution. *Proceedings of 12th IEEE International Conference on e-Health Networking Applications and Services (Healthcom 2010): 12th IEEE International Conference on e-Health Networking Applications and Services*, Lyon 1-3 July 2010, 1(1), pp. 56 – 60, 2010.

Teadustöö põhisuunad

SF0142084As02 Bioelektriliste signaalide interpreteerimine 01.01.02 - 31.12.06

ETF7225 Ajutraumaga patsientide EEG signaalijoonise analüüs ja monitooring 01.01.07 - 31.12.09

SF0140027s07 Biosignaalide interpreteerimine meditsiinitehnikas 01.01.07 - 31.12.12

3.2.1201.13-0015 Algorithms for Automatic detection of brain disorders based on advanced EEG signal processing techniques 01.01.2013 - 31.08.2015

CURRICULUM VITAE

1. Personal data

Name	Andres Anier
Date and place of birth	08.12.1972 Jõhvi, Ida-Virumaa, Estonia
E-mail	andres.anier@mail.ee

2. Education

Educational institution	Graduation year	Education (field of study/degree)
Tallinn University of Technology	1998	System and Computer Engineering. MSc
Tallinn University of Technology	2002	Biomedical engineering. MSc
Tallinn University of Technology		Biomedical engineering. PhD student

3. Language competence/skills (fluent; average, basic skills)

Language	Level
Estonian	Fluent
English	Fluent
Russian	Average
Finnish	Basic

4. Professional employment

Period	Organisation	Position
1995-1998	Aetec AS	Software architect
1998-2002	Philips Estonia OÜ	Medical Systems Engineer
2000-	Girf OÜ	Founder, member of board
2002-2003	Hansabank	Systems Integration Project Manager
2004-	ELIKO Competence Centre	eHealth and Telemedine workpackages manager
2013-	EdgeWise OÜ	Founder, CEO

5. Research activity, including honours and thesis supervised

   Kala, R., (sup) Anier, A. EEG based assessment of depth of sedation in ICU : BSc thesis. Tallinn, Tallinn University of Technology, 2008.

   Anier, A., Kaik, J., and Meigas, K. Method for Reducing Pacing Current Threshold at Transesophageal Stimulation. *IFMBE Proc,* pp. 554 - 557, 2007.

   Anier, A., Kaik, J. and Meigas, K. A Novel Method for Reducing Pain Sensation at Transesopageal Atrial Stimulation. *Engineering in Medicine and Biology Society, 2007. EMBS 2007. 29th Annual International Conference of the IEEE,* pp. 923 - 926, 2007.

   Anier, A., Kaik, J., and Meigas, K. Precise Positioning of Electrodes at Transesophagael Atrial Simulation Using Multichannel Transesophagael Pacemaker and Lead. *IFMBE Proc*, pp. 183 - 185, 2008.

   Anier, An., Kaik, J., and Meigas, K. Device and Methods for Performing Transesophageal Stimulation at Reduced Pacing Current Threshold. *Estonian Journal of Engineering*, 14(2), pp. 154 – 166, 2008.

   Lõõbas, I., Reilent, E., Anier, A., Luberg, A. and Kuusik, A. Towards semantic contextual content-centric assisted living solution. *Proceedings of 12th IEEE International Conference on e-Health Networking Applications and Services (Healthcom 2010): 12th IEEE International Conference on e-Health Networking Applications and Services, Lyon 1-3 July 2010,* 1(1), pp. 56 – 60, 2010.

6. Main areas of scientific work

   SF0142084As02 Bioelectrical signals interpretation 01.01.02 - 31.12.06

   ETF7225 EEG Pattern Analysis and Brain Monitoring of Sedated Trauma Patients 01.01.07 - 31.12.09

   SF0140027s07 Interpretation of Biosignals in Biomedical Engineering 01.01.07 - 31.12.12

   3.2.1201.13-0015 Algorithms for Automatic detection of brain disorders based on advanced EEG signal processing techniques 01.01.2013 - 31.08.2015

DISSERTATIONS DEFENDED AT
TALLINN UNIVERSITY OF TECHNOLOGY ON
NATURAL AND EXACT SCIENCES

1. **Olav Kongas**. Nonlinear Dynamics in Modeling Cardiac Arrhytmias. 1998.

2. **Kalju Vanatalu**. Optimization of Processes of Microbial Biosynthesis of Isotopically Labeled Biomolecules and Their Complexes. 1999.

3. **Ahto Buldas**. An Algebraic Approach to the Structure of Graphs. 1999.

4. **Monika Drews**. A Metabolic Study of Insect Cells in Batch and Continuous Culture: Application of Chemostat and Turbidostat to the Production of Recombinant Proteins. 1999.

5. **Eola Valdre**. Endothelial-Specific Regulation of Vessel Formation: Role of Receptor Tyrosine Kinases. 2000.

6. **Kalju Lott**. Doping and Defect Thermodynamic Equilibrium in ZnS. 2000.

7. **Reet Koljak**. Novel Fatty Acid Dioxygenases from the Corals *Plexaura homomalla* and *Gersemia fruticosa.* 2001.

8. **Anne Paju**. Asymmetric oxidation of Prochiral and Racemic Ketones by Using Sharpless Catalyst. 2001.

9. **Marko Vendelin**. Cardiac Mechanoenergetics *in silico*. 2001.

10. **Pearu Peterson**. Multi-Soliton Interactions and the Inverse Problem of Wave Crest. 2001.

11. **Anne Menert**. Microcalorimetry of Anaerobic Digestion. 2001.

12. **Toomas Tiivel**. The Role of the Mitochondrial Outer Membrane in *in vivo* Regulation of Respiration in Normal Heart and Skeletal Muscle Cell. 2002.

13. **Olle Hints**. Ordovician Scolecodonts of Estonia and Neighbouring Areas: Taxonomy, Distribution, Palaeoecology, and Application. 2002.

14. **Jaak Nõlvak**. Chitinozoan Biostratigrapy in the Ordovician of Baltoscandia. 2002.

15. **Liivi Kluge**. On Algebraic Structure of Pre-Operad. 2002.

16. **Jaanus Lass**. Biosignal Interpretation: Study of Cardiac Arrhytmias and Electromagnetic Field Effects on Human Nervous System. 2002.

17. **Janek Peterson**. Synthesis, Structural Characterization and Modification of PAMAM Dendrimers. 2002.

18. **Merike Vaher**. Room Temperature Ionic Liquids as Background Electrolyte Additives in Capillary Electrophoresis. 2002.

19. **Valdek Mikli**. Electron Microscopy and Image Analysis Study of Powdered Hardmetal Materials and Optoelectronic Thin Films. 2003.

20. **Mart Viljus**. The Microstructure and Properties of Fine-Grained Cermets. 2003.

21. **Signe Kask**. Identification and Characterization of Dairy-Related *Lactobacillus.* 2003

22. **Tiiu-Mai Laht**. Influence of Microstructure of the Curd on Enzymatic and Microbiological Processes in Swiss-Type Cheese. 2003.

23. **Anne Kuusksalu**. 2–5A Synthetase in the Marine Sponge *Geodia cydonium*. 2003.

24. **Sergei Bereznev**. Solar Cells Based on Polycristalline Copper-Indium Chalcogenides and Conductive Polymers. 2003.

25. **Kadri Kriis**. Asymmetric Synthesis of C_2-Symmetric Bimorpholines and Their Application as Chiral Ligands in the Transfer Hydrogenation of Aromatic Ketones. 2004.

26. **Jekaterina Reut**. Polypyrrole Coatings on Conducting and Insulating Substracts. 2004.

27. **Sven Nõmm**. Realization and Identification of Discrete-Time Nonlinear Systems. 2004.

28. **Olga Kijatkina**. Deposition of Copper Indium Disulphide Films by Chemical Spray Pyrolysis. 2004.

29. **Gert Tamberg**. On Sampling Operators Defined by Rogosinski, Hann and Blackman Windows. 2004.

30. **Monika Übner**. Interaction of Humic Substances with Metal Cations. 2004.

31. **Kaarel Adamberg**. Growth Characteristics of Non-Starter Lactic Acid Bacteria from Cheese. 2004.

32. **Imre Vallikivi**. Lipase-Catalysed Reactions of Prostaglandins. 2004.

33. **Merike Peld**. Substituted Apatites as Sorbents for Heavy Metals. 2005.

34. **Vitali Syritski**. Study of Synthesis and Redox Switching of Polypyrrole and Poly(3,4-ethylenedioxythiophene) by Using *in-situ* Techniques. 2004.

35. **Lee Põllumaa**. Evaluation of Ecotoxicological Effects Related to Oil Shale Industry. 2004.

36. **Riina Aav**. Synthesis of 9,11-Secosterols Intermediates. 2005.

37. **Andres Braunbrück**. Wave Interaction in Weakly Inhomogeneous Materials. 2005.

38. **Robert Kitt**. Generalised Scale-Invariance in Financial Time Series. 2005.

39. **Juss Pavelson**. Mesoscale Physical Processes and the Related Impact on the Summer Nutrient Fields and Phytoplankton Blooms in the Western Gulf of Finland. 2005.

40. **Olari Ilison**. Solitons and Solitary Waves in Media with Higher Order Dispersive and Nonlinear Effects. 2005.

41. **Maksim Säkki**. Intermittency and Long-Range Structurization of Heart Rate. 2005.

42. **Enli Kiipli**. Modelling Seawater Chemistry of the East Baltic Basin in the Late Ordovician–Early Silurian. 2005.

43. **Igor Golovtsov**. Modification of Conductive Properties and Processability of Polyparaphenylene, Polypyrrole and polyaniline. 2005.

44. **Katrin Laos**. Interaction Between Furcellaran and the Globular Proteins (Bovine Serum Albumin β-Lactoglobulin). 2005.

45. **Arvo Mere**. Structural and Electrical Properties of Spray Deposited Copper Indium Disulphide Films for Solar Cells. 2006.

46. **Sille Ehala**. Development and Application of Various On- and Off-Line Analytical Methods for the Analysis of Bioactive Compounds. 2006.

47. **Maria Kulp**. Capillary Electrophoretic Monitoring of Biochemical Reaction Kinetics. 2006.

48. **Anu Aaspõllu.** Proteinases from *Vipera lebetina* Snake Venom Affecting Hemostasis. 2006.

49. **Lyudmila Chekulayeva**. Photosensitized Inactivation of Tumor Cells by Porphyrins and Chlorins. 2006.

50. **Merle Uudsemaa**. Quantum-Chemical Modeling of Solvated First Row Transition Metal Ions. 2006.

51. **Tagli Pitsi**. Nutrition Situation of Pre-School Children in Estonia from 1995 to 2004. 2006.

52. **Angela Ivask**. Luminescent Recombinant Sensor Bacteria for the Analysis of Bioavailable Heavy Metals. 2006.

53. **Tiina Lõugas**. Study on Physico-Chemical Properties and Some Bioactive Compounds of Sea Buckthorn (*Hippophae rhamnoides* L.). 2006.

54. **Kaja Kasemets**. Effect of Changing Environmental Conditions on the Fermentative Growth of *Saccharomyces cerevisae* S288C: Auxo-accelerostat Study. 2006.

55. **Ildar Nisamedtinov**. Application of ^{13}C and Fluorescence Labeling in Metabolic Studies of *Saccharomyces* spp. 2006.

56. **Alar Leibak**. On Additive Generalisation of Voronoï's Theory of Perfect Forms over Algebraic Number Fields. 2006.

57. **Andri Jagomägi**. Photoluminescence of Chalcopyrite Tellurides. 2006.

58. **Tõnu Martma**. Application of Carbon Isotopes to the Study of the Ordovician and Silurian of the Baltic. 2006.

59. **Marit Kauk**. Chemical Composition of $CuInSe_2$ Monograin Powders for Solar Cell Application. 2006.

60. **Julia Kois**. Electrochemical Deposition of $CuInSe_2$ Thin Films for Photovoltaic Applications. 2006.

61. **Ilona Oja Açik**. Sol-Gel Deposition of Titanium Dioxide Films. 2007.

62. **Tiia Anmann**. Integrated and Organized Cellular Bioenergetic Systems in Heart and Brain. 2007.

63. **Katrin Trummal**. Purification, Characterization and Specificity Studies of Metalloproteinases from *Vipera lebetina* Snake Venom. 2007.

64. **Gennadi Lessin**. Biochemical Definition of Coastal Zone Using Numerical Modeling and Measurement Data. 2007.

65. **Enno Pais**. Inverse problems to determine non-homogeneous degenerate memory kernels in heat flow. 2007.

66. **Maria Borissova**. Capillary Electrophoresis on Alkylimidazolium Salts. 2007.

67. **Karin Valmsen**. Prostaglandin Synthesis in the Coral *Plexaura homomalla*: Control of Prostaglandin Stereochemistry at Carbon 15 by Cyclooxygenases. 2007.

68. **Kristjan Piirimäe**. Long-Term Changes of Nutrient Fluxes in the Drainage Basin of the Gulf of Finland – Application of the PolFlow Model. 2007.

69. **Tatjana Dedova**. Chemical Spray Pyrolysis Deposition of Zinc Sulfide Thin Films and Zinc Oxide Nanostructured Layers. 2007.

70. **Katrin Tomson**. Production of Labelled Recombinant Proteins in Fed-Batch Systems in *Escherichia coli*. 2007.

71. **Cecilia Sarmiento**. Suppressors of RNA Silencing in Plants. 2008.

72. **Vilja Mardla**. Inhibition of Platelet Aggregation with Combination of Antiplatelet Agents. 2008.

73. **Maie Bachmann**. Effect of Modulated Microwave Radiation on Human Resting Electroencephalographic Signal. 2008.

74. **Dan Hüvonen**. Terahertz Spectroscopy of Low-Dimensional Spin Systems. 2008.

75. **Ly Villo**. Stereoselective Chemoenzymatic Synthesis of Deoxy Sugar Esters Involving *Candida antarctica* Lipase B. 2008.

76. **Johan Anton**. Technology of Integrated Photoelasticity for Residual Stress Measurement in Glass Articles of Axisymmetric Shape. 2008.

77. **Olga Volobujeva**. SEM Study of Selenization of Different Thin Metallic Films. 2008.

78. **Artur Jõgi**. Synthesis of 4'-Substituted 2,3'-dideoxynucleoside Analogues. 2008.

79. **Mario Kadastik**. Doubly Charged Higgs Boson Decays and Implications on Neutrino Physics. 2008.

80. **Fernando Pérez-Caballero**. Carbon Aerogels from 5-Methylresorcinol-Formaldehyde Gels. 2008.

81. **Sirje Vaask**. The Comparability, Reproducibility and Validity of Estonian Food Consumption Surveys. 2008.

82. **Anna Menaker**. Electrosynthesized Conducting Polymers, Polypyrrole and Poly(3,4-ethylenedioxythiophene), for Molecular Imprinting. 2009.

83. **Lauri Ilison**. Solitons and Solitary Waves in Hierarchical Korteweg-de Vries Type Systems. 2009.

84. **Kaia Ernits**. Study of In_2S_3 and ZnS Thin Films Deposited by Ultrasonic Spray Pyrolysis and Chemical Deposition. 2009.

85. **Veljo Sinivee**. Portable Spectrometer for Ionizing Radiation "Gammamapper". 2009.

86. **Jüri Virkepu**. On Lagrange Formalism for Lie Theory and Operadic Harmonic Oscillator in Low Dimensions. 2009.

87. **Marko Piirsoo**. Deciphering Molecular Basis of Schwann Cell Development. 2009.

88. **Kati Helmja**. Determination of Phenolic Compounds and Their Antioxidative Capability in Plant Extracts. 2010.

89. **Merike Sõmera**. Sobemoviruses: Genomic Organization, Potential for Recombination and Necessity of P1 in Systemic Infection. 2010.

90. **Kristjan Laes**. Preparation and Impedance Spectroscopy of Hybrid Structures Based on $CuIn_3Se_5$ Photoabsorber. 2010.

91. **Kristin Lippur**. Asymmetric Synthesis of 2,2'-Bimorpholine and its 5,5'-Substituted Derivatives. 2010.

92. **Merike Luman**. Dialysis Dose and Nutrition Assessment by an Optical Method. 2010.

93. **Mihhail Berezovski**. Numerical Simulation of Wave Propagation in Heterogeneous and Microstructured Materials. 2010.

94. **Tamara Aid-Pavlidis**. Structure and Regulation of BDNF Gene. 2010.

95. **Olga Bragina**. The Role of Sonic Hedgehog Pathway in Neuro- and Tumorigenesis. 2010.

96. **Merle Randrüüt**. Wave Propagation in Microstructured Solids: Solitary and Periodic Waves. 2010.

97. **Marju Laars**. Asymmetric Organocatalytic Michael and Aldol Reactions Mediated by Cyclic Amines. 2010.

98. **Maarja Grossberg**. Optical Properties of Multinary Semiconductor Compounds for Photovoltaic Applications. 2010.

99. **Alla Maloverjan**. Vertebrate Homologues of Drosophila Fused Kinase and Their Role in Sonic Hedgehog Signalling Pathway. 2010.

100. **Priit Pruunsild**. Neuronal Activity-Dependent Transcription Factors and Regulation of Human *BDNF* Gene. 2010.

101. **Tatjana Knjazeva**. New Approaches in Capillary Electrophoresis for Separation and Study of Proteins. 2011.

102. **Atanas Katerski**. Chemical Composition of Sprayed Copper Indium Disulfide Films for Nanostructured Solar Cells. 2011.

103. **Kristi Timmo.** Formation of Properties of $CuInSe_2$ and $Cu_2ZnSn(S,Se)_4$ Monograin Powders Synthesized in Molten KI. 2011.
104. **Kert Tamm**. Wave Propagation and Interaction in Mindlin-Type Microstructured Solids: Numerical Simulation. 2011.
105. **Adrian Popp**. Ordovician Proetid Trilobites in Baltoscandia and Germany. 2011.
106. **Ove Pärn**. Sea Ice Deformation Events in the Gulf of Finland and This Impact on Shipping. 2011.
107. **Germo Väli**. Numerical Experiments on Matter Transport in the Baltic Sea. 2011.
108. **Andrus Seiman**. Point-of-Care Analyser Based on Capillary Electrophoresis. 2011.
109. **Olga Katargina**. Tick-Borne Pathogens Circulating in Estonia (Tick-Borne Encephalitis Virus, *Anaplasma phagocytophilum*, *Babesia* Species): Their Prevalence and Genetic Characterization. 2011.
110. **Ingrid Sumeri**. The Study of Probiotic Bacteria in Human Gastrointestinal Tract Simulator. 2011.
111. **Kairit Zovo**. Functional Characterization of Cellular Copper Proteome. 2011.
112. **Natalja Makarytsheva**. Analysis of Organic Species in Sediments and Soil by High Performance Separation Methods. 2011.
113. **Monika Mortimer**. Evaluation of the Biological Effects of Engineered Nanoparticles on Unicellular Pro- and Eukaryotic Organisms. 2011.
114. **Kersti Tepp**. Molecular System Bioenergetics of Cardiac Cells: Quantitative Analysis of Structure-Function Relationship. 2011.
115. **Anna-Liisa Peikolainen**. Organic Aerogels Based on 5-Methylresorcinol. 2011.
116. **Leeli Amon**. Palaeoecological Reconstruction of Late-Glacial Vegetation Dynamics in Eastern Baltic Area: A View Based on Plant Macrofossil Analysis. 2011.
117. **Tanel Peets**. Dispersion Analysis of Wave Motion in Microstructured Solids. 2011.
118. **Liina Kaupmees**. Selenization of Molybdenum as Contact Material in Solar Cells. 2011.
119. **Allan Olspert**. Properties of VPg and Coat Protein of Sobemoviruses. 2011.
120. **Kadri Koppel**. Food Category Appraisal Using Sensory Methods. 2011.
121. **Jelena Gorbatšova**. Development of Methods for CE Analysis of Plant Phenolics and Vitamins. 2011.
122. **Karin Viipsi**. Impact of EDTA and Humic Substances on the Removal of Cd and Zn from Aqueous Solutions by Apatite. 2012.
123. **David Schryer**. Metabolic Flux Analysis of Compartmentalized Systems Using Dynamic Isotopologue Modeling. 2012.
124. **Ardo Illaste**. Analysis of Molecular Movements in Cardiac Myocytes. 2012.
125. **Indrek Reile**. 3-Alkylcyclopentane-1,2-Diones in Asymmetric Oxidation and Alkylation Reactions. 2012.
126. **Tatjana Tamberg**. Some Classes of Finite 2-Groups and Their Endomorphism Semigroups. 2012.

127. **Taavi Liblik**. Variability of Thermohaline Structure in the Gulf of Finland in Summer. 2012.
128. **Priidik Lagemaa**. Operational Forecasting in Estonian Marine Waters. 2012.
129. **Andrei Errapart**. Photoelastic Tomography in Linear and Non-linear Approximation. 2012.
130. **Külliki Krabbi**. Biochemical Diagnosis of Classical Galactosemia and Mucopolysaccharidoses in Estonia. 2012.
131. **Kristel Kaseleht**. Identification of Aroma Compounds in Food using SPME-GC/MS and GC-Olfactometry. 2012.
132. **Kristel Kodar**. Immunoglobulin G Glycosylation Profiling in Patients with Gastric Cancer. 2012.
133. **Kai Rosin**. Solar Radiation and Wind as Agents of the Formation of the Radiation Regime in Water Bodies. 2012.
134. **Ann Tiiman**. Interactions of Alzheimer's Amyloid-Beta Peptides with Zn(II) and Cu(II) Ions. 2012.
135. **Olga Gavrilova**. Application and Elaboration of Accounting Approaches for Sustainable Development. 2012.
136. **Olesja Bondarenko**. Development of Bacterial Biosensors and Human Stem Cell-Based *In Vitro* Assays for the Toxicological Profiling of Synthetic Nanoparticles. 2012.
137. **Katri Muska**. Study of Composition and Thermal Treatments of Quaternary Compounds for Monograin Layer Solar Cells. 2012.
138. **Ranno Nahku**. Validation of Critical Factors for the Quantitative Characterization of Bacterial Physiology in Accelerostat Cultures. 2012.
139. **Petri-Jaan Lahtvee**. Quantitative Omics-level Analysis of Growth Rate Dependent Energy Metabolism in *Lactococcus lactis*. 2012.
140. **Kerti Orumets**. Molecular Mechanisms Controlling Intracellular Glutathione Levels in Baker's Yeast *Saccharomyces cerevisiae* and its Random Mutagenized Gluthatione Over-Accumulating Isolate. 2012.
141. **Loreida Timberg**. Spice-Cured Sprats Ripening, Sensory Parameters Development, and Quality Indicators. 2012.
142. **Anna Mihhalevski**. Rye Sourdough Fermentation and Bread Stability. 2012.
143. **Liisa Arike**. Quantitative Proteomics of *Escherichia coli*: From Relative to Absolute Scale. 2012.
144. **Kairi Otto**. Deposition of In_2S_3 Thin Films by Chemical Spray Pyrolysis. 2012.
145. **Mari Sepp**. Functions of the Basic Helix-Loop-Helix Transcription Factor TCF4 in Health and Disease. 2012.
146. **Anna Suhhova**. Detection of the Effect of Weak Stressors on Human Resting Electroencephalographic Signal. 2012.
147. **Aram Kazarjan**. Development and Production of Extruded Food and Feed Products Containing Probiotic Microorganisms. 2012.
148. **Rivo Uiboupin**. Application of Remote Sensing Methods for the Investigation of Spatio-Temporal Variability of Sea Surface Temperature and Chlorophyll Fields in the Gulf of Finland. 2013.
149. **Tiina Kriščiunaite**. A Study of Milk Coagulability. 2013.

150. **Tuuli Levandi**. Comparative Study of Cereal Varieties by Analytical Separation Methods and Chemometrics. 2013.
151. **Natalja Kabanova**. Development of a Microcalorimetric Method for the Study of Fermentation Processes. 2013.
152. **Himani Khanduri**. Magnetic Properties of Functional Oxides. 2013.
153. **Julia Smirnova**. Investigation of Properties and Reaction Mechanisms of Redox-Active Proteins by ESI MS. 2013.
154. **Mervi Sepp**. Estimation of Diffusion Restrictions in Cardiomyocytes Using Kinetic Measurements. 2013.
155. **Kersti Jääger**. Differentiation and Heterogeneity of Mesenchymal Stem Cells. 2013.
156. **Victor Alari**. Multi-Scale Wind Wave Modeling in the Baltic Sea. 2013.
157. **Taavi Päll**. Studies of CD44 Hyaluronan Binding Domain as Novel Angiogenesis Inhibitor. 2013.
158. **Allan Niidu**. Synthesis of Cyclopentane and Tetrahydrofuran Derivatives. 2013.
159. **Julia Geller**. Detection and Genetic Characterization of *Borrelia* Species Circulating in Tick Population in Estonia. 2013.
160. **Irina Stulova**. The Effects of Milk Composition and Treatment on the Growth of Lactic Acid Bacteria. 2013.
161. **Jana Holmar**. Optical Method for Uric Acid Removal Assessment During Dialysis. 2013.
162. **Kerti Ausmees**. Synthesis of Heterobicyclo[3.2.0]heptane Derivatives *via* Multicomponent Cascade Reaction. 2013.
163. **Minna Varikmaa**. Structural and Functional Studies of Mitochondrial Respiration Regulation in Muscle Cells. 2013.
164. **Indrek Koppel**. Transcriptional Mechanisms of BDNF Gene Regulation. 2014.
165. **Kristjan Pilt**. Optical Pulse Wave Signal Analysis for Determination of Early Arterial Ageing in Diabetic Patients. 2014.